USGS
science for a changing world

Conceptual Models of Groundwater Flow in the Grand Canyon Region, Arizona

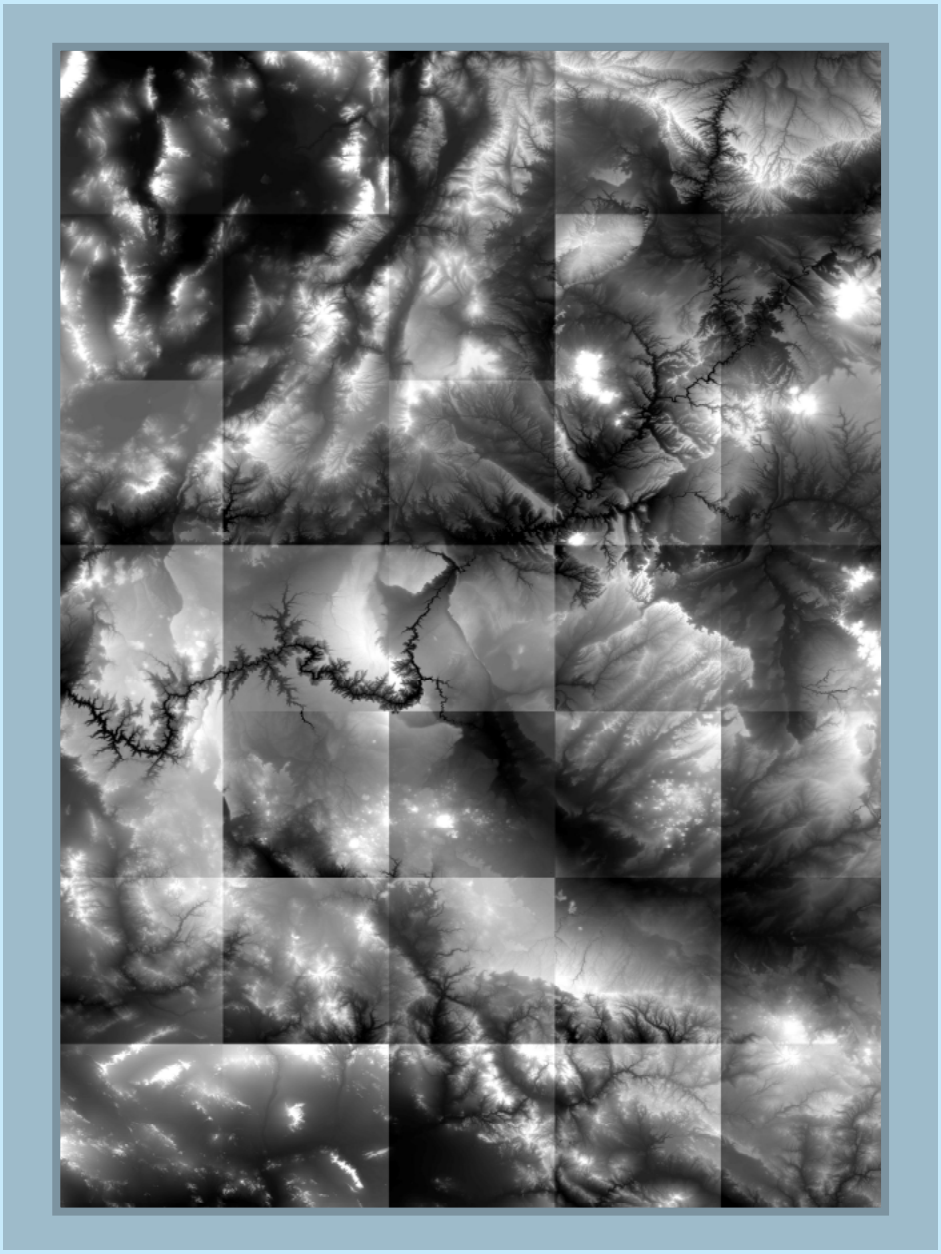

Scientific Investigations Report 2022–5037

U.S. Department of the Interior
U.S. Geological Survey

Cover. Mosaic of digital elevation models (DEMs) showing the Colorado River in the Grand Canyon region. Dark hues represent areas of lower elevation, whereas lighter hues represent areas of higher elevation. Digital elevation models from U.S. Geological Survey (2017) and separate DEMs are available for download at https://apps.nationalmap.gov/downloader/#/.

Conceptual Models of Groundwater Flow in the Grand Canyon Region, Arizona

By Jacob E. Knight and Peter W. Huntoon

Scientific Investigations Report 2022–5037

U.S. Department of the Interior
U.S. Geological Survey

U.S. Geological Survey, Reston, Virginia: 2022

For more information on the USGS—the Federal source for science about the Earth, its natural and living resources, natural hazards, and the environment—visit https://www.usgs.gov or call 1–888–ASK–USGS.

For an overview of USGS information products, including maps, imagery, and publications, visit https://store.usgs.gov.

Suggested citation:
Knight, J.E., and Huntoon, P.W., 2022, Conceptual models of groundwater flow in the Grand Canyon region, Arizona: U.S. Geological Survey Scientific Investigation Report 2022–5037, 51 p., https://doi.org/10.3133/sir20225037.

Associated data for this publication:
Knight, J.E., and Jones, C.J., 2022, Soil-Water-Balance (SWB) model archive used to simulate potential mean annual recharge in the Grand Canyon region, Arizona: U.S. Geological Survey data release, https://doi.org/10.5066/P9FQ7BSY.

ISSN 2328-0328 (online)

Contents

Figures

Conversion Factors

U.S. customary units to International System of Units

Multiply	By	To obtain
	Length	
inch (in.)	2.54	centimeter (cm)
inch (in.)	25.4	millimeter (mm)
foot (ft)	0.3048	meter (m)
mile (mi)	1.609	kilometer (km)
	Area	
acre	4,047	square meter (m^2)
acre	0.4047	hectare (ha)
acre	0.4047	square hectometer (hm^2)
acre	0.004047	square kilometer (km^2)
square mile (mi^2)	259.0	hectare (ha)
square mile (mi^2)	2.590	square kilometer (km^2)
	Volume	
gallon (gal)	3.785	liter (L)
gallon (gal)	0.003785	cubic meter (m^3)
gallon (gal)	3.785	cubic decimeter (dm^3)
cubic foot (ft^3)	28.32	cubic decimeter (dm^3)
acre-foot (acre-ft)	1,233	cubic meter (m^3)
acre-foot (acre-ft)	0.001233	cubic hectometer (hm^3)
	Flow rate	
cubic foot per second (ft^3/s)	0.02832	cubic meter per second (m^3/s)
cubic foot per day (ft^3/d)	0.02832	cubic meter per day (m^3/d)

International System of Units to U.S. customary units

Multiply	By	To obtain
	Length	
meter (m)	3.281	foot (ft)
kilometer (km)	0.6214	mile (mi)
kilometer (km)	0.5400	mile, nautical (nmi)
meter (m)	1.094	yard (yd)

Temperature in degrees Fahrenheit (°F) may be converted to degrees Celsius (°C) as follows:

$$°C = (°F - 32) / 1.8.$$

Datum

Vertical coordinate information is referenced to the North American Vertical Datum of 1988 (NAVD 88).

Horizontal coordinate information is referenced to the North American Datum of 1983 (NAD 83).

Elevation, as used in this report, refers to distance above the vertical datum.

Abbreviations

API	American Petroleum Institute
ADWR	Arizona Department of Water Resources
AZOGCC	Arizona Oil and Gas Conservation Commission
DEM	digital elevation model
HSG	hydrologic soil group
HUC	hydrologic unit code
MRLC	multi-resolution land characteristics
NLCD	National Land Cover Database
PRISM	parameter-elevation regression on independent slopes model
ROD	Record of Decision
SWB	soil-water-balance
UDOGM	Utah Department of Natural Resources Division of Oil, Gas and Mining
UNESCO	United Nations Educational, Scientific, and Cultural Organization
USDA	U.S Department of Agriculture
USGS	U.S. Geological Survey

Conceptual Models of Groundwater Flow in the Grand Canyon Region, Arizona

By Jacob E. Knight[1] and Peter W. Huntoon[2]

Abstract

The conceptual models of groundwater flow outlined herein synthesize what is known and hypothesized about the groundwater-flow systems that discharge to the Grand Canyon of Arizona. These models interpret the hydrogeologic characteristics and hydrologic dynamics of the physical systems into a framework for understanding key aspects of the physical systems as they relate to groundwater flow and contaminant transport. This report describes five individual groundwater-flow systems draining to the Grand Canyon: Kaibab, Uinkaret-Kanab, Marble-Shinumo, Cataract, and Blue Spring. These systems are present in the saturated parts of the lower Paleozoic carbonate section exposed on the walls of the Grand Canyon; specifically, the Mississippian Redwall Limestone down through the Cambrian Muav Limestone of Tonto Group. Together, the systems described in this report compose the regional groundwater-flow system. Local to subregional flow systems in the sedimentary units of the overlying Permian section could provide transport pathways from the land surface to the regional flow system. Despite the potential importance of the local systems, the focus of this report is on the systems present in the lower Paleozoic section because all major springs in the Grand Canyon discharge from those units.

The most important hydrogeologic characteristics include system boundaries imposed by major tectonic structures, and the degree to which karstification influences the magnitude and direction of flow in each system. Important hydrologic dynamics include locations and rates of potential groundwater recharge, vertical pathways to the regional aquifer, and the locations, magnitude, geochemical signature, and hydrostratigraphic setting of groundwater discharge from springs. Unknown properties or conditions that represent the greatest uncertainties in our current understanding of the regional groundwater-flow system are identified for additional consideration.

Groundwater data are sparse owing to geographic remoteness and extreme depth to water throughout much of the study area. This paucity of information was diminished with the development of a structural contour map of the top and bottom surfaces of the regional aquifer, and a Soil-Water-Balance model that produces spatial distributions of rates of potential recharge. Investigation of the five groundwater-flow systems reveals important, though mostly qualitative, characteristics controlling the rates and directions of groundwater flow. Karstification has produced dissolution-enhanced conduit flow pathways to various degrees in each of the systems. Parts of each system exhibit relative structural uplift or downdropping of the hydrostratigraphic units of the regional aquifer, with some uplifted sections dipping inward toward the Grand Canyon and others dipping outward. The Kaibab groundwater system is archetypical of an uplifted, inward-dipping karst system, whereas the Blue Spring groundwater system and most of the Cataract groundwater system are representative instances of a downdropped or basin karst system. The Uinkaret-Kanab groundwater-flow system is structurally similar to the basin karst systems but karstification has not progressed to nearly the same degree. The Marble-Shinumo groundwater system does not fall cleanly into either category and its boundaries are the most uncertain of all the groundwater systems.

Introduction

The Grand Canyon of Arizona is a United Nations World Heritage Site (UNESCO, 2018), a visually stunning geologic wonder and an international tourist destination for millions of people. The Grand Canyon region is a home or sacred place of origin for many Native Americans and its cultural significance goes back thousands of years. The Colorado River, which occupies the Grand Canyon, is a primary source of drinking and irrigation water for millions of people in the United States and Mexico.

There are few perennial streams on the plateaus surrounding the Grand Canyon (fig. 1), so most users are dependent solely on deep wells or water extracted from springs that discharge deep in the canyon. For example, Grand Canyon village on the South Rim in Grand Canyon National Park is visited annually by more than 4 million tourists and is supplied entirely by water transported about 12 miles from Roaring Springs, which are situated north of the Colorado River near the bottom of a tributary canyon. Water at Supai village, which is home to the Havasupai Tribe, is supplied by a well drilled into alluvium in the floor of Cataract Canyon that draws water from Cataract Creek. That water originates from Havasu Springs at the bottom of the canyon 1.5 miles

[1]U.S. Geological Survey

[2]Self-employed, Boulder City, Nevada

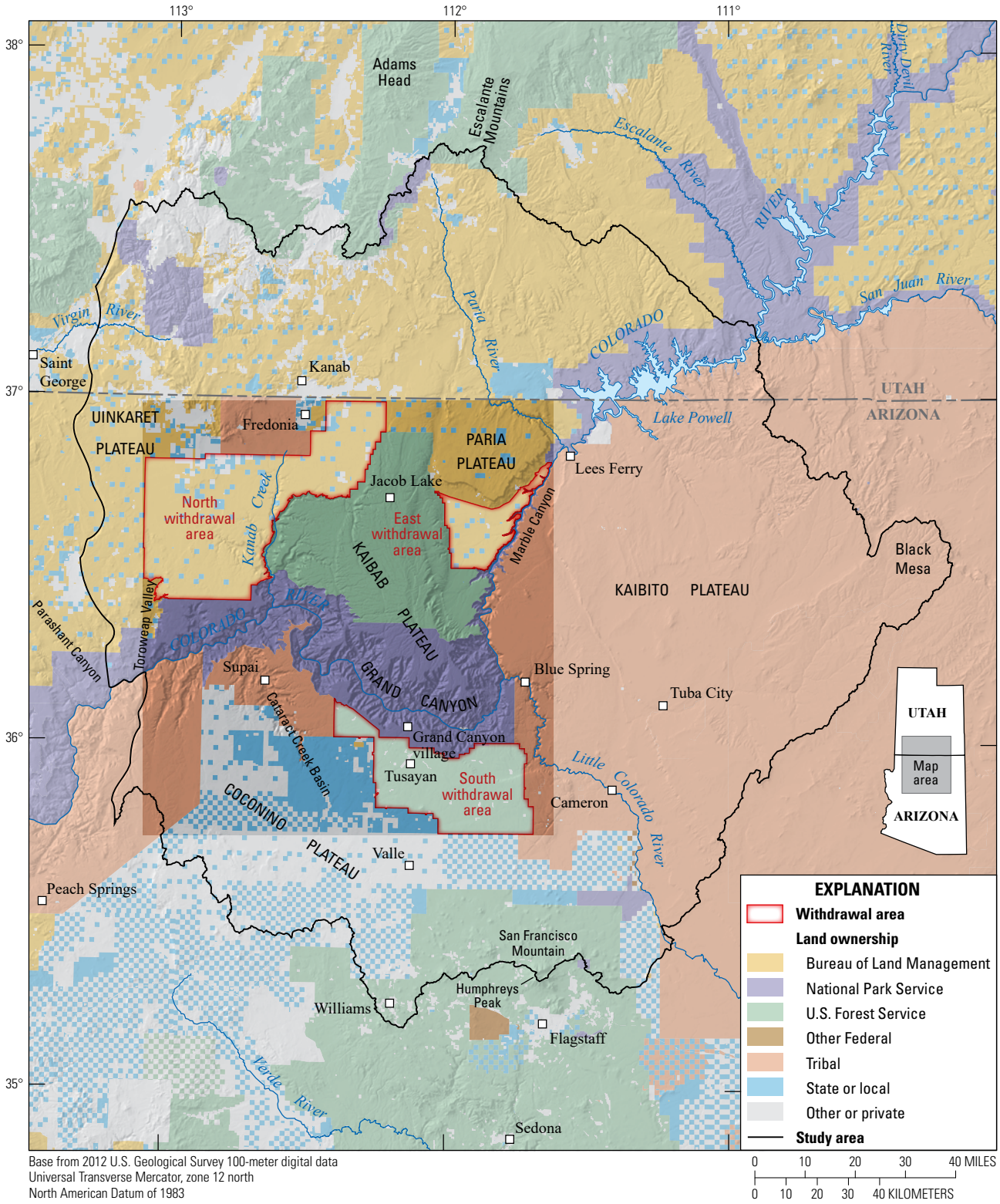

Figure 1. Map of geographic locations and land ownership in the study area in southern Utah and northern Arizona. Withdrawal areas represent Federal lands removed from availability for future mineral claims beginning July 2009.

upstream from the alluvial well. The town of Tusayan south of Grand Canyon is supplied by deep wells drilled into the regional aquifer, and the Jacob Lake community north of Grand Canyon is supplied by springs that discharge from a perched aquifer. In addition to human needs, critical habitats and ecosystems are present at springs throughout the study area (Alpine, 2010).

The groundwater system in the study area consists of both perched groundwater of limited spatial extent and the considerably deeper regional aquifer. Confining strata in structurally undeformed parts of the plateaus preclude downward circulation of recharge, thus creating the perched zones. The perched and regional systems are generally separated by 2,000 feet or more of unsaturated strata. Steeply dipping faults and fault zones complicate groundwater circulation patterns by serving as barriers to lateral flow perpendicular to them where there are large offsets of the water-bearing strata (fig. 2). In contrast, fracture and dissolution permeability within or parallel to the planes of the faults commonly provide high-capacity vertical and horizontal flow paths. This allows for downward circulation of groundwater from the perched groundwater zones to the deep regional aquifer and for very rapid flow of groundwater laterally from beneath distant recharge areas to karst springs deep in the canyons.

During extreme circumstances, groundwater discharging through the major karst springs localized along fault zones in the regional aquifer under the Kaibab Plateau tends to be sporadic wherein storm water recharge has been observed to transit tens of miles from recharge areas on the plateau to springs deep in the canyon in a matter of a couple of days (Huntoon, 2000; Jones and others, 2018). This contrasts with groundwater sampled from small springs from the undeformed interior parts of the regional aquifer under the adjacent Kanab Plateau, which exhibit resident times likely measured in thousands of years (Beisner and others, 2017b).

The plateaus adjacent to the Grand Canyon hosts some of the highest-grade uranium ore deposits in the United States (Alpine, 2010). Uranium ore was discovered in the Lost Orphan Mine on the South Rim of the Grand Canyon in 1951. This led to widespread exploration for ore bodies in the Grand Canyon region in the late 1970s as prices for uranium increased; however, exploration declined as prices decreased in the early 1990s. A brief uranium price spike in 2007 renewed interest, leading to thousands of new mining claims in the Grand Canyon region by 2009 (Department of the Interior, 2012). On July 21, 2009, U.S. Secretary of the Interior Ken Salazar proposed a 2-year withdrawal of approximately 1 million acres of Federal lands in the Grand Canyon region from future mineral entry; this withdrawal included three areas in the region (fig. 1). In 2012, Secretary Salazar signed a Record of Decision (ROD) to withdraw these same Federal lands from new mineral activity, which include new claims, for the next 20 years, subject to valid existing rights (fig. 1).

A key factor leading to the ROD was the limited amount of scientific data and resulting uncertainty on potential effects of uranium mining activities on the cultural, biological, and hydrological resources in the area. Potential vectors for exposure from uranium and associated elements include wind-borne dusts, surface-water runoff, groundwater flow, soil, sediment, and food-chain pathways. The U.S. Geological Survey (USGS) is tasked with addressing the data gaps underlying the uncertainty of the potential effects of uranium exploration and mining on people, ecology, and water resources within the Grand Canyon watershed.

Purpose and Scope

This report describes one of several USGS studies designed to address the scientific data gaps underlying the uncertainty of potential effects to groundwater resources owing to uranium mining in the Grand Canyon watershed. It comprises a summary of regional hydrogeologic characteristics followed by a series of conceptual models describing each of the groundwater-flow systems that discharge to the Grand Canyon. A summary of the regional hydrogeologic framework provides a common reference from which to describe and compare the characteristics of the individual groundwater systems.

The conceptual model for each system details what is currently known or hypothesized about hydrologic conditions and hydrogeologic characteristics of that system, particularly those that influence the rate and direction of groundwater flow. Locations and long-term mean rates of potential groundwater recharge are simulated based on spatially distributed temperature, precipitation, and land-cover data. Locations and approximate rates of groundwater discharge are mapped from previous reports. Major tectonic structures are identified as system boundaries and (or) conduits for vertical and horizontal movement of water. The degree of karstification and conduit network development varies by system and strongly influences groundwater residence time and direction of flow. Unknown hydrogeologic aquifer characteristics or hydrologic conditions are noted that represent the greatest uncertainties in our current understanding of the regional groundwater-flow system.

Description of Study Area

The study area is defined to include all groundwater basins that discharge to the Grand Canyon that underlie at least one of the uranium withdrawal areas specified in the 2012 ROD (Department of the Interior, 2012). HUC-8 (hydrologic unit code) level drainages representing medium-sized river basins are used as a convenient proxy for the aerial extent of underlying groundwater systems but are not expected to be perfect representations. The geographic limits of the study area are the Hurricane Fault to the west, the Escalante Mountains to the north, Black Mesa to the east, and the San Francisco Mountain (San Francisco Peaks) to the south (fig. 1).

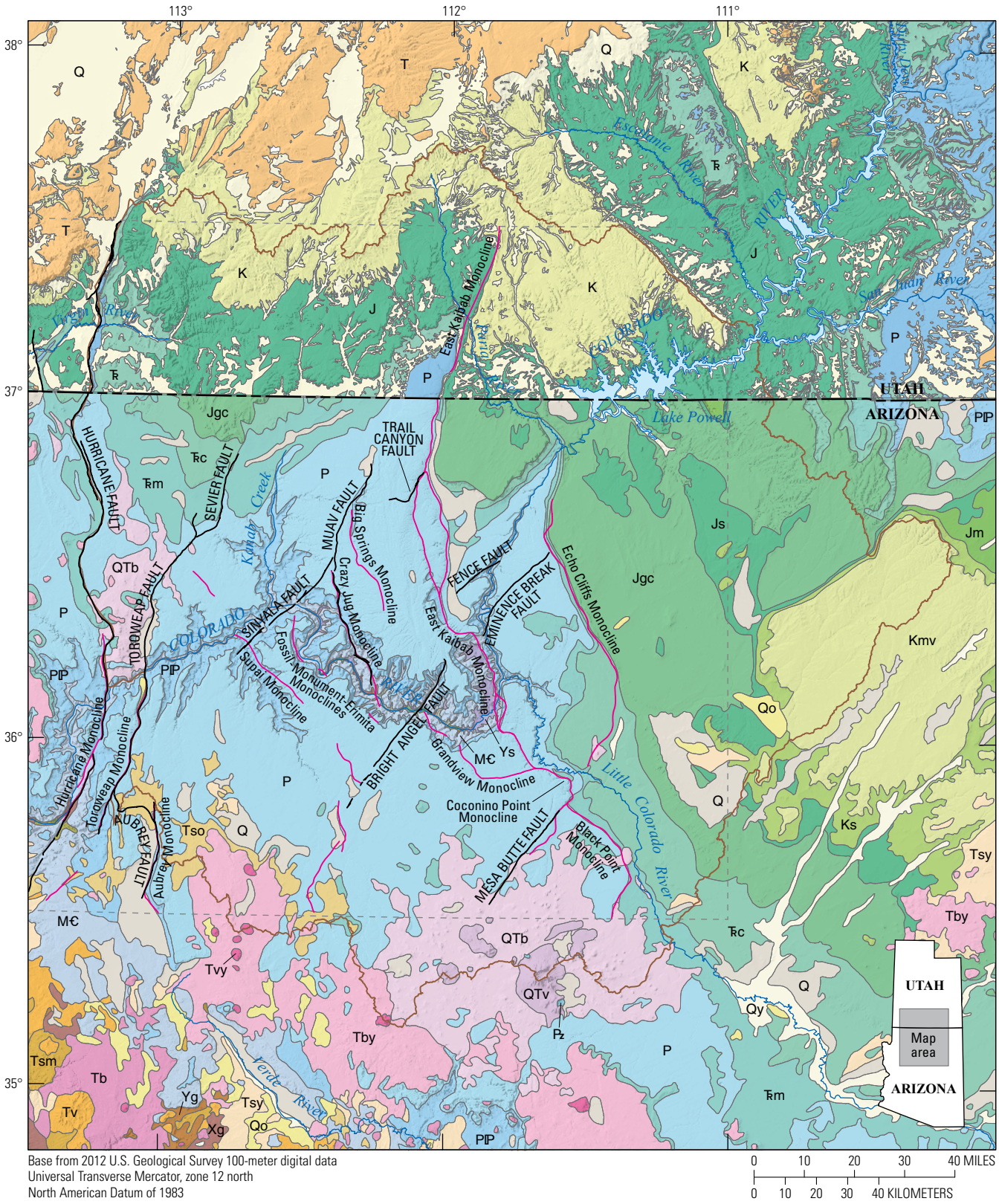

Base from 2012 U.S. Geological Survey 100-meter digital data
Universal Transverse Mercator, zone 12 north
North American Datum of 1983

0 10 20 30 40 MILES
0 10 20 30 40 KILOMETERS

Figure 2. Map of surface geology and structural features of the study area in southern Utah and northern Arizona, adapted from Richard and others (2000) and Hintze and others (2000). Select regional linear structural features are modified from Billingsley and Hampton (2000), Billingsley and Workman (2000), Billingsley and Wellmeyer (2003), Billingsley and others (2006a, b, 2007, 2008, 2012), and Billingsley and Priest (2013).

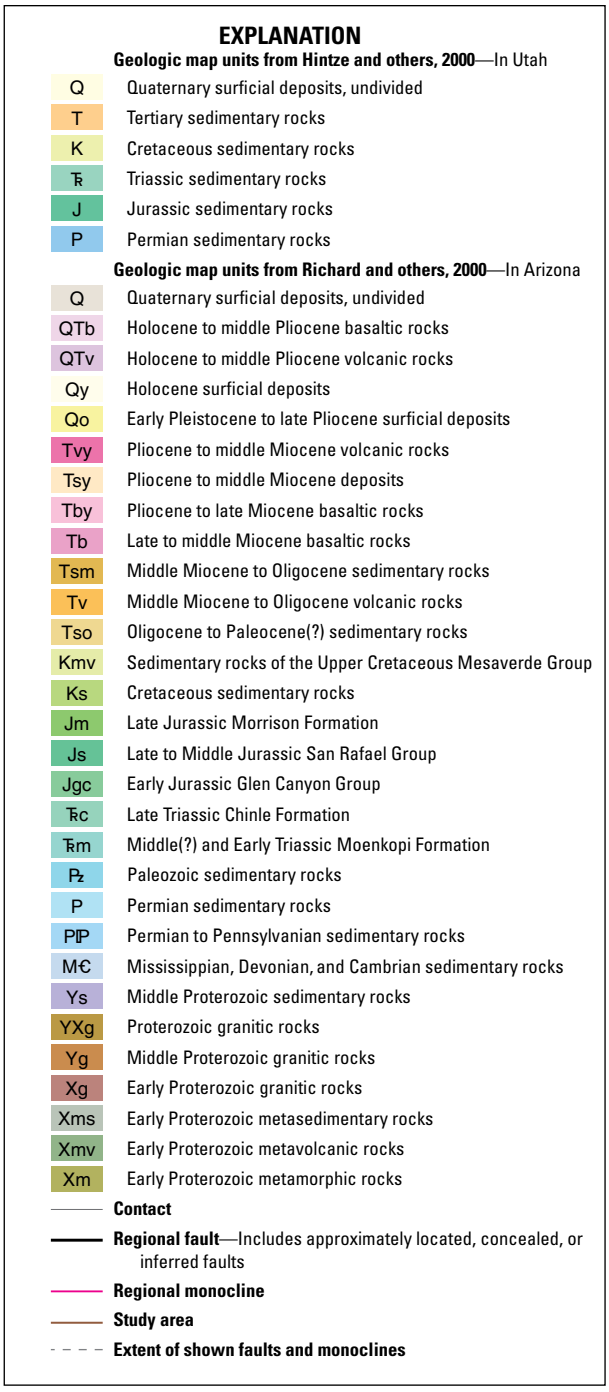

The topography within the study area is classic for the western Colorado Plateau; that is, broad plateaus dissected by the deeply incised canyons of the westward-flowing Colorado River. The plateaus consist generally of flat to gently dipping thick sequences of Paleozoic and Mesozoic sedimentary rocks punctuated by northerly trending, widely spaced, east-dipping Laramide monoclines and late Tertiary fault zones (Huntoon and others, 2003) (fig. 2).

Land surface elevations on the plateaus generally range between 5,000 and 6,000 feet, except on the Kaibab Plateau where elevations exceed 9,000 feet. The north and south edges of the study area reach similar elevations in the Escalante Mountains (Adams Head is 10,426 feet) and in the San Francisco Mountain (Humphreys Peak is 12,633 feet). The surface of the Colorado River decreases from 3,080 feet at Lees Ferry to 1,200 feet at the mouth of Spencer Creek where Lake Mead backs up into the Grand Canyon, 40 miles upstream from the mouth of the canyon (fig. 1).

Climate in the study area varies greatly with elevation. The lower elevation plateaus are hot and arid with mean summer highs exceeding 90 degrees Fahrenheit (°F) and annual rainfall of less than 10 inches (Western Regional Climate Center, 2020). The Kaibab Plateau and the upper elevations of the Escalante Mountains and San Francisco Mountain are much cooler and wetter, with an average summer high between 70 and 80 °F and annual precipitation greater than 30 inches (Western Regional Climate Center, 2020). Shrub and grassland accounts for the vast majority of land cover on the lower plateaus. Higher elevations are dominated by evergreen forests (Multi-Resolution Land Characteristics Consortium, 2020). The plateaus surrounding the Grand Canyon are characterized by a near total absence of perennial streams. This occurs primarily because the potential evaporation rate is much greater than the available precipitation (fig. 3). Only a small fraction of precipitation is available to eventually recharge the aquifer systems in much of the region.

Population centers are sparse and lightly populated (fig. 1). Tusayan (population 587), Valle (population 238), and Grand Canyon village (population 2,004) on the Coconino Plateau and Supai village (population 208) in Havasu Canyon include most of the people living within the study area south of the Grand Canyon. Fredonia (population 1,300) and Kanab (population 4,698), which are located on either side of the Arizona-Utah border, are the nearest towns north of the Grand Canyon (U.S. Census Bureau, 2020).

Previous Investigations

In 1869, John Wesley Powell led the first U.S. Government sponsored exploration of the Colorado River and its tributaries. Over the 150 years since, many scientists have produced works to describe and explain the natural wonders of the Grand Canyon. Chief among them is Edwin D. McKee, who produced books and reports describing the depositional environment of each of the Paleozoic units exposed in the canyon. His book Ancient Landscapes of the Grand Canyon Region was published in 1931 and reprinted in 30 new editions throughout the remainder of his life (Spamer, 1999). From the mid-20th century to present, geologic investigations have become more diverse and specialized. Highly detailed geologic maps of the Grand Canyon began to be published in the 1970s (for example, Huntoon and others, 1976). Between 2000 and 2013, the USGS produced a series of nine 30′ × 60′ quadrangle geologic maps encompassing most of the study area (appendix 1). Timmons and Karlstrom (2012) produced detailed geologic maps and cross sections of the eastern Grand Canyon.

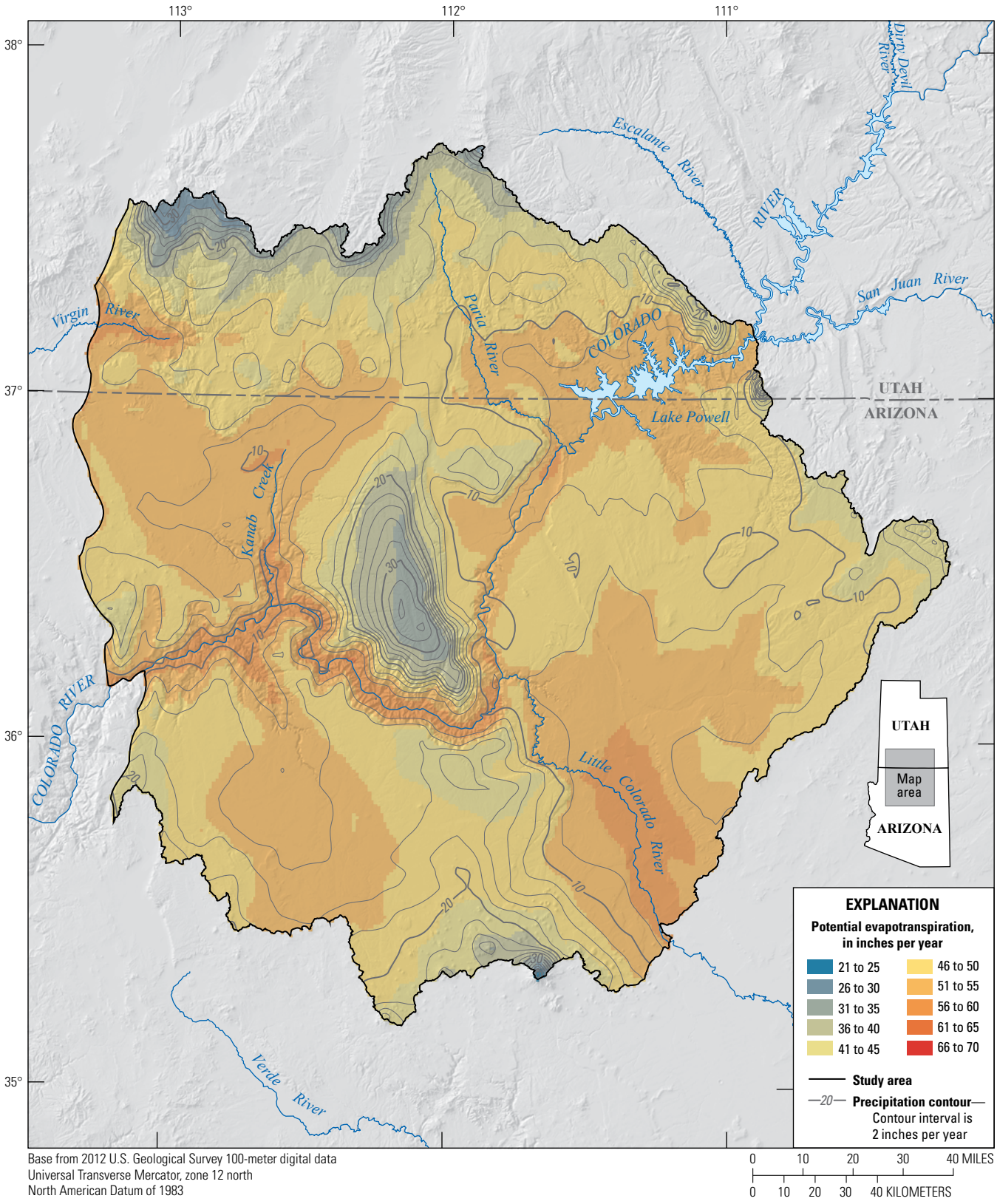

Figure 3. Map of precipitation and potential evapotranspiration of the study area. Potential evapotranspiration is represented by the color scale and precipitation is represented by the contour lines. Modified from PRISM Climate Group, 2017.

LaRue (1925) provided the first collection of detailed hydrologic data from the Grand Canyon as part of a survey examining the potential for hydroelectric power generation below the junction of the Green and Colorado Rivers. Between 1950 and 1965, the USGS carried out a series of field surveys collecting spring discharge and water quality data, culminating in a summary report by Johnson and Sanderson (1968). In the same year, McGavock (1968) published an extensive dataset collected from wells and springs on the Coconino Plateau.

Subsequent studies focused more on the availability and flow of groundwater. Metzger (1961) investigated the availability of water supplies along the South Rim of the Grand Canyon for use by the Grand Canyon National Park. Twenter (1962) outlined potential target areas for groundwater development on the Hualapai Indian Reservation. Cooley (1976) examined the presence and movement of groundwater toward the Blue Spring groundwater system of the Little Colorado River. Huntoon conducted hydrogeologic surveys on the Kaibab Plateau (Huntoon, 1974) and Hualapai Plateau (Huntoon, 1977). Huntoon also produced a paleo-reconstruction of the regional groundwater circulation that led to the uranium mineralization in breccia pipes in the region (Huntoon, 1996) and qualitatively contrasted the karstic permeability within the confined and unconfined aquifers that drained to the Grand Canyon (Huntoon, 2000). His unpublished manuscript dating from 1982 on the planimetric extent of the regional groundwater-flow systems that discharge to the Grand Canyon (Peter W. Huntoon, written commun., 2017) provided additional information for this report.

Several regional hydrogeologic investigations within the study area have been carried out since the late 1990s. The Kaibab National Forest commissioned an environmental impact statement for proposed growth of Tusayan (Kaibab National Forest, 1999). That report included a summary of hydrogeologic conditions in the area and potential effects of proposed groundwater withdrawals on the Coconino Plateau; the assessment was in part determined through simulations of a numerical groundwater-flow model (Errol L. Montgomery and Associates, 1999). The USGS published a report on the hydrogeology of the regional aquifer in and near the Little Colorado River Basin (Hart and others, 2002). A later report studied the hydrogeology of the regional aquifer beneath the Coconino Plateau (Bills and others, 2007). Information from these reports contributed to the development of the Northern Arizona Regional Groundwater Flow Model (Pool and others, 2011). The Utah Geological Survey investigated regional groundwater flow in the Virgin River Basin of southern Utah and northern Arizona (Inkenbrandt and others, 2013).

Recent studies include environmental site assessments and geochemical investigations. The USGS published a Scientific Investigations Report (Alpine, 2010) containing the latest comprehensive site characterization of mined breccia pipe uranium deposits in northern Arizona, including information on geological, hydrological, and biological systems as they relate to the mineral withdrawal areas. Crossey and others (2006) showed the influence of deeply derived fluids on spring geochemistry. Beisner and others (2017b) published results of a geochemical survey of springs north of the Grand Canyon that provide an understanding of what constitutes naturally occurring background concentrations of uranium and associated trace elements in the region's groundwater. The USGS is planning to conduct a similar survey of springs on the south side of the Grand Canyon, previously carried out by Monroe in 2001 (Monroe and others, 2004). The USGS is also planning to investigate the flux of uranium and associated trace elements in the Colorado River and major tributaries (USGS, 2014).

Methods of Investigation

Conceptual models are useful to summarize what is known and deduced about the character of the groundwater-flow systems in a study area. The qualitative assembly and analysis of relevant field data and system characteristics provide a foundation upon which mathematical and (or) numerical simulations can be formulated. Important components of a conceptual model include the identification and characteristics of system boundaries, delineation of hydrostratigraphy and aquifer properties, deduction of flow directions between recharge and discharge areas, and assembly of a gross regional groundwater budget (Anderson and others, 2015). The conceptual models presented in this report were developed through analysis of previously published investigations and datasets, supplemented by new maps illustrating the structural elevation of the base of the regional aquifer and simulated potential recharge rates. Special attention is given to the location and character of boundary conditions. Ambiguous system boundaries are identified and explained.

Regional Aquifer Structural Contour Map

The top and bottom surface elevations of the regional aquifer were spatially interpolated from point data using Esri ArcMap software. The method of generating the surfaces is similar to that presented by Inkenbrandt and others (2013). Data sources consist of (1) 30′ × 60′ geologic maps intersected with a 10-meter resolution digital elevation model (DEM) where contacts of the bottom and (or) top surfaces of the regional aquifer are exposed at the surface, (2) well logs from State agencies that include information on depth to formation, and (3) thematic cross sections that are included with 30′ × 60′ geologic maps of the area. Description of map construction and data used for the interpolations are itemized, and sources are referenced in appendix 1 and table 1.1 of this report.

Potential Recharge Model

A Soil-Water-Balance (SWB) model (Westenbroek and others, 2010) was created to estimate long-term average rates and spatial distributions of potential recharge. Potential recharge is defined as water available to infiltrate deep into the subsurface after accounting for surface and near-surface processes, such as precipitation, runoff, and evapotranspiration. Simulating these processes in the SWB model is dependent on property variables describing land use and soil type, such as curve number, root zone depth, soil water capacity, and soil moisture retention. These properties are supplied to SWB as spatially gridded data that influence simulated rates of infiltration to the soil and simulated volumes of water stored in the soil over time.

In this application, the SWB model estimates potential evaporation rates on a daily time step using the Hargreaves-Samani method (Hargreaves and Samani, 1985) and spatially gridded daily temperature data. Potential evaporation serves as an upper bound to simulate actual evapotranspiration. In both the real physical system and modeled system, evapotranspiration in this case is generally limited by water availability in the root zone of the soil.

Gridded daily precipitation data supplies water input to the SWB model. Temperature data determines whether the precipitation is assumed to be immediately available for routing (in the form of rain) or stored temporarily above the surface (in the form of snow). Soil and land-cover properties determine the amount of precipitation or snow melt that can infiltrate versus that classified as overland runoff. Infiltrated water is added to a running balance of water stored in the unsaturated root zone of each model cell. Likewise, simulated evapotranspiration removes water from the balance. When water content exceeds the root zone capacity, excess water is assumed to move downward as potential recharge to the aquifer.

The time period of the SWB model simulation was 1981–2016, determined by availability of gridded daily temperature and precipitation data (PRISM Climate Group, 2017). Land cover data from Multi-Resolution Land Characteristics (MRLC) and soil data from the U.S. Department of Agriculture (USDA) were processed for model input using ArcMap and Python tools. The model grid was set up using 1,000-meter by 1,000-meter cells. This cell size was chosen to balance the goals of (1) adequately representing the heterogeneity in soil and land cover, and (2) obtaining reasonably short model run times.

Model output is presented in terms of mean annual rates calculated in each model cell over the 36-year simulation period. This level of detail is useful for identifying locations and relative magnitude of potential recharge within each groundwater system. Simulated values of potential recharge should not be considered accurate representations of actual recharge. Model inputs, particularly soil and land cover properties, are highly uncertain and in some cases purely speculative. A rudimentary sensitivity analysis was performed to help bound the results by running the simulation with higher and lower values of the most important system properties.

SWB model results are described as potential results to emphasize the high degree of uncertainty inherent in the modeling process. The SWB model is a mass-balance calculation of water at the land surface and within the root zone, but the regional aquifer is as much as 3,000 feet or more below the surface. Soil and land cover properties, such as available water capacity and root zone depth, influence model results but are not precisely known at the model scale. Limitations notwithstanding, the model is still useful in some important ways. It serves as a repository of available climatic and land use data of the study area, and it allows for comparative analysis of the factors determining relative rates of recharge within different subregions of the study area. Input datasets used to execute the model are illustrated and data sources cited in appendix 2 of this report. A model archive containing the SWB input and output datasets is available in Knight and Jones (2022).

Hydrogeologic Framework

Investigations of groundwater flow in the Grand Canyon region typically consider two major aquifer systems: the C- and R-aquifers (fig. 4). They are described here for clarity and consistency with previous reports, followed by a definition of an alternative classification scheme that is more useful to the hydrogeologic setting of the Grand Canyon.

C-Aquifer

The C-aquifer is defined as the saturated parts of the Kaibab Formation, Toroweap Formation, and the Coconino Sandstone, all of Permian age (Cooley and others, 1969). These units lie above the Permian Hermit Formation and the Pennsylvanian to Permian Supai Group, which, unless faulted, serve as a very effective confining intervals that prevent downward leakage from the C-aquifer (Hart and others, 2002). The rocks composing the C-aquifer generally are elevated and well-drained by canyons or extensional fault zones, and the saturated zones are spatially discontinuous and unconfined (Bills and others, 2007). Reported depths to water in the C-aquifer range from less than 300 feet to more than 1,500 feet. Saturated thickness is greatest east of the Mesa Butte Fault (fig. 2) and reaches an extreme of 2,200 feet south of Flagstaff where the Permian section is thickest (Hart and others, 2002).

Generally, the intercrystalline permeabilities associated with the carbonate rocks that form most of the Kaibab and Toroweap Formations are negligible, but secondary permeability in the form of dissolution-widened joints and fractures coupled with a well-developed epikarst allows for recharge (label 1 in fig. 4). The interstitial permeability found in the underlying Coconino Sandstone, although modest, is the largest found in any of the clastic units in the Grand Canyon Paleozoic section (McKee and Resser, 1945) and accounts for most of the storage that is present in the C-aquifer (label 2 in fig. 4). The result is that perched saturated zones develop

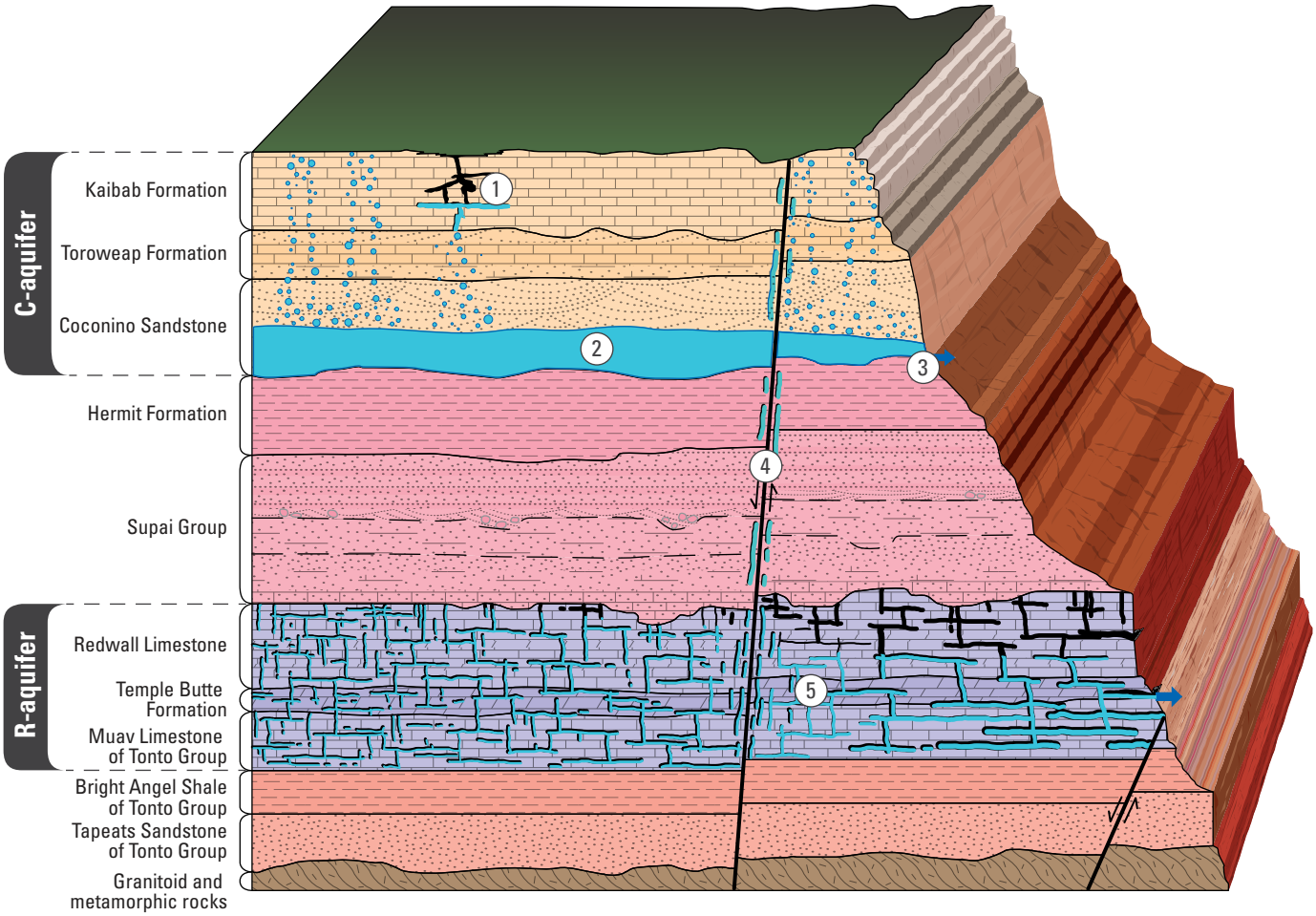

Figure 4. Conceptual block diagram of hydrogeologic units. (1) Occurrence of recharge to C-aquifer can be widely distributed in space but is likely focused around areas of highly developed epikarst. (2) The majority of groundwater storage in the C-aquifer occurs in the Coconino Sandstone overlying the Hermit Formation confining unit. (3) Discharge from the C-aquifer occurs at springs exposed in canyon walls, or (4) as downward flow to the R-aquifer where substantial fracturing breaks the confining interval. (5) Groundwater flow in the R-aquifer occurs via interconnected voids that have dissolved and widened over geologic time.

above the confining strata of the underlying Hermit Formation and Supai Group. Groundwater then flows laterally to seeps at the base of the Coconino Sandstone along canyon walls (label 3 in fig. 4) or to extensional fault zones that allow the water to descend vertically and recharge the underlying R-aquifer (label 4 in fig. 4). The groundwater going into transient storage within the C-aquifer can achieve long residence times under the lower, poorly drained plateaus (Bills and others, 2007).

Wholesale dissolution of gypsum units in the Toroweap Formation has resulted in classic karst landscape with numerous sinkholes on the elevated Kaibab Plateau (fig. 1) (Huntoon, 1974). Similar populations of sinkholes are present on the Coconino Plateau where thick gypsum deposits and carbonate layers are present in the Kaibab Formation between Grand Canyon village and Supai village. Consequently, the highly organized karstic permeability within the epikarst developed on the Kaibab Formation, as well as the underlying karst networks in the gypsum layers, provide well-integrated conduits that allow for rapid circulation of recharge from storms and snow melt to nearby extensional fault zones.

Active extensional faulting is concentrated in three vicinities within the Grand Canyon region; specifically, (1) areas centered around the Blue Spring along the Little Colorado River, (2) in Cataract Creek Basin upstream from Supai village, and (3) along the Hurricane Fault surrounding the mouth of Parashant Canyon (figs. 1 and 2). Extensional rifting of the Paleozoic section has progressed sufficiently in these areas to the extent that the plateau surface is depressed and the rocks are riven with normal faults (Huntoon and others, 2003). Many of these faults and associated subsidiary fractures are highly permeable and serve as high-capacity conduits that allow groundwater circulation pathways from the C- to underlying R-aquifer (label 4 in fig. 4). The vertical permeabilities in these extensional fault zones can equal that in well-developed karst (Caine and others, 1996). An excellent example of this is found in Cataract Creek Basin, 20 miles upstream from Supai village.

Sinkholes are present along normal faults that are crossed by the ephemeral Cataract Creek at the level of the Kaibab Formation (Billingsley and others, 2006b). These features host swallow holes that can consume substantial percentages of flood flows that move down the channel. The water descends into and circulates through karst networks developed in the R-aquifer, ultimately discharging at Havasu Springs.

R-Aquifer

The R-aquifer is defined as the saturated parts of the lower Paleozoic carbonate rocks that are present below the Supai Group throughout the Colorado Plateau (fig. 4) (Cooley and others, 1969). Those strata in the Grand Canyon region include the Mississippian Redwall Limestone, Devonian Temple Butte Formation, undivided Cambrian carbonates, and the Cambrian Muav Limestone of Tonto Group (hereafter, Muav Limestone) (fig. 4) (Cooley, 1976).

The Redwall Limestone is named for the massive vertical cliffs forming red iron-stained walls in the Grand Canyon. The unit is composed almost entirely of highly soluble calcium and magnesium carbonate minerals. It thickens steadily and uniformly to the northwest, from a thin edge against the Defiance Uplift in western New Mexico to more than 750 feet thick in southern Utah (McKee, 1960). The Temple Butte Formation is a sandy dolomite containing thin sandstone and limestone beds. In the eastern Grand Canyon, it appears as thin, discontinuous lenses filling paleochannels no more than 100 feet thick in the upper surface of the Cambrian Muav Limestone. It gradually thickens to the west, reaching a maximum thickness of 650 feet west of the mouth of Grand Canyon (Beus, 2003). The Muav Limestone, as defined by McKee and Resser (1945), consists of the carbonate units in the Tonto Group. The base of the Muav Limestone is complex; the limestones that form the Muav Limestone intertongue with the underlying Bright Angel Shale of Tonto Group (hereafter, Bright Angel Shale) (Leighty, 2021).

For hydrologic purposes, the base of the R-aquifer in the eastern Grand Canyon region is defined as the base of the Peach Springs Canyon Member of the Muav Limestone because all of the major karst springs that discharge from the R-aquifer are present at or above the base of that member (Johnson and Sanderson, 1968). Westward of the Toroweap Valley (fig. 1), the largest springs are present at the base of the Rampart Cave Member of the Muav Limestone, some 200 feet below the Peach Springs Canyon Member (Twenter, 1962). Therefore, it is convenient to define the base of the aquifer as the base of the Rampart Cave Member in the western Grand Canyon region.

The structural contours present in figures 5 and 6 are spatially interpolated estimates of elevations at the top of the Redwall Limestone and base of the Muav Limestone. These units crop out on the Hualapai Plateau and along the west and south edges of the Colorado Plateau outside of the study area (Richard and others, 2000). They are continuously exposed in the canyon walls from Marble Canyon to the mouth of the Grand Canyon. Average thickness between the top of the Redwall Limestone and the base of the Muav Limestone in the study area is 1,000 feet (Bills and others, 2007).

Active groundwater circulation in the study area takes place at great depth in the R-aquifer, in many places more than 3,000 feet below land surface. Depth to the top of the Redwall Limestone (fig. 7) increases greatly to the north and east owing to the regional dip of the rocks and the presence of progressively thickening overlying Mesozoic section (fig. 2).

The R-aquifer is a karst aquifer; that is, the permeability in the aquifer is the result of dissolution of the host rock into interconnected voids and caves that have developed over geologic time (label 5 in fig. 4). In contrast, the intercrystalline permeabilities of the carbonate rocks that compose the aquifer are negligible. Hydraulic gradients within karst aquifers dictate the development of the permeability architecture, which is hierarchical and organized in a down-gradient direction, much like a surface stream network. The following is a general classification of the groundwater flow regimes found in the R-aquifer in the Grand Canyon region. Details of the individual systems follow.

Hydrogeologic Regimes of the Grand Canyon

Huntoon (2000) defined two end members for the karst systems found in the Grand Canyon region: basin karst and uplift karst. The distinguishing characteristic is the structural elevation of the base of the aquifer relative to the Colorado River, which serves as the ultimate sink for water within these systems.

The basin karst systems are confined wherein hydraulic gradients are small and permeabilities are large owing to widespread development of two-dimensional maze caves preferentially dissolved parallel to stratigraphic bedding. The passageways dissolved through the rocks are localized predominantly on joints and fractures. The springs emerge from the top of the R-aquifer where it is exposed in the floors of canyons, where the top of the R-aquifer is exposed, or where it is present a short distance below the surface. The water discharges under artesian pressure from the systems, sometimes upward through fractures that penetrate overlying confining strata.

The water from these basin karst systems exhibits minimal fluctuation in discharge rates and lengthy resident times characterized by warmer temperatures and elevated dissolved solids. The basin karst systems are characterized by pulse-through hydraulics; that is, discharge rates vary in accord with seasonal or longer climatic recharge pulses in distant recharge areas yet the actual water that discharges from the springs has been in transit for years to centuries (Huntoon, 2000).

Uplift karst systems are simpler drain systems than basin karst systems, they exhibit steep hydraulic gradients between the recharge areas and springs in the walls of the

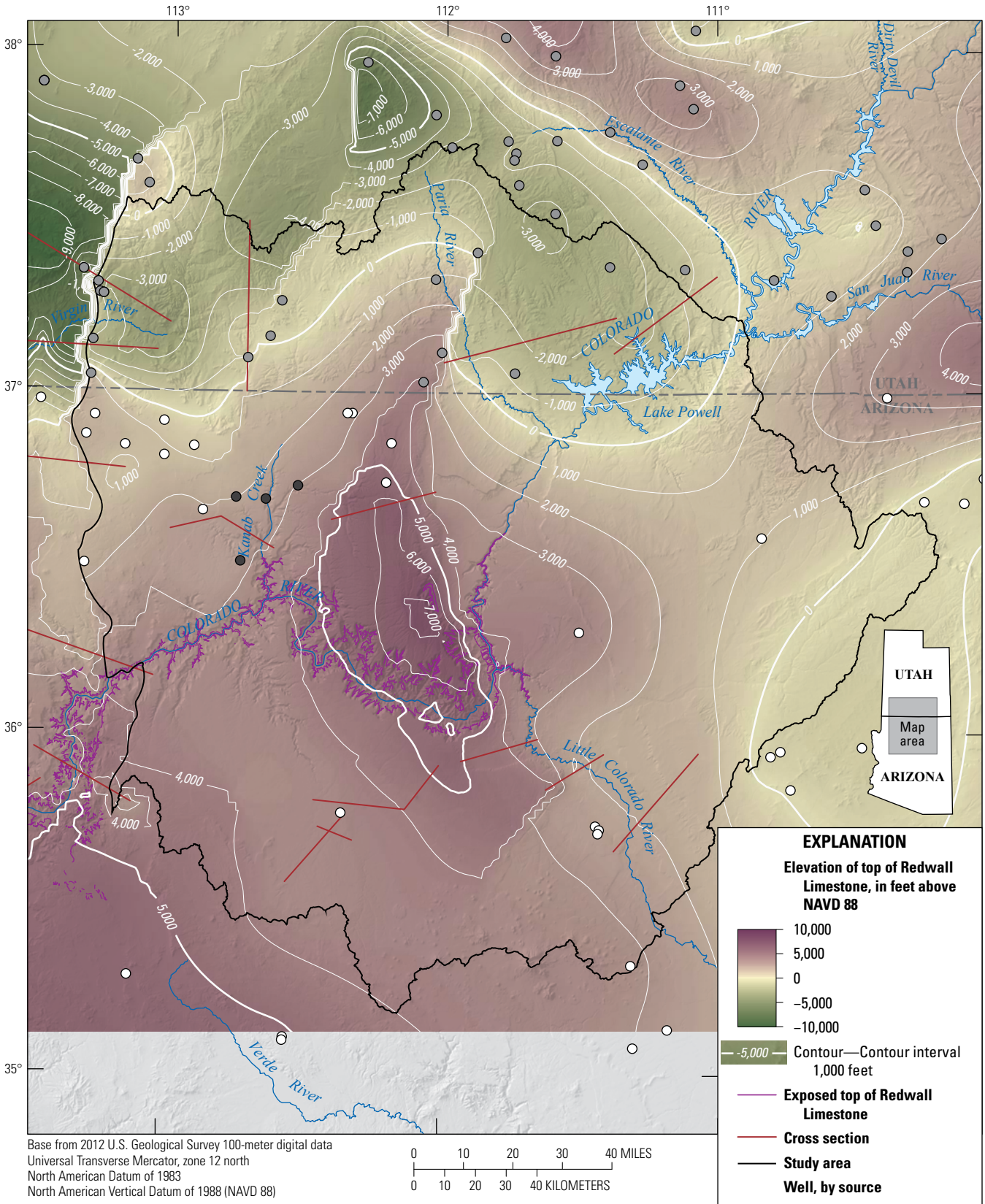

Figure 5. Map of structural contours of the top surface elevation of the Redwall Limestone, in feet. Structural contours are interpolated from data provided by Arizona Department of Water Resources, Arizona Oil and Gas Conservation Commission, and Utah Department of Natural Resources Division of Oil, Gas and Mining. See appendix 1 for summary of and access to data used.

canyon. Dissolution permeability, commonly in the form of linear passageways, tends to be extremely anisotropic with the maximum permeability oriented parallel to the hydraulic gradient. The caves tend to localize along extensional fault zones or fractures parallel to extensional faults within the carbonate rocks because those cavities commonly provided the initial integrated flow pathways through the host rocks. The caves can also develop along favorably oriented joints parallel to the hydraulic gradient.

Uplift karst systems are unconfined, possess minimal groundwater storage, and exhibit flashy and highly variable seasonal discharge rates. They exhibit flow-through hydraulics; that is, water discharging from the springs consists largely of the water that recently entered the uplift karst system in the recharge area. Consequently, both the temperatures and total dissolved solids in the spring waters are low (Huntoon, 2000).

There is one caveat to describing the uplifted karst systems. Groundwater flow paths pass through the rocks that compose the overlying C-aquifer where those rocks are present (Huntoon, 1974). This is the case throughout the Grand Canyon region, except for the Hualapai Plateau

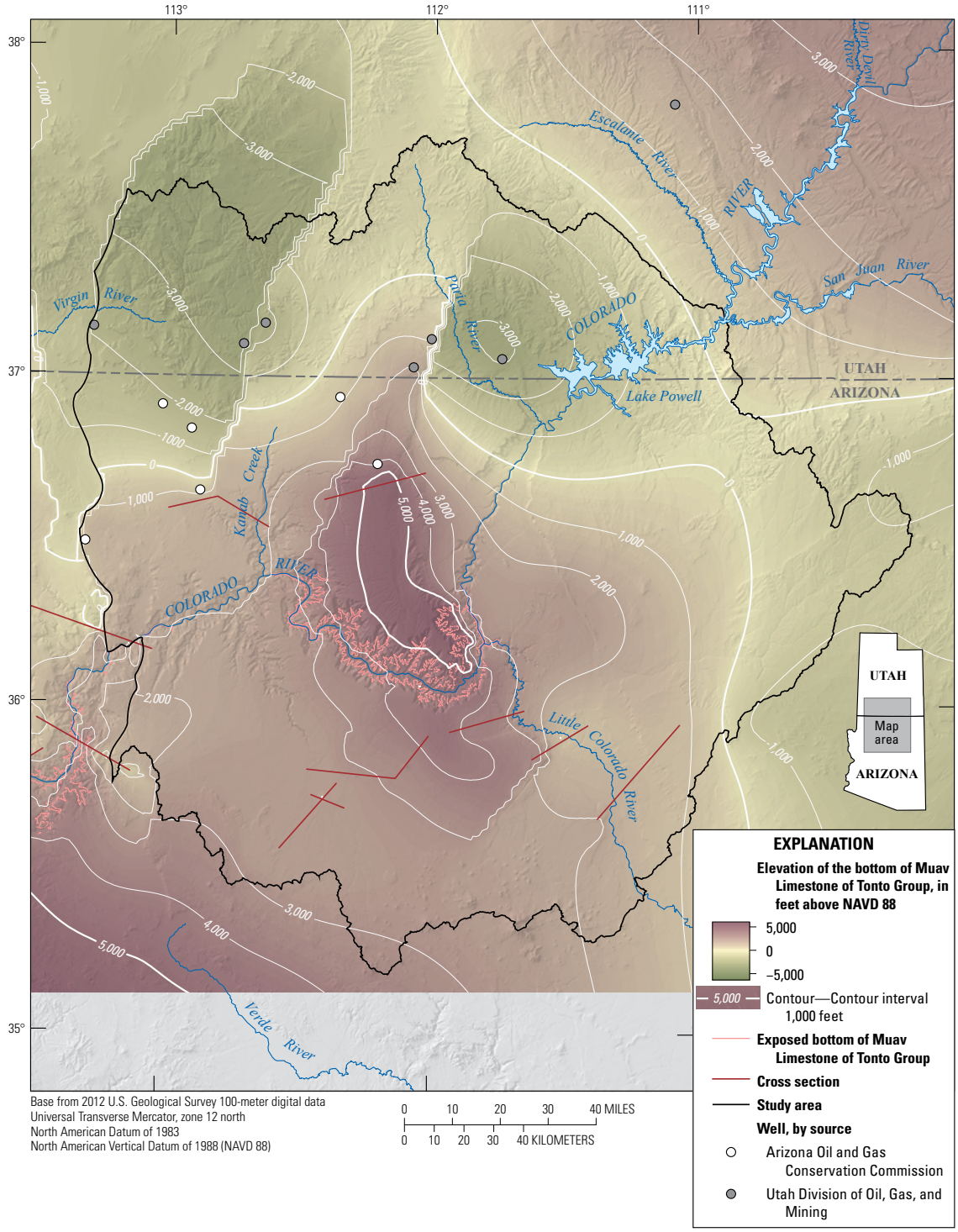

Figure 6. Map of structural contours of the bottom surface elevation of the Muav Limestone of Tonto Group, in feet. Structural contours are interpolated from data provided by Arizona Oil and Gas Conservation Commission, and Utah Department of Natural Resources Division of Oil, Gas and Mining. See appendix 1 for summary of and access to data used. Note: Lack of data west of Hurricane Fault and north of the Arizona-Utah border leads to high uncertainty in the interpolated bottom surface elevation of the Muav Limestone of Tonto Group, which can be in conflict with the interpolated top surface elevation of the Redwall Limestone.

just west of the study area, where the rocks that form the C-aquifer have been removed by erosion. Much of the water entering these systems passes quickly through the fault zones that hydraulically link the C- and R-aquifers as well as through the epikarst and conduits dissolved in the rocks of the C-aquifer. However, some recharge goes into transient storage in the Permian section, particularly in the Coconino Sandstone (Jones and others, 2018). Hydraulic gradients develop beneath the areas of recharge toward fractures that allow water to descend to the R-aquifer. Those delayed waters form the base flows from the uplifted karst systems and tend to moderate the discharge rates from the springs and lengthen the recessions of the pulsed recharge events. Larger systems impose greater moderation on discharge response to recharge events and exhibit longer periods of recession from peak discharge.

The dip of the strata adjacent to the Grand Canyon strongly influences the size of the springs that discharge from both the uplifted C- and R-aquifer systems. Seeps and springs are small or absent in domains where the strata dip away from the canyon, whereas they can be very large where the strata dip toward the canyon.

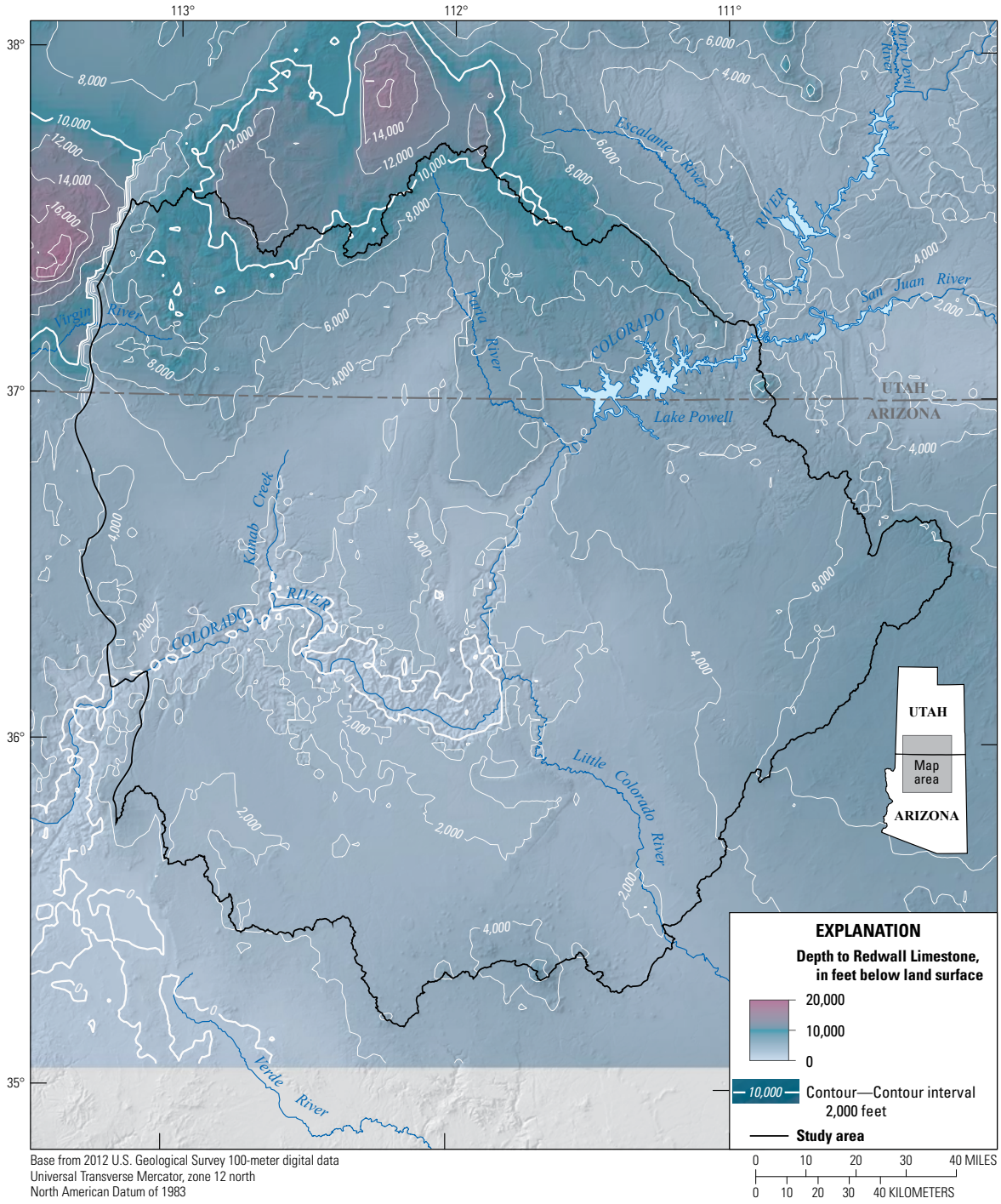

Figure 7. Map of depth to the top surface of Redwall Limestone, in feet below land surface, in the Grand Canyon region.

This association exists because the structural dip of the strata strongly influences the hydraulic gradients within unconfined uplift karst systems. A highly asymmetric groundwater mound develops above the confining layer at the base of the aquifer where the strata dip away from canyons (fig. 8). The crest of the mound, which constitutes a groundwater divide, parallels the canyon wall where the setback is a function of the thickness of the saturated zone, the dip and permeability of the rocks, and the rate of recharge. The setback can be hundreds to thousands of feet. The water between the exposed outcrop and the divide emerges from seeps and small springs on the canyon wall. However, the water beyond the divide flows away from the canyon. The setback of this mound is transient. During periods of drought, the saturated thickness decreases, so the crest of the mound moves closer to the canyon wall, and spring flows decrease.

The identical phenomenon occurs within the planes of permeable fracture and fault zones in the R-aquifer that intersect the canyon wall in domains where the rocks forming the aquifer dip away from the canyon. Indian Garden Spring (station 360439112073901; USGS 2018b), a spring that discharges from the Bright Angel Fault near the Indian Garden Campground in Grand Canyon National Park, is an example. The spring derives water from the part of the groundwater mound within the fault zone that slopes toward the canyon. The crest of that mound is probably setback a few miles from the canyon wall. However, much of the water circulating downward in the fault zone lies beyond the divide and circulates away from the canyon to ultimately discharge through Havasu Springs (fig. 9). The dip of formations toward or away from the canyon does not have the same influence on the functioning of basin karst systems. The hydraulic gradients controlling groundwater flow under confined conditions form independently from the structural dip.

The largest springs discharging from the Muav Limestone at the base of the R-aquifer are in the uplifted inward-dipping regimes, whereas the largest springs discharging from the Redwall Limestone at the top of the R-aquifer are in the basin regimes (fig. 9).

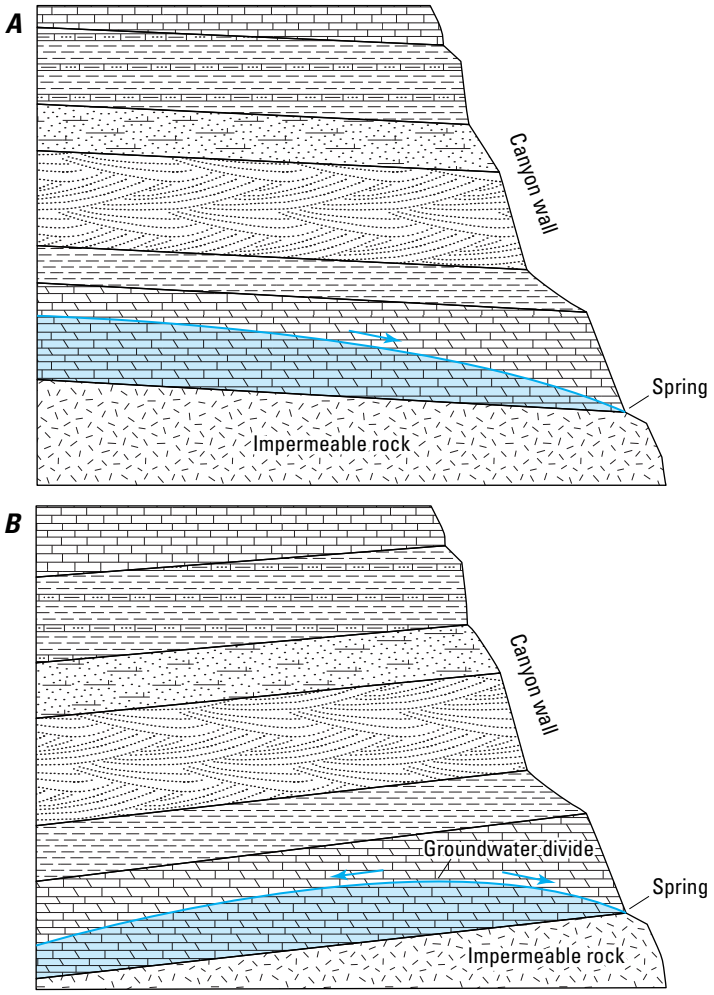

Figure 8. Conceptual illustration of a potentiometric surface in an uplift karst regime. The blue line represents the groundwater mound that develops above impermeable rock. Seeps and springs are generally larger and steadier where the strata dip toward the canyon wall such as in *A*, in contrast to *B*, where the strata dip away from the canyon wall.

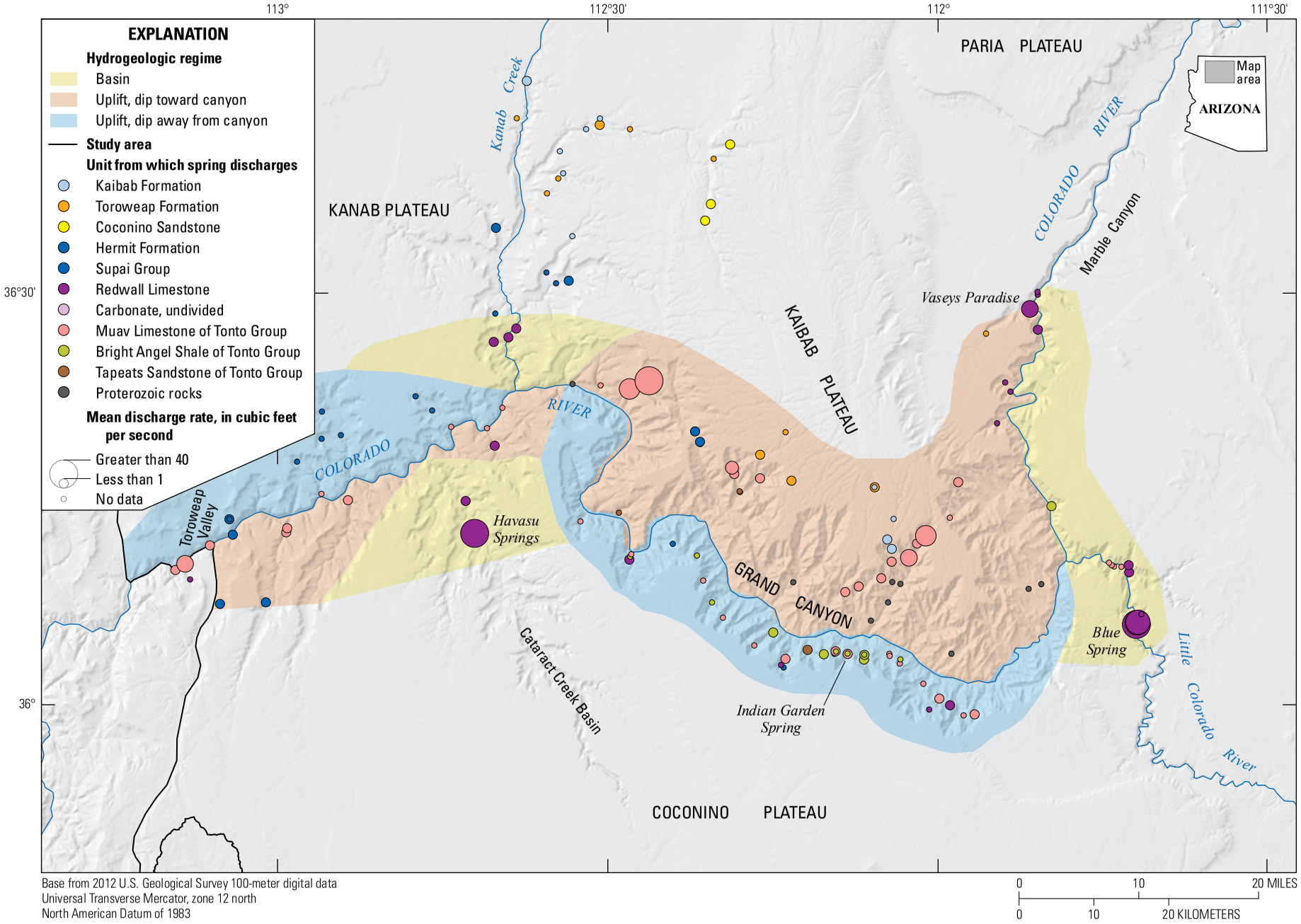

Figure 9. Map of the hydrogeologic regimes of springs and their designated geologic units discharging to the Grand Canyon. Symbol size indicates relative magnitude of mean discharge rate.

Geologic Structure

The mapping of major geologic structures in the Paleozoic section—faults, monoclines, axes of anticlines and synclines (fig. 2)—helps delineate the extent of the groundwater-flow systems within the R-aquifer in the study area and classify them into types. Delineation of structural highs and offsets of permeable units across large-displacement faults allows for the division of the R-aquifer into discrete flow systems. In the elevated plateaus, fractures align with geologic structure, particularly extensional faults, which indicate preferential flow directions via localized high-capacity karst drains.

Laramide compression and Cenozoic extension created most of the structural deformation that influences groundwater flow in the study area. The Laramide orogeny caused widespread uplift and crustal shortening in the east-northeast direction, resulting in north-striking, east-dipping monoclines (fig. 2) formed over thrust faults, and reverse displacements along reactivated Proterozoic basement rocks (Huntoon and others, 2003). Subsidiary blocks in the Grand Canyon region were alternately uplifted (for example, the Kaibab Plateau) or downwarped (for example, the Cataract Creek Basin). Extensive erosion removed most of the Mesozoic rocks in the southern and western sections of the region. Cenozoic crustal extension began to affect the Grand Canyon region around mid-Pliocene time. East-west extension caused normal faulting along many of the Laramide monoclines, followed by additional normal faults and extensional basins forming between them. These subsidiary faults propagate upward from either the upper part of the Proterozoic basement or the carbonate rocks of the lower Paleozoic section. Fault density and displacement is partially attenuated by shallower, more ductile units, including the Supai Group and the Hermit Formation (Huntoon and others, 2003).

The faults and folds of the Grand Canyon region influence groundwater flow in several ways. Vertical offset of faults can juxtapose permeable units against impermeable units. Fault gouge derived from fine-grained units can form a vertical wall of low permeability. The presence of either condition can greatly decrease groundwater flow across the fault. Conversely, the damaged zone of fractures on either side of a fault can provide a highly permeable, highly anisotropic setting for groundwater flow in the direction of the fractures. This is especially the case with normal faults formed under extensional forces, and relatively young or still-active faults in which associated fractures have not been sealed with mineral precipitate (Caine and others, 1996).

Recharge

A Soil-Water-Balance (SWB) model (Westenbroek and others, 2010) was used to estimate spatial distributions and relative rates of potential recharge for the study area (appendix 2; Knight and Jones, 2022). Model results show essentially zero potential recharge across much of the study area (fig. 10). This is reasonable given the generally high potential evaporation rates and low precipitation rates on the lower plateaus. Relatively high rates of potential recharge are simulated in isolated locations at high elevations on the high plateaus of southern Utah, San Francisco Mountain, and atop the Kaibab Plateau in the center of the study area.

Discharge

Discharge from the regional R-aquifer occurs through springs and seeps where the aquifer is exposed in the Grand Canyon and its tributary canyons, which serve as the ultimate drains for the region. There are two important characteristics common among springs discharging to the Grand Canyon: (1) the water discharges from the lower Paleozoic carbonates, and (2) faults are the dominant geologic factor on the locations of springs (Cooley, 1963). All springs in the region that have discharge larger than ~2 cubic feet per second (ft^3/s) are from fractures associated with faults, indicating that fractures not only provide the pathways for vertical circulation through the Paleozoic section, but also collect and transport water laterally to springs deep in the canyons.

The largest springs discharge from the lower Paleozoic units composing the R-aquifer (fig. 11), such as the Redwall Limestone and the Muav Limestone. Fewer springs discharge at lower rates from the upper Paleozoic units of the C-aquifer. Many small springs have been identified in the Mesozoic and Cenozoic units covering the northern, eastern, and southeastern extents of the study area. Much of the potential recharge simulated in the northern extent of the study area (fig. 10) probably never reaches the regional aquifer and instead discharges from these springs.

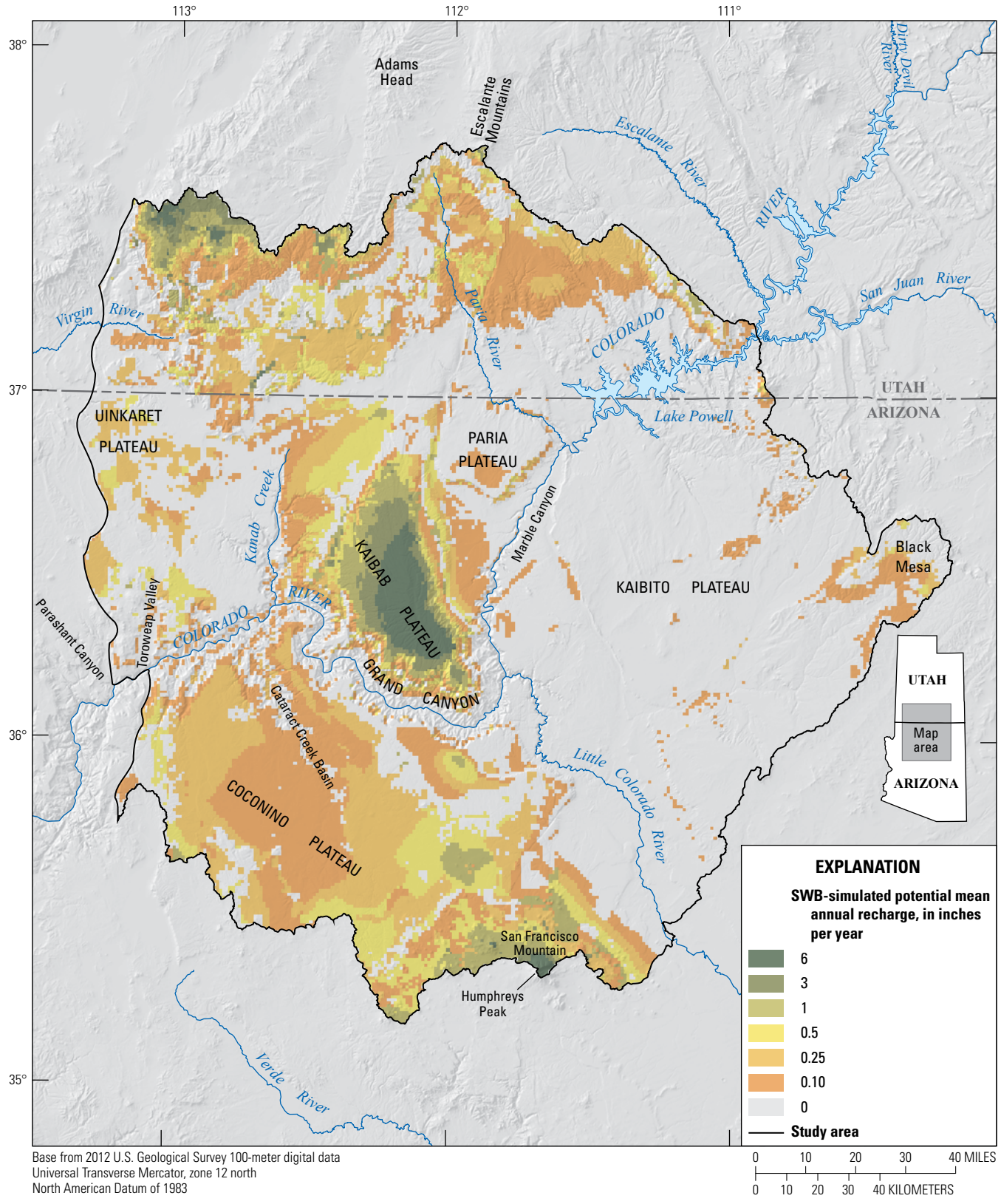

Figure 10. Map of the simulated potential mean annual recharge in the Grand Canyon region using a Soil-Water-Balance (SWB) model (Knight and Jones, 2022) from 1981–2016, in inches per year.

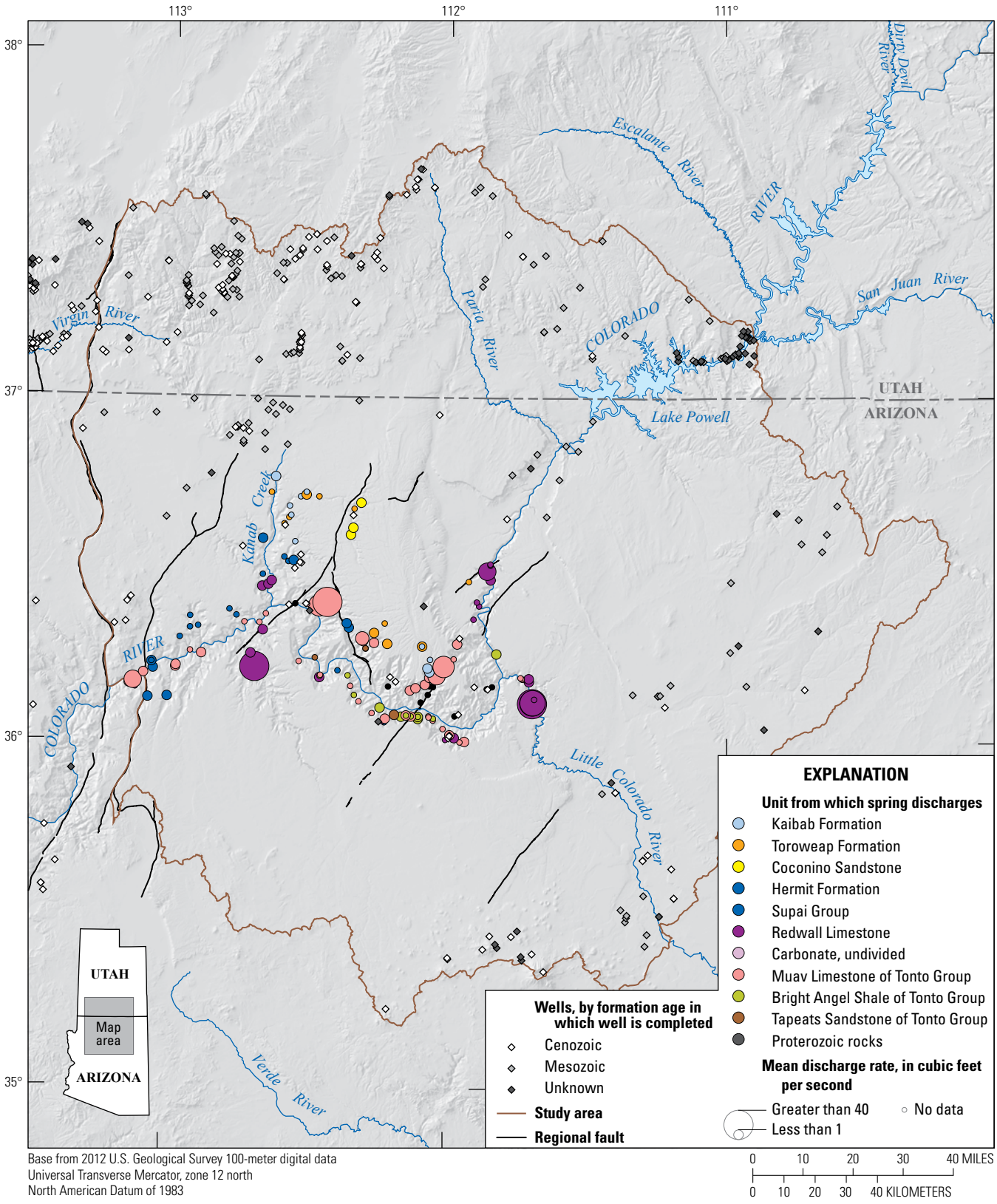

Figure 11. Map of spring locations, stratigraphic settings, and aquifer age in the Grand Canyon region.

Conceptual Models of Groundwater-Flow Systems in the Grand Canyon Region

Water-bearing strata beneath the plateaus surrounding the Grand Canyon are laterally partitioned by geologic structure into individual groundwater-flow systems that function independently from each other (fig. 12). Provided that accurately identified system boundaries are imposed by geologic structure, a contaminant source located in one system will not affect the springs in another. For this reason, geologic structure was used to identify system boundaries wherever possible. Presumed groundwater divides were used as necessary to delineate system extents but are substantially more uncertain because hydraulic boundaries can change location over time in response to changes in aquifer recharge or pumping withdrawals.

For each proposed individual groundwater system, three major attributes are discussed: potential recharge locations, discharge locations, and system boundaries. Hydrogeologic units and geologic structure are considered as they relate to these attributes. Primary attention is given to flow in the lower Paleozoic rocks that compose the R-aquifer.

The exact areal extents of the proposed groundwater systems are unknown because insufficient water level data are available to accurately define all of the bounding groundwater divides (fig. 12). Major topographic divides sufficiently far from the Grand Canyon and mineral withdrawal areas are used to limit the extent of the study area, outside of which there are no discharge locations related to the groundwater flow within. The Cataract groundwater system provides one exception as the outer boundary of the system is likely coincident with the study area extent. The Blue Spring groundwater system is known to be substantially truncated in this report, which only focuses on the lower portion adjacent to the Grand Canyon between the neighboring Cataract and Marble-Shinumo groundwater systems. For a full account of the Blue Spring groundwater system, refer to Hart and others (2002). The three groundwater systems north of the Grand Canyon probably do not extend to the study area boundary. There is unlikely to be active groundwater circulation in the R-aquifer rocks where they dip deeply below Mesozoic strata.

Kaibab Groundwater System

The Kaibab Plateau is the most elevated of the plateaus adjacent to the Grand Canyon (fig. 13). It is a lushly forested environment that sharply contrasts with the adjacent deserts. Because the plateau is high in elevation, it is an orographic barrier. Average precipitation ranges from 16 inches per year on its flanks to more than 30 inches per year at the summit. Evaporation potential varies between 58 and 62 inches per year (Farnsworth and others, 1982), which is low for the region. The ratio between potential evaporation and actual precipitation is lower for the Kaibab Plateau than any other area near the Grand Canyon, creating greater opportunity for water to enter the groundwater system. Although the Kaibab Plateau receives the most precipitation in the area, no perennial surface streams drain from it (USGS, 2016).

The groundwater system that drains the Kaibab Plateau is an uplifted karst system (fig. 9). Large quantities of water discharge from a small number of large springs deep within the Grand Canyon. The springs are fed by extensive cave networks that transport the water miles from under the Kaibab Plateau. Flash flooding in the caves is common. The flood waters travel several tens of miles between the surface of the plateau and the springs in a period of several hours to a few days (Jones and others, 2018).

The hydraulic boundaries of the Kaibab groundwater system are predominately fixed by extensional faults that bound the plateau to the west or intersect it from the east. The permeability of the R-aquifer within the plateau is dominated by fracture and karstic permeability developed along the strikes of the extensional faults. As a result, almost all flow occurs parallel to the faults, whereas flow perpendicular to them is negligible, including from adjacent flow systems.

The west boundary of the Kaibab groundwater system is formed by the West Kaibab Fault Zone, a network of interconnected extensional faults with displacements as great as 1,300 feet (Billingsley and others, 2008). Fracture and dissolution permeabilities along the faults are well developed and serve as lateral drains toward the wall of the Grand Canyon for about two-thirds of the plateau surface. The permeable extensional faults that trend north-south along the axis of the uplift either deliver their water to intersections with the West Kaibab Fault Zone to the northwest or directly toward the wall of the Grand Canyon to the south (Huntoon, 1974).

The East Kaibab Monocline marks the eastern geographic extent of the Kaibab Plateau, but groundwater likely flows across it in places (fig. 13). The Fence Fault and subsidiary parallel fractures that trend perpendicular to the uplift impinge on the crest of the uplift and serve as drains to Marble Canyon. A similar situation appears to the north, where normal faults aligned with the Trail Canyon Fault cut across the monocline. There is no clearly identifiable point of discharge associated with groundwater flow along these faults, but it is possible that they allow water to move deep into the subsurface below House Rock Valley to emerge eventually at springs in Marble Canyon. For these reasons the east boundary of the Kaibab groundwater system is defined along the crest of the Kaibab Plateau south to the Fence Fault. The eastern area of Kaibab Plateau, north of the Fence Fault, is thereby considered a part of the neighboring Marble-Shinumo groundwater system.

Huntoon (1974) delineated groundwater catchment areas within the Kaibab groundwater system based on the elevation of the Bright Angel Shale confining unit and the elevations of springs that drain from it. This configuration of catchment areas has been substantiated by dye tracing analyses conducted by Jones and others (2018).

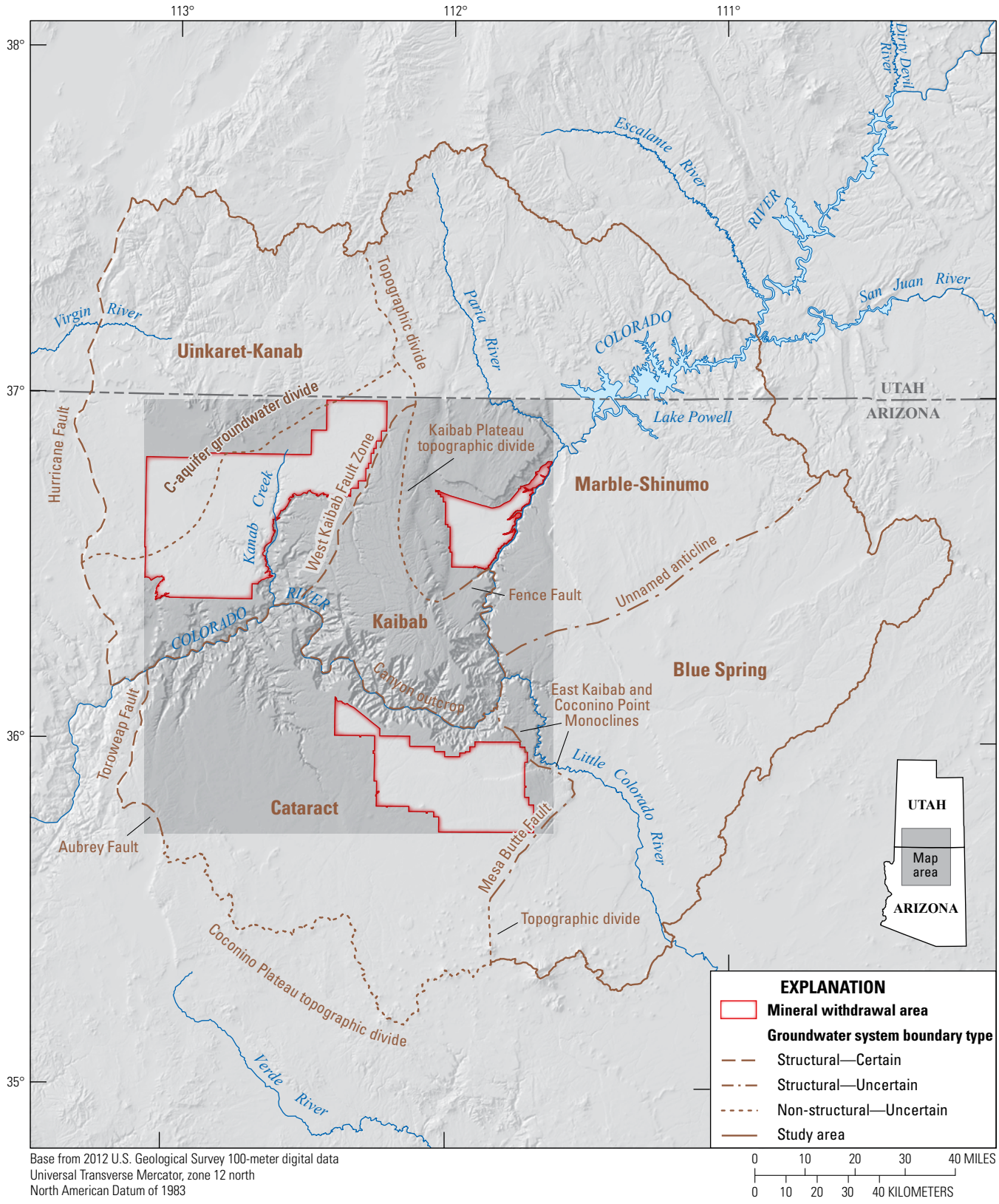

Figure 12. Map of the Grand Canyon region showing groundwater-system boundaries, topographic and groundwater divides, mineral withdrawal areas, and geologic structures.

The SWB model output reveals the greatest potential for recharge at the higher elevations of the Kaibab Plateau with smaller amounts present on the flanks (fig. 13). The surface of the Kaibab Plateau is dotted with sinkholes related to the dissolution of gypsum in the underlying Toroweap Formation. Many sinkholes, especially those in the grassy parks, drain extensive areas of closed surface topography. The distribution of the sinkholes is strongly correlated to mapped faults (Jones and others, 2018).

Fractures associated with the faults mapped on the surface of the Kaibab Plateau provide permeable vertical pathways that allow recharge from large storms or rapid snow melts to pass directly through the section to the base of the C-aquifer, thus allowing for rapid transport of water between the recharge area and the springs. In areas without faults, recharge water goes into transient storage, primarily in the Coconino Sandstone above the Hermit Formation confining unit, where it circulates laterally to faults. This delayed drainage accounts for the base flows from the springs deep in the canyons (Huntoon, 1974).

The major springs in the Kaibab groundwater system discharge from the R-aquifer at the base of the Muav Limestone above its contact with a thick underlying section of Bright Angel Shale. The springs discharge from the basal carbonate strata in the Peach Springs Member of the Muav Limestone and are localized where caves and dissolution-widened fractures associated with extensional fault zones intersect the canyon walls (Huntoon, 1974).

The largest springs that discharge from the Kaibab Plateau are the Tapeats, Thunder, and Deer Springs (fig. 13), which drain most of the plateau via the West Kaibab Fault Zone. The base flows from these springs are about 50 ft^3/s, although flood flows can be several times this amount (Johnson and Sanderson, 1968). Bright Angel Spring and Roaring Springs drain the south-central part of the plateau via caves present on fractures or parallel to the Bright Angel Fault, which in turn is hydraulically linked to normal faults that trend along the axis of the Kaibab uplift. Roaring Springs serves as the sole water supply for both the north and south rim developments in Grand Canyon National Park via pipelines where the water is pumped as much as 4,000 feet vertically up to the rims (Historic American Engineering Record, 2015).

Vaseys Paradise, on the wall of Marble Canyon (fig. 13), is the primary visible spring that drains the east side of the Kaibab Plateau. The water discharges from a cave dissolved along fractures parallel to the Fence Fault at the base of the Mooney Falls Member of the Redwall Limestone. Submerged springs discharge water originating on the plateau directly from the Fence Fault into the Colorado River.

The only continuous streamflow records that exist for the Kaibab Plateau springs are daily measurements of the Bright Angel Creek (station 09403000) from 1924 to 1974 and continuous measurements from 1991 to 1993 (USGS, 2018b). Those measurements serve as a useful proxy for spring discharge because the creek is fed by a series of karst springs. Recently, Jones and others (2018) collected continuous discharge data from Roaring Springs and performed hydrograph recession analyses to distinguish contributions arising from throughput via caves, fracture porosity, and matrix porosity after precipitation and snow melt events.

The superposition of rapid flash flows and longer-term releases from storage is more evident in the Kaibab groundwater system than any other systems investigated in this study. Flash floods through the cave networks are characteristic (Huntoon, 1974); however, sustained base flow during droughts and the dry fall season occur owing to discharge of water from transient storage in the clastic rocks high in the section and saturated fractured rocks at the base of the section.

The primary uncertainties associated with the Kaibab groundwater system are the extent of active groundwater circulation to the north and the location of the east boundary north of the Fence Fault. The strata plunge northward off the Kaibab uplift under a thick cover of Mesozoic rocks in southern Utah. Circulation in that area is likely negligible owing to diminished permeability and less steep hydraulic gradients, both of which are poorly quantified.

Uinkaret-Kanab Groundwater System

The Uinkaret and Kanab Plateaus, which are separated by the Toroweap-Sevier Fault, are uplifted but otherwise undisturbed on the north side of the Grand Canyon (fig. 14). The strata dip gently to the north-northeast toward the axis of a very broad gently north-plunging downwarp that trends along Kanab Canyon. The Permian Kaibab Formation forms the surface of the southern half of these plateaus within the Unikaret-Kanab groundwater system. The northern halves of the plateaus are buried by a progressively thickening section of Mesozoic rocks that compose the high plateaus of southern Utah. Kanab Canyon is the predominant surface feature, which incises progressively deeper into the Paleozoic strata toward the Colorado River.

Circulation rates through the system are minimal, evident by the lack of prominent springs discharging from it to the Grand Canyon. The regionally notable north-trending extensional Toroweap-Sevier Fault (Billingsley and others, 2008; Biek and others, 2015) and Hurricane Fault are the only laterally continuous faults in the region, with the Toroweap-Sevier Fault extending down through the middle of the Uinkaret-Kanab groundwater system and the Hurricane Fault bounding it to the west. Both prominent faults intersect the Grand Canyon, yet no springs discharge from either on the north side of the Colorado River. It is apparent that neither of these extensional fault zones has evolved into a lateral karst drain for the R-aquifer.

The Hurricane Fault is what defines the west boundary of the Uinkaret-Kanab groundwater system primarily because the upthrown strata along the east side of the fault establishes a structural high in the system. The lack of springs where the fault is dissected by Whitmore Canyon reveals that no

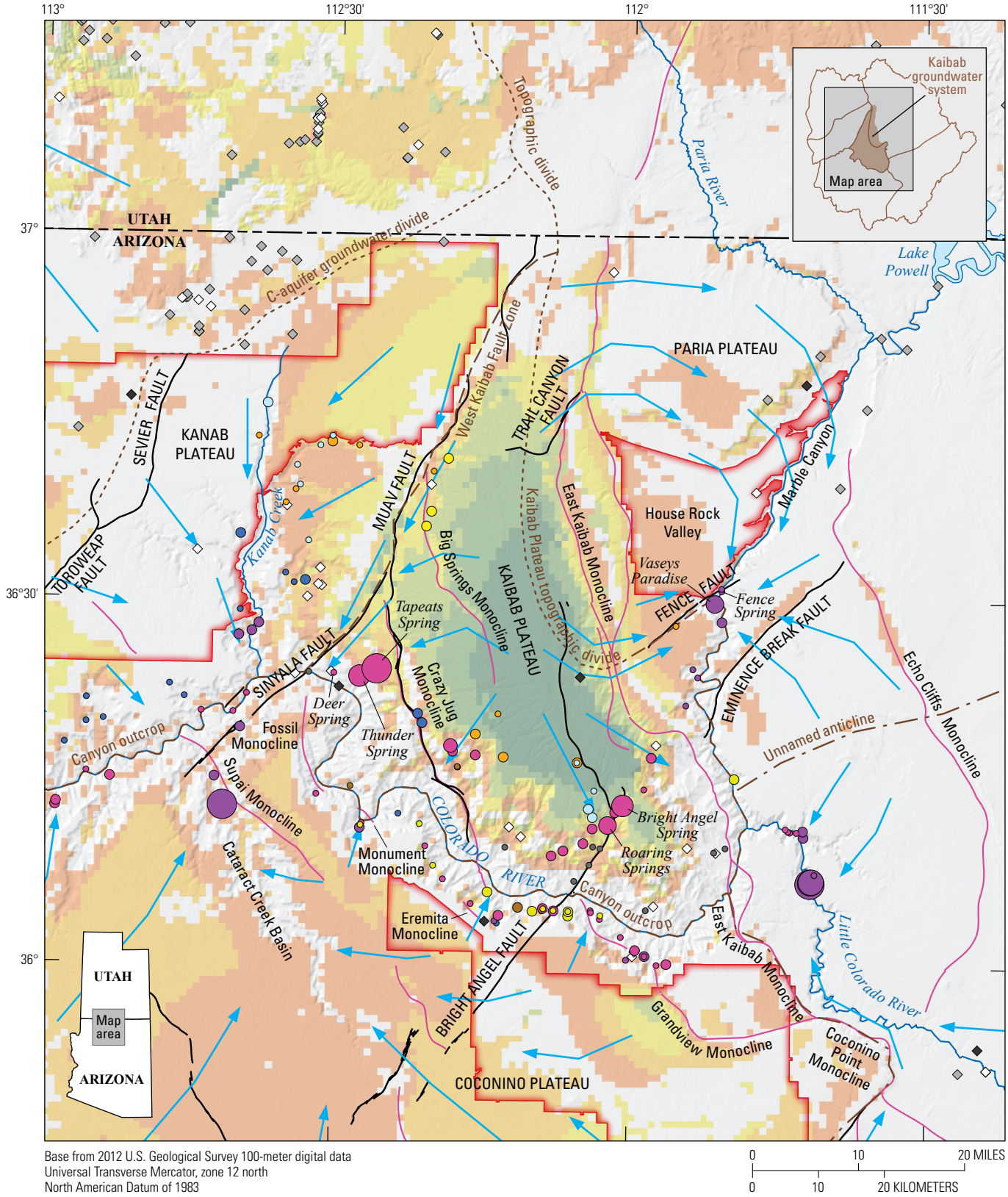

Figure 13. Map of the Grand Canyon region showing simulated potential mean annual recharge (Knight and Jones, 2022), in inches per year, spring locations, geologic structures, and proposed boundaries of the Kaibab groundwater system. SWB, Soil-Water-Balance model.

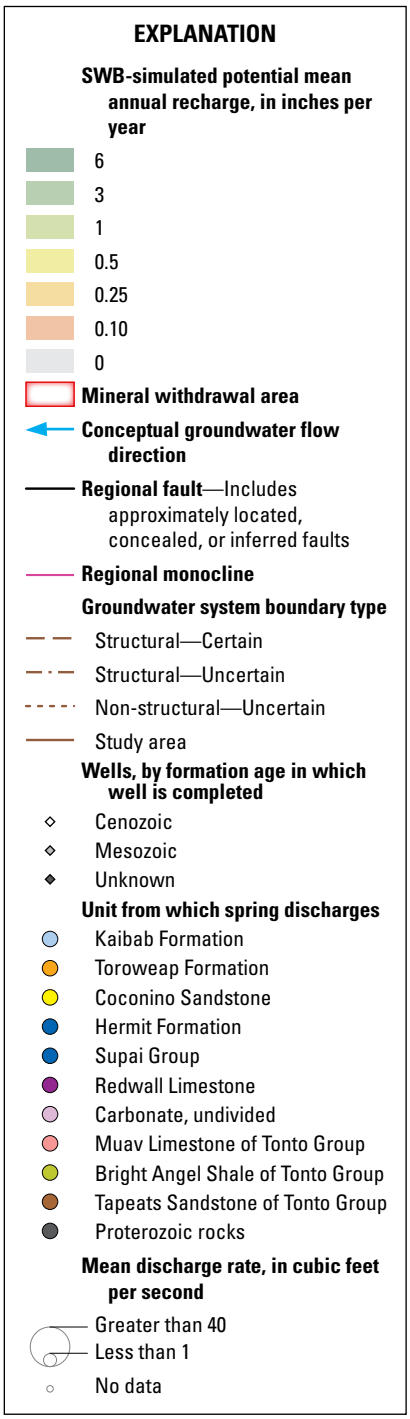

groundwater circulates along the fault to the Grand Canyon. The strata dip gently to the northeast away from the Hurricane Fault toward Kanab Canyon and to the north beyond Kanab, Utah (Doelling, 2008). A progressively thicker section of Mesozoic confining strata in Utah overlies the Paleozoic rocks in the system. Similar to the northern extent of the Kaibab groundwater system, the lack of recharge through the Mesozoic cover implies a lack of active circulation. The eastern limit of the Unikaret-Kanab groundwater system is defined by the West Kaibab Fault Zone. The southern limit is the Grand Canyon.

A groundwater divide in the C-aquifer, previously suggested by Inkenbrandt and others (2013) based on groundwater level measurements, roughly coincides with the surface water divide between the Colorado River and Virgin River (see dotted line, fig. 14). If caused by a structural high, the same divide probably applies to the R-aquifer but there are no available groundwater level measurements in the R-aquifer west of the Sevier Fault. The only known point of discharge that could be an outlet for regional flow north of the potential divide are the Dixie Hot Springs (also known as Pah Tempe Springs), just east of the Hurricane Fault in southern Utah. The springs contribute approximately 11 ft^3/s of flow to the Virgin River (Gardner, 2018), some of which could possibly discharge from the R-aquifer. The spring water is very warm with high levels of dissolved solids (Gardner, 2018). The R-aquifer is approximately 3,000 feet below the land surface, but geochemical analysis shows that the source of water could be between 2,000 and 19,000 feet below the surface (Dutson, 2005).

The lack of dynamic circulation through the R-aquifer under the Uinkaret-Kanab groundwater system is explained by a lack of recharge (fig. 14). Annual rainfall on the plateaus is only 10–14 inches per year, most of which quickly evaporates or transpires. Results from the SWB model reveal that there is substantial potential recharge in the higher elevations of southern Utah along the north boundary of the Uinkaret-Kanab groundwater system (fig. 10). However, that recharge flows into and through the Mesozoic section before discharging from springs far above the stratigraphic level of the R-aquifer.

Most springs and seeps discharging from the Paleozoic rocks within the system are in Kanab Canyon and its tributaries. Despite Kanab Canyon being one of the largest tributaries to the Grand Canyon, the base flow from the canyon (station 09403850) averages only 4 ft^3/s (USGS, 2018b). This is a trivial amount considering the topographic catchment area is more than 2,300 square miles.

Side Canyon, Showerbath, and Kanab springs above the mouth of Kanab Canyon discharge a combined total of approximately 1 ft^3/s from the rocks that compose the R-aquifer. Seeps in Snake Gulch discharge from the Permian rocks of the C-aquifer. Water quality samples from Pigeon Spring, also from the C-aquifer, have high concentrations of uranium, but their geochemical signatures reveal that they are not sourced by circulation from the reclaimed Pigeon Mine located 1 mile to the west (fig. 14) (Beisner and others, 2017a).

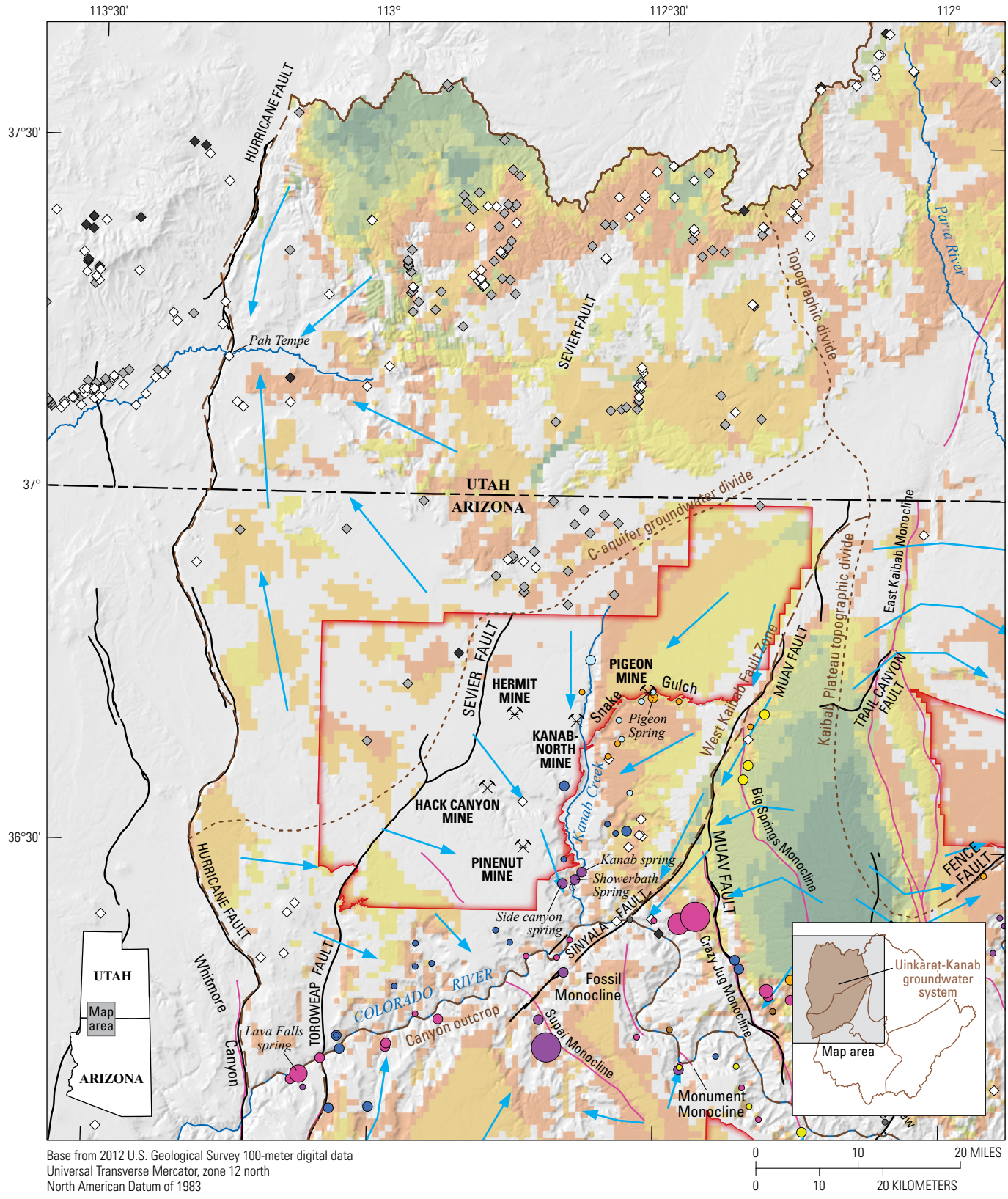

Figure 14. Map of the Grand Canyon region showing simulated potential mean annual recharge (Knight and Jones, 2022), in inches per year, spring locations, geologic structures, and proposed boundaries of the Uinkaret-Kanab groundwater system. SWB, Soil-Water-Balance model.

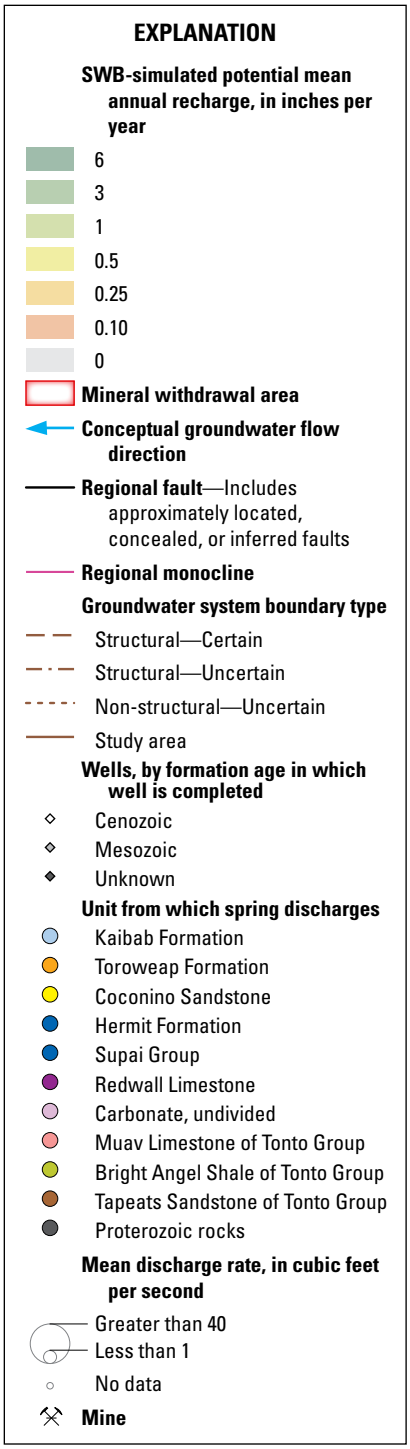

Minor springs and seeps discharge from the north wall of the Grand Canyon west of Kanab Creek from the rocks of the Hermit Formation, Supai Group, and Redwall Limestone. Their diminutive size and relatively high total dissolved solids content (for example, station 362157112451601; USGS, 2018b) reveal that groundwater circulation through that part of the system is very slow and that karstic development is minimal.

Several wells were drilled into the R-aquifer to supply potable water for various uranium mining operations. The withdrawal rates from them are negligible on a system scale. Informal historical water-level measurements from wells at the Hermit, Kanab-North, Hack Canyon, and Pinenut mines (fig. 14) have yielded inconsistent results. Recent samples from the Pinenut well (station 363003112440901) indicate long groundwater residence time consistent with low aquifer permeability. Tritium values are less than the laboratory reporting level, indicating no substantial component of water recharged after 1952 (USGS, 2018b). Radiocarbon age dating indicates groundwater at the well may be tens of thousands of years old.

The greatest uncertainties with respect to the R-aquifer in the Uinkaret-Kanab groundwater system are regional permeabilities, flow directions, flow rates, and the absolute positions of the groundwater divide between the Virgin River and Colorado River.

Marble–Shinumo Groundwater System

The Marble-Shinumo groundwater system underlies the plateaus on either side of Marble Canyon and likely extends beneath parts of adjacent plateaus to the east and north (fig. 15). The R-aquifer within it is a basin-type karst system. The east mineral withdrawal area is located entirely within the Marble-Shinumo groundwater system in House Rock Valley between the eastern slope of the Kaibab Plateau and the western rim of Marble Canyon.

The east boundary of the Marble-Shinumo groundwater system is likely defined by a reverse fault underlying the Echo Cliffs Monocline that appears to sever the R-aquifer. The south boundary is a possible groundwater divide between the Marble-Shinumo and Blue Spring groundwater systems, coinciding with an unnamed subtle anticline and topographic divide between the Colorado and Little Colorado River drainages. The west boundary is coincident with the east boundary of the Kaibab groundwater system, making the eastern portion of the Kaibab Plateau, north of the Fence Fault part of the Marble-Shinumo groundwater system. The north boundary is subjectively placed at the Vermillion Cliffs, beyond which there appears to be little circulation in the R-aquifer.

The Permian Kaibab Formation forms the surface of the plateaus adjacent to Marble Canyon. The overlying Mesozoic strata step up behind the Vermillion Cliffs and Echo Cliffs at distances up to several miles from the canyon rim to the north and east. There the Paria and Kaibito Plateaus rise 2,000 feet above the rim of Marble Canyon. The Kaibab Plateau is an

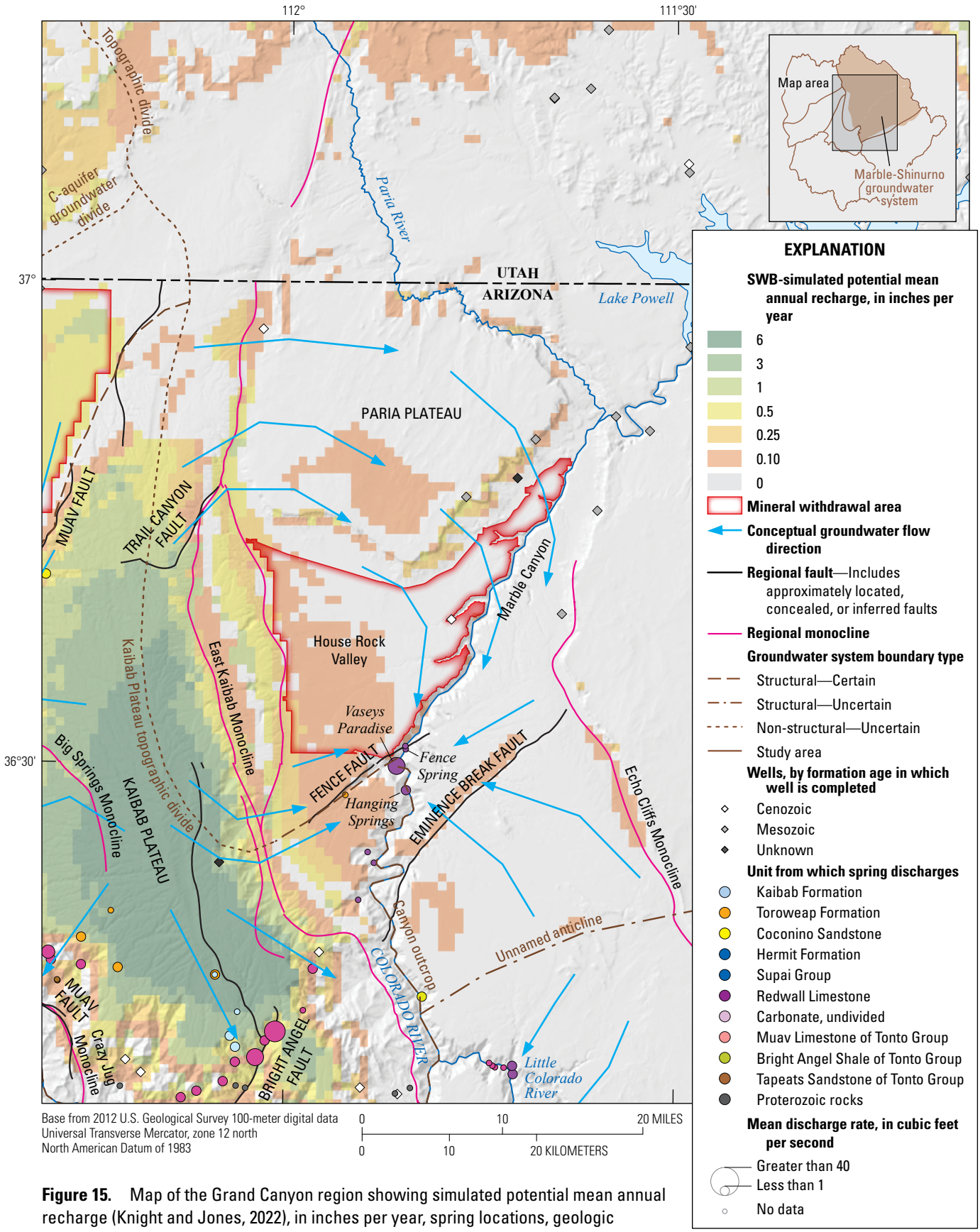

Figure 15. Map of the Grand Canyon region showing simulated potential mean annual recharge (Knight and Jones, 2022), in inches per year, spring locations, geologic structures, and proposed boundaries of the Marble-Shinumo groundwater system. SWB, Soil-Water-Balance model.

orographic barrier to the west of the Marble-Shinumo groundwater system, which greatly limits precipitation over House Rock Valley and Marble Canyon. The SWB model results reveal very minimal potential recharge across much of the Marble-Shinumo groundwater system (fig. 15), owing to low precipitation rates and high potential evaporation rates (fig. 3).

Glen Canyon Dam and Lake Powell are located to the east of the Marble-Shinumo groundwater system. The Jurassic Navajo Sandstone is the principal water-bearing unit in the Lake Powell region and the lake is developed on it (Thomas, 1996). However, there is no evidence that the water in the lake or the Navajo aquifer, which is contained within overlying Mesozoic strata, is in hydraulic communication with either the C- or R-aquifers that are the focus of this analysis. Thick confining strata in the lower part of the Mesozoic section, and a reverse fault underlying the Echo Cliffs Monocline that probably severs lateral continuity of the R-aquifer, makes a hydraulic connection unlikely.

A very broad, gently dipping anticline plunges north-northeast toward Lees Ferry, coincident with the course of Marble Canyon. The extensional Fence and Eminence Faults trend northeast diagonally across both the anticline and Marble Canyon. The faults are present between the East Kaibab and Echo Cliffs Monoclines. The two faults bound the Eminence graben, which is approximately 20 miles long and 5 miles wide. The rocks composing the R-aquifer within the graben are internally faulted and highly karstified yielding large permeabilities (Huntoon, 1981).

Most of the groundwater that discharges from the Marble-Shinumo groundwater system emerges at Fence Spring. The water discharges from the east bank at river level from the Fence Fault. The spring is situated in the uppermost part of the Redwall Limestone on the downthrown side of the fault. The water is warm and there is a high concentration of total dissolved solids, revealing long residence times. The spring water originates at least partly from the section of the Marble-Shinumo groundwater system located between Marble Canyon and Echo Cliffs Monocline. Potential recharge rates in this section are very low, and there is no evidence of the Fence Fault extending through the Echo Cliffs Monocline, so there may be another source area contributing flow to the east Fence Spring.

The northeast quadrant of the Kaibab Plateau could potentially be the additional source area. Extensional faults exist across the northern reach of the East Kaibab Monocline, which could allow groundwater from the recharge areas atop the northern Kaibab Plateau to move downward and eastward beneath the Paria Plateau. Flow paths in this possible scenario would eventually intersect fractures parallel to the Echo Cliffs Monocline, which would direct flow south toward the Fence Fault. The length and depth of this flow path would help to explain the high temperatures and total dissolved solids observed at east Fence Spring. Another possible scenario could involve deep-basin circulation originating east of the Echo Cliffs Monocline, but there is no evidence that the Fence or Eminence Faults extend past the monocline.

No springs that discharge water from the west side of the Marble-Shinumo groundwater system have been observed in Marble Canyon upstream from the Fence Fault. Unobserved discharge directly through the floor of the river could be another possible destination for potential groundwater flow originating from the northeast quadrant of the Kaibab Plateau.

Cataract Groundwater System

The Cataract groundwater system underlies most of the Coconino Plateau (fig. 16). It is bounded on the west by the Aubrey and Toroweap Faults, on the east by the Grand View Monocline and the Mesa Butte Fault. The southeastern limit of the system is a groundwater divide under the topographic divide between the Cataract and Little Colorado drainage basins and similarly to the south by a groundwater divide that coincides approximately with the topographic divides between the Cataract Creek and the Chino Valley and Verde River Basins (Bills and others, 2007). These divides coincide with structural highs of the bases of the C- and R-aquifers. The Paleozoic strata dip gently inward and northward from these elevated boundaries in a broad downwarp that plunges toward the mouth of Havasu Canyon. A large part of the south mineral withdrawal area lies within the Cataract groundwater system, as do the communities of Valle, Tusayan, Supai village, Grand Canyon village, and Williams.

The Cataract groundwater system contains both the C- and R-aquifers. The C-aquifer within the Cataract groundwater system is discontinuous. The rocks composing the aquifer are saturated in the southern part of the system but mostly unsaturated in the northern parts. Where saturated, it is largely unconfined. The permeability is greatest in areas of extensional faulting wherein the fracturing imparts a very strong anisotropy on the permeability.

The R-aquifer within most of the Cataract groundwater system is a classic basin-type karst system with a main discharge point at Havasu Springs in the floor of Cataract Canyon. The rocks that compose the R-aquifer are fully saturated under the lower reaches of Havasu Canyon. In contrast, the rocks are mostly dewatered where they are exposed along the South Rim of the Grand Canyon high above the Colorado River and dipping outward, away from the river and canyon wall. The narrow band along the South Rim to the east and west of Cataract Canyon is better described as an uplifted, outward-dipping karst system.

Only a handful of wells are drilled into the R-aquifer within the Cataract groundwater system and very few water-level measurements are recorded besides those reported as part of well completion reports. Those sparse data coupled with the elevation of Havasu Springs support the convergence of flow on Havasu Springs depicted on figure 16 (Bills and others, 2007).

The SWB model results reveal high levels of potential recharge on the north slope of San Francisco Mountain, and moderate levels in isolated locations east of Valle and Tusayan near the groundwater divide with the adjacent Blue Spring

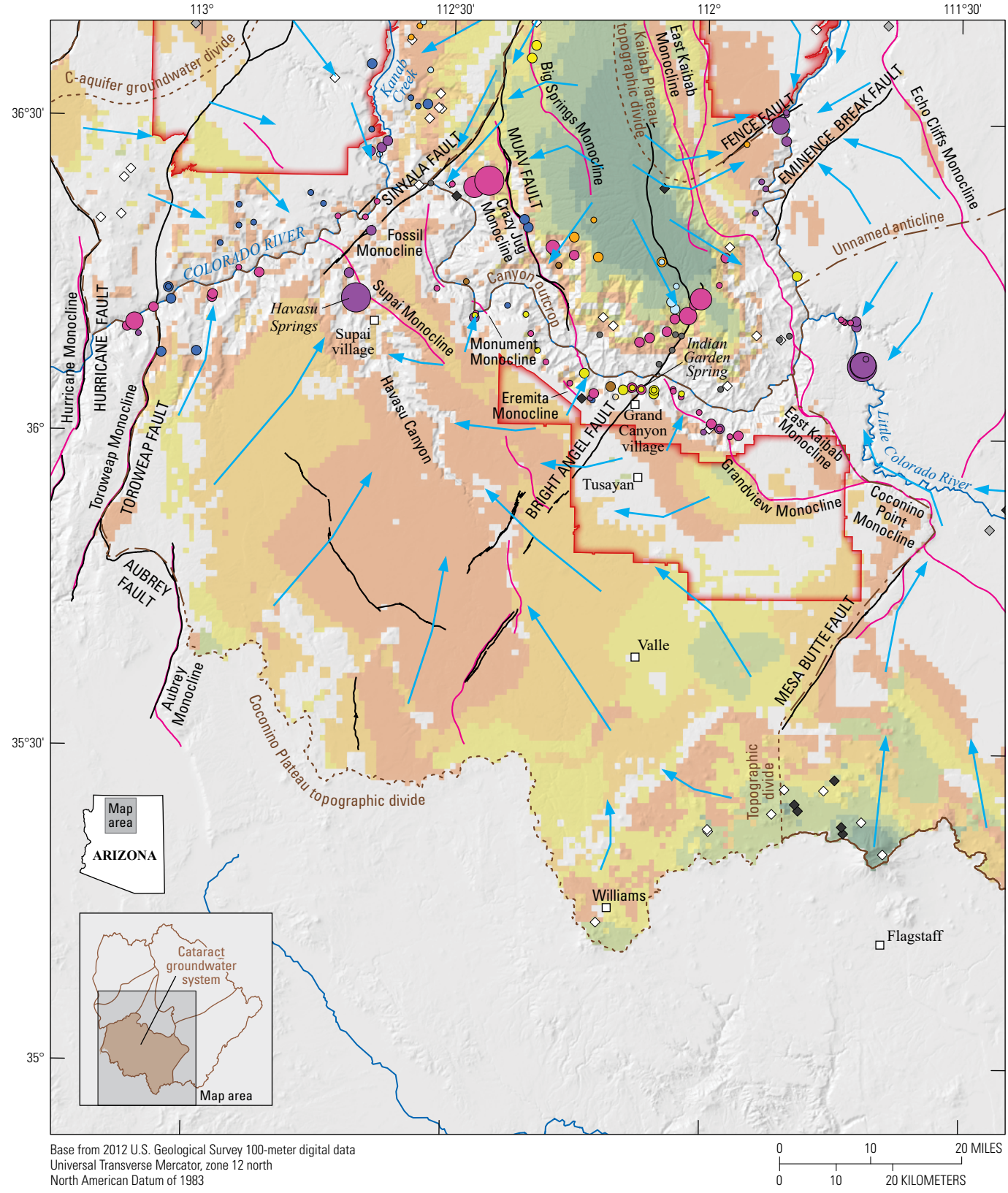

Figure 16. Map of the Grand Canyon region showing simulated potential mean annual recharge (Knight and Jones, 2022), in inches per year, spring locations, geologic structures, and proposed boundaries of the Cataract groundwater system. SWB, Soil-Water-Balance model.

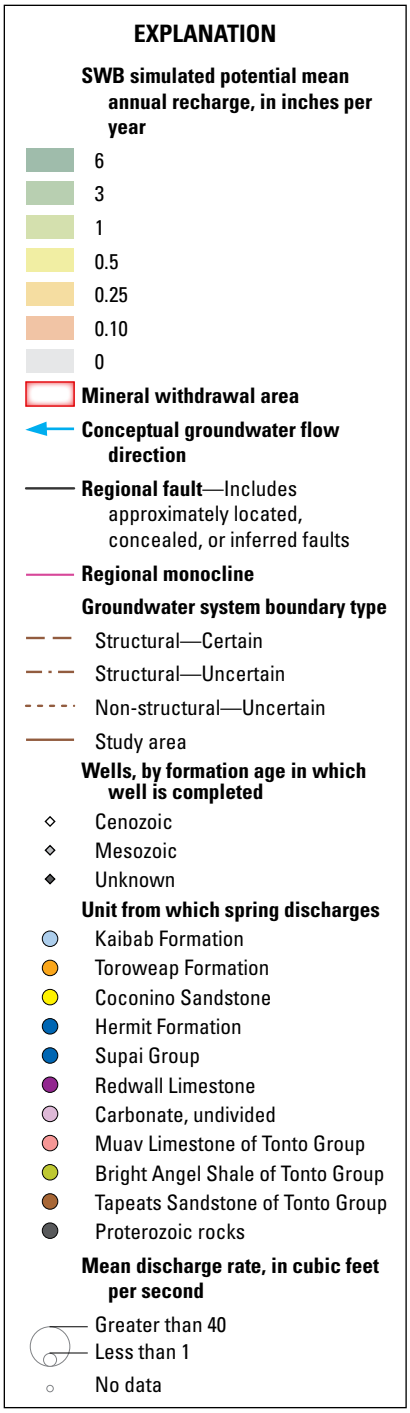

groundwater system. Recharge rates are likely negligible over much of the remainder of the system.

However, the interior of the Cataract Canyon drainage basin is riven by a network of closely spaced, orthogonally intersecting, small-displacement normal faults that are well exposed in the Kaibab Formation at the surface. Approximately 20 percent of the surface area of the basin is internally drained by sinks along these faults, which may conduct available surface waters down through the C-aquifer directly to the R-aquifer (Melis and others, 1996). This extensional fault zone is centered approximately 40 miles upstream from Havasu Springs.

Havasu Springs, just upstream from Supai village, is the primary point of discharge for groundwater from the Cataract groundwater system. The water rises to the floor of Cataract Canyon along a small normal fault that serves as a conduit through a thin section of the Supai Formation that overlies the Redwall Limestone at the spring.

Although not exposed, the karstic character of the flow system supplying Havasu Springs can be readily inferred. The volume of water flowing from the spring reveals that it is fed by a cavern network dissolved in the Redwall Limestone that is analogous to the dewatered two-dimensional planimetric cavern networks exposed within the interior of the Eminence graben in the walls of Marble Canyon (fig. 4).

A major flood in 1993 coursed down the otherwise ephemeral Cataract Creek with losses of water into sinkholes that opened along fissures in the fault system 40 miles upstream from Havasu Springs (Melis and others, 1996). Within 2 years, the water quality at the spring freshened (concentration of total dissolved solids decreased), noticeably revealing that the flood waters had diluted the water in the R-aquifer and arrived (Huntoon, 2000). It is reasonable to infer that preferential dissolution enhancement of permeability within the R-aquifer aligned with the regional hydraulic gradient, and accounts for the hydraulic connection between the upstream fault zone and Havasu Springs.

The water from Havasu Springs is turquoise in color from the spontaneous precipitation of dissolved calcium carbonate, much like the water at Blue Spring, and has created world famous travertine dams and falls between the springs and the Colorado River. The temperature of the water at the spring is about 70 °F and the discharge is fairly uniform at about 60 ft^3/s (Johnson and Sanderson, 1968). The steady discharge, warm temperature, and poor water quality attest to the large size of the groundwater system and generally lengthy residence time for the groundwater in it.

More than 40 springs and seeps are located below the South Rim of eastern Grand Canyon, but the combined total discharge from them is only a few cubic feet per second. These springs generally discharge from the strata comprising the lower R-aquifer in an uplifted, outward dipping hydrologic regime (fig. 9). The source for the water is recharge from distances probably no greater than a few miles south of the southern Grand Canyon rim. There is little to no groundwater storage in the strata at the south Grand Canyon Rim (Metzger, 1961).

Therefore, water has been transported via pipeline from the Roaring Springs from the Kaibab groundwater system to Grand Canyon village on the South Rim.

The Cataract groundwater system is the only system in the study area with substantial groundwater withdrawals from the R-aquifer. Approximately 500 acre-feet per year are pumped from the R-aquifer for use by the towns of Valle and Tusayan (USGS, 2018a). The City of Williams municipal water system also utilizes the R-aquifer to supplement reservoir storage.

It is important to determine flow vectors to the R-aquifer, either in the subsurface or overland, that can be expected from contaminant sources including mined ore and waste rock stored on the surface and mine production water. Of particular concern are migration pathways to the swallow holes in the floor of Cataract Creek upstream from Havasu Springs. No quantitative work has been carried out in the form of dye traces to determine flow rates between Havasu Springs and the sinks in the floor of Cataract Creek in the fault zone 40 miles upstream. The transmissive character of the R-aquifer, particularly where it is fractured by highly conductive extensional faults, remains unquantified.

The setback and temporal behavior of the groundwater divide behind the South Rim of the Grand Canyon have not been adequately delineated. The divide separates groundwater discharge to numerous small springs along the walls of the Grand Canyon from regional flow in the R-aquifer that moves away from the canyon toward Havasu Springs.

Blue Spring Groundwater System

The Blue Spring groundwater system is a basin-type karst system. It is the largest groundwater system that drains to the Grand Canyon, encompassing 27,000 square miles underlying the Little Colorado River drainage basin in Arizona and western New Mexico. This report focuses on the discharge end of the Blue Spring groundwater system downstream from Wupatki National Monument (fig. 17). The eastern part of the south mineral withdrawal area possibly impinges from the west onto this part of the Blue Spring groundwater system.

The north and southwest groundwater system boundaries, which are the only boundaries relevant to this discussion, are those previously defined respectively for the south boundary of the Marble-Shinumo groundwater system and east and southeast boundary of the Cataract groundwater system (fig. 17).

The SWB model results reveal high rates of potential recharge around San Francisco Mountain but negligible rates throughout the rest of the system within the study area. Additional potential recharge would likely be simulated in the upgradient portions of the Blue Spring groundwater system outside of the study area.

Blue Spring is a collective description of at least 36 individual springs on the floor of the Little Colorado River canyon within about 13 river miles of its confluence with the Colorado River. According to Cooley (1976), base flow upstream from Blue Spring is only about 5–7 ft^3/s. Blue Spring discharges at a constant rate of about 90 ft^3/s, which is almost half of the perennial flow at the mouth of the Little Colorado River. Cooley (1976) also recorded 60 ft^3/s contribution to streamflow from two unnamed springs just downstream from Blue Spring, 40–45 ft^3/s from other springs before river mile 10, and another 20 ft^3/s before river mile 3.1. In total, the springs of the Blue Spring groundwater system contribute 220 ft^3/s to the Little Colorado River (Cooley, 1976).

The large and steady discharge rate from the springs is consistent with the size of its catchment area. The water emerges at an average temperature of 70 °F and is turquoise in color owing to the spontaneous precipitation of calcium carbonate (Johnson and Sanderson, 1968). Deposits of calcium carbonate create a continuous series of travertine dams and rimstone pools between the springs and the Colorado River.

The Blue Spring is situated within an extensional rift zone riven by a dense set of generally north-south trending small displacements owing to normal faults. The regional dip of the Paleozoic strata is very gentle toward the southeast and a structural low near or upstream from Cameron, Arizona (fig. 17). The result is that the floor of the Little Colorado River cuts ever deeper into the Paleozoic section in the downstream direction along this reach. Most of the water emerges from a few major springs in the Mooney Falls Member of the Redwall Limestone, which discharge from saturated caves and dissolution-widened fractures associated with faulting.

Work by Cooley (1976) demonstrated that most of the Blue Spring water is derived from the C-aquifer underlying the Little Colorado River Basin. In Cooley's (1976) conceptual model, the water circulates laterally through the C-aquifer downstream within the basin until it is intercepted by the north-trending extensional faults oriented subparallel to the East Kaibab Monocline west of Cameron. It circulates downward within the fault zone to the R-aquifer where it then follows dissolution-widened fractures and caves in the Redwall Limestone that developed along the faults, emerging at the downstream springs.

Hart and others (2002) estimated 140,000 acre-feet of groundwater withdrawals from the C-aquifer in 1995, approximately 20,000 acre-feet of which withdrawal occurs near Flagstaff, just within the study area (Bills and others, 2007). This is the most developed of the groundwater systems considered in this report.

The positions of the groundwater divides in both the C- and R-aquifers that separate the Cataract and Blue Spring groundwater systems are poorly defined owing to a lack of wells in that region. However, knowledge of the positions of these divides is material to this assessment because they are overlain by the south mineral withdrawal area. Without additional knowledge of the potentiometric surface, the groundwater flow directions within the aquifers in the eastern part of the withdrawal area can only be speculated.

Groundwater circulation rates through the fault zone that supplies the Blue Spring groundwater system are likely to be exceptionally fast given the expected karstic permeabilities. However, those rates have not been quantified.

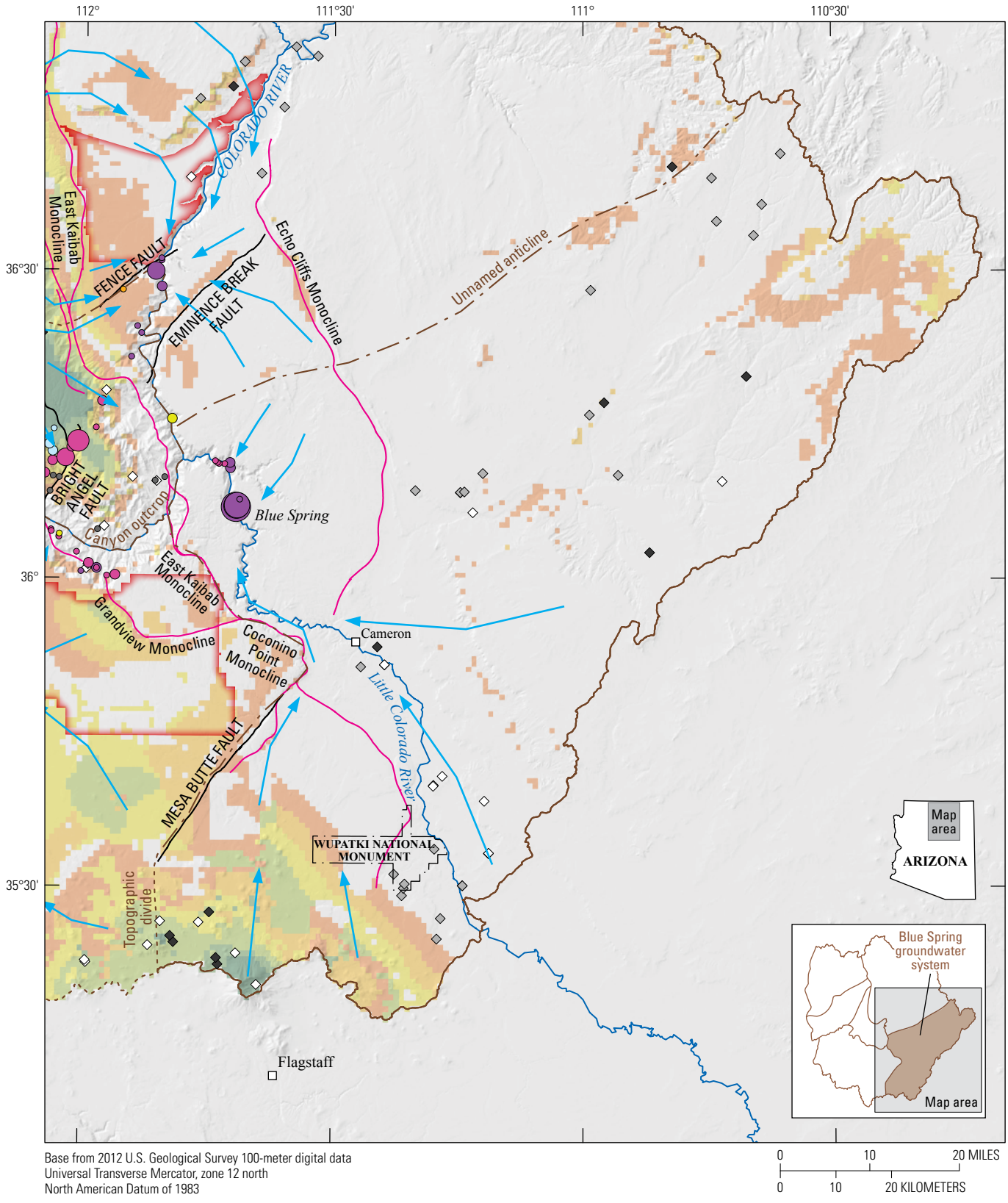

Figure 17 (pages 31–32). Map of the Grand Canyon region showing simulated potential mean annual recharge (Knight and Jones, 2022), in inches per year, spring locations, geologic structure, and proposed boundaries of the Blue Spring groundwater system. SWB, Soil-Water-Balance model.

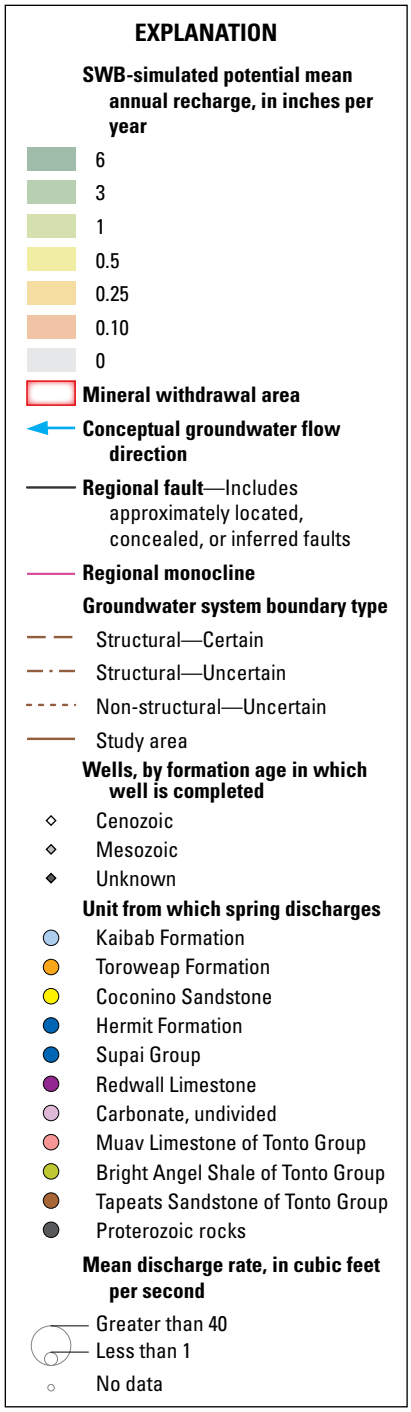

Figure 17 (pages 31–32). —Continued

Summary

Development of a conceptual model is useful in summarizing what is known or hypothesized about a groundwater system. The assembly and analysis of relevant field data and system characteristics into a qualitative representation of a groundwater system provides a foundation upon which further quantitative analyses and (or) numerical simulations can be built. Of equal importance is the determination of unknown aquifer properties or conditions that cause the greatest uncertainties in our understanding of the system. This report presents a summary and interpretation of available groundwater data from the Grand Canyon region and proposes that groundwater flow to the Grand Canyon occurs via five distinct groundwater systems.

The Kaibab groundwater system has the highest elevation, most precipitation, and presumably the most recharge per surface area of the groundwater systems in the area. It is an inward-dipping uplifted karst system characterized by rapid flow paths between recharge and discharge at springs. The Kaibab groundwater system is probably separated from the Uinkaret-Kanab groundwater system by the West Kaibab Fault Zone, which functions as an effective drain owing to high permeability from dissolution-enhanced fractures.

The Uinkaret-Kanab groundwater system is lower in elevation, hotter, and more arid. The Kanab Plateau is a basin karst system, but relatively undeformed and therefore less conducive to groundwater flow. Recharge is assumed to be minimal. Only a few cubic feet per second of discharge is observed from springs in Kanab Creek. Dixie Hot Springs (also known as Pah Tempe Springs) discharges deep-sourced groundwater to the Virgin River. The location of a regional groundwater divide between these two discharge points is unknown and has important implications for predicting the effects of potential contamination originating in the north mineral withdrawal area.

The Marble-Shinumo groundwater system is mostly a basin karst system that also likely includes the northeast quadrant of the uplifted Kaibab Plateau, which is an uplifted karst system. This is the only system with evidence indicating that the aquifer is connected across (beneath) the Colorado River. The Fence Spring discharges water originating apparently from both sides of Marble Canyon. The Eminence graben focuses groundwater flow to springs both visible and submerged in the canyon. The rest of the groundwater system is relatively undeformed, and rates of groundwater flow are likely small.

The Cataract groundwater system is an inward-dipping basin karst system. It is likely separated from the Blue Spring groundwater system by the East Kaibab Monocline and Mesa Butte Fault. The absolute location of this system boundary

determines how much of the south mineral withdrawal area is within the Blue Spring groundwater system. Likewise, a groundwater divide set back from the South Rim of the Grand Canyon separates flow of groundwater to the principal point of discharge for the groundwater system at Havasu Springs from the minor amount of flow that occurs in the springs below the South Rim. This divide likely runs through the northern part of the south mineral withdrawal area.

The Blue Spring groundwater system is an outward-dipping basin karst system. It is the largest subsystem in terms of area and volumetric discharge. A total of approximately 220 ft^3/s of groundwater discharges from a group of springs in the Little Colorado River just upstream from the Colorado River.

Numerical groundwater-flow models are typically used to determine likely flow paths and rates of transport for potential groundwater contaminants from source to discharge locations. However, there is insufficient hydrogeologic information to accurately simulate groundwater flow in much of the study area. Wells are sparse owing to the remoteness of much of the area and the great depth to groundwater, so there are few hydraulic head measurements from which to deduce flow directions in the regional aquifer and aquifer properties are poorly quantified.

Although sufficient data are not available at this time to confidently develop a numerical model of the groundwater-flow system in the Grand Canyon region, information is available to help characterize the groundwater systems in the area. System boundaries are important to define. Aside from the groundwater divide location behind the South Rim there is relatively low uncertainty of the Cataract and Blue Spring groundwater system boundaries. A more certain location of the possible regional groundwater divide between the northern and southern parts of the Uinkaret-Kanab groundwater system is a prerequisite to any numerical simulation of groundwater flow in that area. Whether pathways exist for groundwater to flow across the East Kaibab Monocline from the northeast quadrant of Kaibab Plateau has important implications for simulating groundwater flow in the Marble-Shinumo groundwater system.

Additional data that would be necessary for a numerical model include additional measurements of groundwater levels in the regional aquifer, estimates of hydrogeologic properties from pumping tests in the regional aquifer, location and nature of system boundaries, effects of geologic structure on groundwater flow, and additional discharge measurements at R-aquifer springs.

Acknowledgment

The hydrogeologic investigation presented in this report was supported by the USGS Toxic Substances Hydrology Program.

References Cited

Alpine, A.E., 2010, Hydrological, geological, and biological site characterization of breccia pipe uranium deposits in northern Arizona: U.S. Geological Survey Scientific Investigations Report 2010–5025, 353 p.

Anderson, M.P., Woessner, W.W., and Hunt, R.J., 2015, Applied groundwater modelling—Simulation of flow and advective transport: Academic Press, 630 p.

Beisner, K.R., Paretti, N.V., Tillman, F.D., Naftz, D.L., Bills, D.J., Walton-Day, K., and Gallegos, T.J., 2017a, Geochemistry and hydrology of perched groundwater springs—assessing elevated uranium concentrations at Pigeon Spring relative to nearby Pigeon Mine, Arizona (USA): Hydrogeology Journal, v. 25, p. 539–556, accessed on October 2, 2017, at https://doi.org/10.1007/s10040-016-1494-8

Beisner, K.R., Tillman, F.D., Anderson, J.R., Antweiler, R.C., and Bills, D.J., 2017b, Geochemical characterization of groundwater discharging from springs north of the Grand Canyon, Arizona, 2009–2016: U.S. Geological Survey Scientific Investigations Report 2017–5068, 58 p., accessed on August 8, 2017, at https://doi.org/10.3133/sir20175068.

Beus, S.S., 2003, Temple Butte Formation, chap. 7 *of* Beus, S.S., and Morales, M., eds., Grand Canyon Geology: Geological Society of America p. 107–114.

Biek, R.F., Rowley, P.D., Anderson, J.J., Maldonado, F., Moore, D.W., Hacker, D.B., Eaton, J.G., Hereford, R., Sable, E.G., Filkhorn, H.F., and Matyjasik, B., 2015, Geologic map of the Panguitch 30’x60’ quadrangle, Garfield, Iron, and Kane Counties, Utah: Utah Geological Survey, scale 1:50,000 and 1:62,500.

Biek, R.F., Rowley, P.D., Hayden, J.M., Hacker, D.B., Willis, G.C., Hintze, L.F., Brown, K.D., 2010, Geologic map of the St. George and East Part of the Clover Mountains 30’x60’ quadrangles, Washington and Iron Counties, Utah: Utah Geological Survey, scale 1:100,000.

Billingsley, G.H., Block, D.L., and Dyer, H.C., 2006a, Geologic map of the Peach Springs 30’x60’ quadrangle, Mohave and Coconino Counties, northwestern Arizona: U.S. Geological Survey Scientific Investigations Map 2900.

Billingsley, G.H., Felger, T.J., and Priest, S.S., 2006b, Geologic map of the Valle 30’x60’ quadrangle, Coconino County, northern Arizona: U.S. Geological Survey Scientific Investigations Map 2895.

Billingsley, G.H., and Hampton, H.M, 2000, Geologic map of the Grand Canyon 30’x60’ quadrangle, Coconino and Mohave Counties, northwestern Arizona: U.S. Geological Survey Geologic Investigations Series I-2688, scale 1:100,000.

Billingsley, G.H., and Priest, S.S., 2013, Geologic map of the Glen Canyon Dam 30'x60' quadrangle, Coconino County, northern Arizona: U.S. Geological Survey Scientific Investigations Map 3268.

Billingsley, G.H., Priest, S.S., and Felger, T.J., 2007, Geologic map of the Cameron 30'x60' quadrangle, Coconino County, northern Arizona: U.S. Geological Survey Scientific Investigations Map 2977, scale 1:100,000.

Billingsley, G.H., Priest, S.S., and Felger, T.J., 2008, Geologic map of the Fredonia 30'x60' quadrangle, Mohave and Coconino Counties, northern Arizona: U.S. Geological Survey Scientific Investigations Map 3035, scale 1:100,000.

Billingsley, G.H., Stoffer, P.W., and Priest, S.S., 2012, Geologic map of the Tuba City 30'x60' quadrangle, Coconino County, northern Arizona: U.S. Geological Survey Scientific Investigations Map 3227, scale 1:50,000.

Billingsley, G.H., and Wellmeyer, J.L., 2003, Geologic map of the Mount Trumbull 30'x60' quadrangle, Mohave and Coconino Counties, northwestern Arizona: U.S. Geological Survey Geologic Investigations Series I–2766.

Billingsley, G.H., and Workman, J.B., 2000, Geologic map of the Littlefield 30'x60' quadrangle, Mohave County, northwestern Arizona: U.S. Geological Survey Geologic Investigations Series I–2628.

Bills, D.J., Flynn, M.E., and Monroe, S.A., 2007, Hydrogeology of the Coconino Plateau and adjacent areas, Coconino and Yavapai Counties, Arizona: U.S. Geological Survey Scientific Investigations Report 2005–5222, 101 p.

Caine, J.S., Evans, J.P., and Forster, C.B., 1996, Fault zone architecture and permeability structure: Geology, v. 24, no. 11, p. 1025–1028.

Cooley, M.E., 1963, Hydrology of the Plateau uplands province, in Annual report on the ground water in Arizona, spring 1962 to spring 1963, by Natalie D. White, R.S. Stulik, E.K. Morse, and others: Arizona State Land Dept. Water-Resources Report 15, p. 27–37.

Cooley, M.E, 1976, Spring flow from pre-Pennsylvanian rocks in the southwestern part of the Navajo Indian Reservation, Arizona: U.S. Geological Survey Professional Paper 521-F, 14 p.

Cooley, M.E., Harshbarger, J.W., Akers, J.P., and Hardt, W.F., 1969, Regional hydrogeology of the Navajo and Hopi Indian Reservations, Arizona, New Mexico, and Utah, with a section on Vegetation by O.N. Hicks: U.S. Geological Survey Professional Paper 521–A, 61 p.

Crossey, L.J., Fischer, T.P., Patchett, P.J., Karlstrom, K.E., Hilton, D.R., Newell, D.L., and de Leeuw, G.A., 2006, Dissected hydrologic system at the Grand Canyon—Interaction between deeply derived fluids and plateau aquifer waters in modern springs and travertines: Geology, v. 34, no. 1, p. 25–28, accessed July 21, 2016, at https://doi.org/10.1130/G22057.1.

Department of the Interior, 2012, Secretary Salazar announces decision to withdraw public lands near Grand Canyon from new mining claims, accessed July 21, 2016, at https://www.doi.gov/news/pressreleases/Secretary-Salazar-Announces-Decision-to-Withdraw-Public-Lands-near-Grand-Canyon-from-New-Mining-Claims.

Doelling, H.H., 2008, Geologic map of the Kanab 30' x 60' quadrangle Kane and Washington Counties, Utah, and Coconino and Mohave Counties, Arizona: Salt Lake City, Utah, Utah Geological Survey Miscellaneous Publication 08-2DM, 2 sheets, scale 1:100,000. [Also available at https://ugspub.nr.utah.gov/publications/misc_pubs/MP-08-2.pdf.]

Dutson, S.J., 2005, Effects of Hurricane Fault architecture on groundwater flow in the Timpoweap Canyon of southwestern Utah: Brigham Young University, 57 p.

Errol L. Montgomery and Associates, 1999, Supplemental assessment of hydrogeologic conditions and potential effects of proposed groundwater withdrawal, Coconino Plateau Groundwater Subbasin, Coconino County, Arizona: Williams, Ariz., Montgomery and Associates, 256 p.

Farnsworth, R.K., Thompson, E.S., and Peck, E.L., 1982, Evaporation Atlas for the Contiguous 48 United States: National Oceanic and Atmospheric Administration technical report NWS 33, 27 p.

Gardner, P.M., 2018, Effects of groundwater withdrawals from the Hurricane Fault Zone on discharge of saline water from Pah Tempe Springs, Washington County, Utah: U.S. Geological Survey Scientific Investigations Report 2018–5040, 41 p., accessed May 1, 2018, at https://doi.org/10.3133/sir20185040.

Hargreaves, G.H., and Samani, Z.A., 1985, Reference crop evapotranspiration from Temperature: Applied Engineering in Agriculture, v. 1, no. 2, p. 96–99.

Hart, R.J., Ward, J.J., Bills, D.J., and Flynn, M.E., 2002, Generalized hydrogeology and ground-water budget for the C aquifer, Little Colorado River Basin and parts of the Verde and Salt River Basins, Arizona and New Mexico: U.S. Geological Survey Water Resources Investigation Report 2002–4026, 45 p.

Hintze, L.F., Willis, G.C., Laes, Denise Y.M., Sprinkel, D.A., and Brown, K.D., 2000, Digital geologic map of Utah M-179dm: Utah Geological Survey, 1:500,000 scale, accessed May 28, 2020, at https://geology.utah.gov/apps/intgeomap/.

Historic American Engineering Record, 2015, Transcanyon Water Line, beginning 5 miles below North Kaibab Trail and .14 miles east of Roaring Springs and extending to Indian Garden and Indian Garden Pumphouses, Grand Canyon, Coconino County, AZ: Library of Congress, accessed May 17, 2019, at www.loc.gov/item/az0661/.

Huntoon, P.W., 1974, The karstic groundwater basins of the Kaibab Plateau, Arizona: Water Resources Research, v. 10, no. 3, p. 579–590.

Huntoon, P.W., 1977, Relationship of tectonic structure to aquifer mechanics in the western Grand Canyon district, Arizona: U.S. Department of the Interior Office of Water Research and Technology, Water Resources Series no. 66, 51 p., 2 sheets, scale 1:125,000.

Huntoon, P.W., 1981, Fault controlled ground-water circulation under the Colorado River, Marble Canyon, Arizona: Groundwater, v. 19, no.1, p. 20–27.

Huntoon, P.W., 1996, Large-basin ground water circulation and paleo-reconstruction of circulation leading to uranium mineralization in Grand Canyon breccia pipes, Arizona: The Mountain Geologist, v. 33, no. 3, p. 71–84.

Huntoon, P.W., 2000, Variability of karstic permeability between unconfined and confined aquifers, Grand Canyon region, Arizona: Environmental and Engineering Geoscience, v. 6, no. 2, p. 155–170.

Huntoon, P.W., Billingsley, G.H., Jr., Breed, W.J., Sears, J.W., Ford, T.D., Clark, M.D., Babcock, R.S., and Brown, E.H., 1976, Geologic map of the Grand Canyon National Park, Arizona, 1976 edition: Grand Canyon Natural History Association and Museum of Northern Arizona, 1 sheet, scale 1:62,500.

Huntoon, P.W., Peter, W., Beus, S.S., and Morales, M., 2003, Post-Precambrian tectonism in the Grand Canyon region: Grand Canyon Geology, p. 222–259.

Inkenbrandt, P., Thomas, K., and Jordan, J.L., 2013, Regional groundwater flow and water quality in the Virgin River basin and surrounding areas, Utah and Arizona: Utah Geological Survey Report of Investigation 272.

Johnson, P.W., and Sanderson, R.B., 1968, Spring flow into the Colorado River Lees Ferry to Lake Mead, Arizona: Arizona State Land Department, no. 34, 26 p.

Jones, C.J., Springer, A.E., Tobin, B.W., Zappitello, S.J., and Jones, N.A., 2018, Characterization and hydraulic behaviour of the complex karst of the Kaibab Plateau and Grand Canyon National Park, USA: Geological Society of London, p. 237–260.

Kaibab National Forest, 1999, Final environmental impact statement for Tusayan growth, Coconino County, Arizona: U.S. Forest Service, Southwest Region, 399 p.

Knight, J.E., and Jones, C.J., 2022, Soil-Water-Balance (SWB) model archive used to simulate potential mean annual recharge in the Grand Canyon region, Arizona: U.S. Geological Survey data release, https://doi.org/10.5066/P9FQ7BSY.

LaRue, E.C., 1925, Water power and flood control of Colorado River below Green River, Utah: U.S. Geological Survey Water-Supply Paper 556, 176 p.

Leighty, R.S., 2021 Grand Canyon Stratigraphy: Arizona Geological Survey Contributed Report CR-21-D, poster 24x54 inches

McGavock, E.H., 1968, Basic ground-water data for southern Coconino County, Arizona: Arizona State Land Department Water Resources Report 33, 49 p.

McKee, E.D., 1960, Lithologic subdivisions of the Redwall Limestone in northern Arizona—Their paleogeographic and economic significance: U.S. Geological Survey Professional Paper 400-B, B243–B245.

McKee, E.D., and Resser, C.E., 1945, Cambrian history of the Grand Canyon region: Washington, D.C., Carnegie Institution of Washington Publication 563, 232 p.

Melis, T.S., Phillips, W.M., Webb, R.H., and Bills, D.J., 1996, When the blue-green waters turn red, historical flooding in Havasu Creek, Arizona: U.S. Geological Survey Water Resources Investigation Report 96-4059, 136 p.

Metzger, D.G., 1961, Geology in relation to availability of water along the South Rim Grand Canyon National Park Arizona: U.S. Geological Survey Water-Supply Paper 1475-C, p. 105–138.

Monroe, S.A., Antweiler, R.C., Hart, R.J., Taylor, H.E., Truini, M., Rihs, J.R., and Felger, T.J., 2004, Chemical characteristics of ground-water discharge along the South Rim of Grand Canyon in Grand Canyon National Park, Arizona, 2000–2001: U.S. Geological Survey Scientific Investigations Report 2004–5146, 71 p.

Multi-Resolution Land Characteristics Consortium, 2020, National Land Cover Dataset 2016 Landcover (CONUS), accessed May 28, 2020, at https://www.mrlc.gov/data/nlcd-2016-land-cover-conus.

Pool, D.R., Blasch, K.W., Callegary, J.B., Leake, S.A., and Graser, L.F., 2011, Regional groundwater-flow model of the Redwall-Muav, Coconino, and alluvial basin aquifer systems of northern and central Arizona: U.S. Geological Survey Scientific Investigations Report 2010–5180, 101 p.

PRISM Climate Group, 2017, Recent daily precipitation, minimum and maximum temperature grid data: Oregon State University, accessed August 9, 2017, at http://prism.oregonstate.edu/recent/.

Richard, S.M., Reynolds, S.J., Spencer, J.E. and Pearthree, P.A., 2000, Geologic Map of Arizona. Arizona Geological Survey Map-35, 1,000,000 map scale, Accessed May 28, 2020, at http://repository.azgs.az.gov/uri_gin/azgs/dlio/1705.

Spamer, E.E., 1999, Grand vision of Edwin D. McKee: GSA Today, p. 18–19.

Thomas, B.E., 1996, Simulation analysis of water-level changes in the Navajo sandstone due to changes in the altitude of Lake Powell near Wahweap Bay, Utah and Arizona: U.S. Geological Survey Water-Resources Investigation Report 85–4207, 45 p.

Tillman, F.D., 2015, Documentation of input datasets for the soil-water-balance groundwater recharge model of the Upper Colorado River Basin: U.S. Geological Survey Open-File Report 2015–1160, 17 p., accessed November 6, 2018, at https://doi.org/10.3133/ofr20151160.

Timmons, J.M., and Karlstrom, K.E., 2012, Grand Canyon geology—Two billion years of Earth's history: Geological Society of America, 156 p., accessed June 6, 2018, https://doi.org/10.1130/SPE489.

Twenter, F.R., 1962, Geology and promising areas for groundwater development in the Hualapai Indian Reservation, Arizona: U.S. Geological Survey Water-Supply Paper 1576-A, 38 p.

U.S. Census Bureau, 2020, City and town population totals—2010–2018, accessed May 5, 2020, at https://www.census.gov/data/tables/time-series/demo/popest/2010s-total-cities-and-towns.html

U.S. Geological Survey [USGS], 2014, Grand Canyon Science Plan, accessed August 6, 2021, at https://webapps.usgs.gov/uraniummine/.

U.S. Geological Survey [USGS], 2016, USGS National Hydrography Dataset (NHD) Downloadable Data Collection - National Geospatial Data Asset (NGDA) National Hydrography Dataset (NHD): USGS - National Geospatial Technical Operations Center (NGTOC): Rolla, MO and Denver, CO, accessed December 1, 2018, at http://nhd.usgs.gov.

U.S. Geological Survey, 2017, 1/3rd arc-second Digital Elevation Models (DEMs)- USGS National Map 3DEP Downloadable Data Collection: U.S. Geological Survey [separate DEMs are available for download at https://apps.nationalmap.gov/downloader/#/.]

U.S. Geological Survey [USGS], 2018a, Arizona Water Use Project: U.S. Geological Survey Arizona Water Science Center, accessed January 7, 2019, at https://www.usgs.gov/centers/az-water/science/arizona-water-use?qt-science_center_objects=0#qt-science_center_objects.

U.S. Geological Survey [USGS], 2018b, USGS water data for the Nation: U.S. Geological Survey National Water Information System database, accessed December 1, 2018, at https://doi.org/10.5066/F7P55KJN.

UNESCO, 2018, UNESCO world heritage list, accessed October 25, 2018, at https://whc.unesco.org/en/list/.

Westenbroek, S.M., Kelson, V.A., Dripps, W.R., Hunt, R.J., and Bradbury, K.R., 2010, SWB—A modified Thornthwaite-Mather Soil-Water-Balance code for estimating groundwater recharge: U.S. Geological Survey Techniques and Methods 6–A31, 60 p.

Western Regional Climate Center, 2020, Cooperative Climatological Data Summaries, accessed May 1, 2020, at https://wrcc.dri.edu/ summary/Climsmaz.html.

Appendix 1—2

Appendix 1. Source Data and Development of a Structural Contour Map of the Regional R-Aquifer

Exposed upper and lower aquifer contacts were identified in Esri ArcMap software using the shape files and the geologic maps referenced in table 1.1. The polygon features representing geologic units were dissolved by unit name using the dissolve tool. Then, the resulting polygons were converted to polylines using the polygon to line tool. The polylines were spatially joined to identify coincident contacts of the geologic units that form the upper surface (lower part of the Pennsylvanian Supai Formation overlying Mississippian Redwall Limestone) and lower surface (Cambrian Muav Limestone of Tonto Group [hereafter Muav Limestone] overlying Cambrian Bright Angel Shale of Tonto Group [hereafter Bright Angel Shale]) of the regional aquifer. The vertices to points tool was used to generate (X, Y) points from the polylines. Land surface elevation at each point was extracted from a 10-meter digital elevation model raster using the extract multi-values to points tool.

Well logs with depth to formation information of either the Redwall Limestone or Bright Angel Shale were selected from geodatabases provided by State oil and gas agencies of Arizona (Arizona Oil and Gas Conservation Commission, 2016) and Utah (Utah Department of Natural Resources Division of Oil, Gas and Mining, 2016), and Arizona Department of Water Resources (2016). Land surface elevation was extracted to each well's point location and upper or lower surface elevation was calculated by subtracting depth to formation from land surface.

A series of 30′ x 60′ geologic maps cover the study area (table 1.1). Most of these maps include interpreted elevations and thicknesses of the subsurface units along the traces of selected cross sections. Graphic illustration software was used to select points along the top and bottom surfaces of the illustrated R-aquifer and measure the height above the bottom of the cross section in pixels. This measurement was converted to meters above mean sea level based on the scale provided at either end of the cross-section illustration. Points were selected along each section at a regular interval that captured the variability of the surface elevations, typically 1–2 kilometers. Additional points were placed on either side of faults that caused substantial offset.

Surface interpolation was executed with the spline with barriers tool in ArcMap. Mapped faults with substantial vertical offset were used as barriers to interpolation. Contours were created from the resulting elevation raster using the contour with barriers tool.

Table 1.1. Geologic maps used in combination with digital elevation models to determine elevations along mapped exposures of the top and bottom of the R-aquifer.

Geologic Map	Authors	Features Utilized
Cameron 30′ x 60′ quadrangle	Billingsley and others, 2007	Upper surface exposure, cross sections A, B, and C
Fredonia 30′ x 60′ quadrangle	Billingsley and others, 2008	Upper and lower surface exposures, cross sections A and B
Glen Canyon Dam 30′ x 60′ quadrangle	Billingsley and Priest, 2013	Upper surface exposure
Grand Canyon 30′ x 60′ quadrangle	Billingsley and Hampton, 2000	Upper and lower surface exposures
Littlefield 30′ x 60′ quadrangle	Billingsley and Workman, 2000	Cross section A
Mount Trumbull 30′ x 60′ quadrangle	Billingsley and Wellmeyer, 2003	Upper and lower surface exposures, cross sections A and B
Peach Springs 30′ x 60′ quadrangle	Billingsley and others, 2006a	Upper and lower surface exposures, cross sections A, B, and C
St. George 30′ x 60′ quadrangle	Biek and others, 2010	Cross sections A and B
Tuba City 30′ x 60′ quadrangle	Billingsley and others, 2012	Upper and lower surface exposures
Valle 30′ x 60′ quadrangle	Billingsley and others, 2006b	Cross sections A, B, and C

Table 1. 2. Top surface elevation of the Redwall Limestone derived from driller's logs.

[API, American Petroleum Institute; AZDWR, Arizona Department of Water Resources; AZOGCC, Arizona Oil and Gas Conservation Commission; ID, identification; m, meter; UDOGM, Utah Department of Natural Resources Division of Oil, Gas and Mining; —, not applicable]

API number	Other ID	Source	Redwall Limestone top elevation (m)	Latitude	Longitude
02-017-05065	AZOGCC:0013	AZOGCC (2016)	954	36.9888567	−110.380729269891
02-001-05196	AZOGCC:01-78	AZOGCC (2016)	984	36.9770393	−109.909650110244
02-001-05187	AZOGCC:0248	AZOGCC (2016)	−157	36.9649786	−109.77273031988
02-001-05186	AZOGCC:0295	AZOGCC (2016)	−248	36.9649103	−109.682457349998
02-001-05334	AZOGCC:0226	AZOGCC (2016)	−227	36.9560768	−109.667862689642
02-001-05177	AZOGCC:0245	AZOGCC (2016)	−250	36.9500952	−109.680621070266
02-001-05179	AZOGCC:0266	AZOGCC (2016)	−241	36.9503208	−109.668143120257
02-001-05164	AZOGCC:0260	AZOGCC (2016)	−149	36.9101327	−109.605045219943
02-001-05301	AZOGCC:0060	AZOGCC (2016)	−45	36.8874472	−109.627212900079
02-001-00247	AZOGCC:0247	AZOGCC (2016)	−162	36.8877388	−109.798201760501
02-001-05153	AZOGCC:0145	AZOGCC (2016)	−28	36.8510851	−109.604250719825
02-001-00265	AZOGCC:0265	AZOGCC (2016)	−21	36.8012784	−109.81061044054
02-001-00292	AZOGCC:0292	AZOGCC (2016)	−34	36.804409	−109.815119250876
02-001-05150	AZOGCC:0272	AZOGCC (2016)	8	36.7604033	−109.651784440655
02-017-00270	AZOGCC:0270	AZOGCC (2016)	−164	36.7498159	−110.03042345964
02-017-00283	AZOGCC:0283	AZOGCC (2016)	−43	36.6830089	−110.24782078994
02-017-00281	AZOGCC:0281	AZOGCC (2016)	−74	36.6777864	−110.102405850327
02-001-20077	AZOGCC:0455	AZOGCC (2016)	122	36.6417158	−109.649425360268
02-001-00311	AZOGCC:0311	AZOGCC (2016)	366	36.6242464	−109.445425729583
02-001-20086	AZOGCC:0476	AZOGCC (2016)	630	36.5942792	−109.391679609983
02-005-05030	AZOGCC:03-06	AZOGCC (2016)	317	36.5789511	−110.840177909148
02-001-05149	AZOGCC:0300	AZOGCC (2016)	777	36.5617269	−109.374533969153
02-001-05318	AZOGCC:0325	AZOGCC (2016)	58	36.5344456	−109.945755490816
02-001-20059	AZOGCC:0435	AZOGCC (2016)	853	36.4932557	−109.478253420045
02-001-20097	AZOGCC:0494	AZOGCC (2016)	596	36.4992413	−109.482369209699
02-001-05317	AZOGCC:0308	AZOGCC (2016)	84	36.474317	−109.943797239947
02-001-20171	AZOGCC:0594	AZOGCC (2016)	1,058	36.4454007	−109.208624250523
02-001-20078	AZOGCC:0461	AZOGCC (2016)	1,216	36.4058226	−109.273525909095
02-001-20088	AZOGCC:0478	AZOGCC (2016)	1,133	36.4068842	−109.180406889322
02-001-20125	AZOGCC:0526	AZOGCC (2016)	1,251	36.4020322	−109.470327979784
02-001-20061	AZOGCC:0438	AZOGCC (2016)	1,372	36.3776015	−109.337199949552
02-001-20128	AZOGCC:0531	AZOGCC (2016)	836	36.3647685	−109.510694449773
02-001-20060	AZOGCC:0437	AZOGCC (2016)	1,382	36.3537999	−109.34044793939
02-001-20062	AZOGCC:0439	AZOGCC (2016)	1,415	36.3394746	−109.318709139813
02-001-20056	AZOGCC:0432	AZOGCC (2016)	1,420	36.3366485	−109.274603290022
02-001-20080	AZOGCC:0466	AZOGCC (2016)	1,299	36.3283579	−109.412370850354
02-001-20089	AZOGCC:0480	AZOGCC (2016)	1,411	36.318928	−109.215865309094
02-001-20127	AZOGCC:0529	AZOGCC (2016)	648	36.3265212	−109.570441749851
02-001-20063	AZOGCC:0440	AZOGCC (2016)	1,434	36.3144866	−109.323419540023
02-001-20054	AZOGCC:0430	AZOGCC (2016)	1,450	36.3013297	−109.203225949555
02-005-05022	AZOGCC:03-05	AZOGCC (2016)	1,166	36.3017037	−111.50248308994
02-001-20052	AZOGCC:0428	AZOGCC (2016)	1,504	36.2798955	−109.259634020119

Table 1. 2. Top surface elevation of the Redwall Limestone derived from driller's logs.—Continued

API number	Other ID	Source	Redwall Limestone top elevation (m)	Latitude	Longitude
02-001-20053	AZOGCC:0429	AZOGCC (2016)	1,603	36.2524136	−109.189320170026
02-001-20129	AZOGCC:0534	AZOGCC (2016)	978	36.2459064	−109.52766720941
02-001-20087	AZOGCC:0477	AZOGCC (2016)	1,597	36.2278318	−109.156118810725
02-001-20075	AZOGCC:0453	AZOGCC (2016)	1,656	36.2050958	−109.307061419574
02-001-20098	AZOGCC:0496	AZOGCC (2016)	1,566	36.2025847	−109.25282880009
02-001-05148	AZOGCC:01-77	AZOGCC (2016)	287	36.1223836	−109.856139410206
02-001-20100	AZOGCC:0499	AZOGCC (2016)	1,700	36.0720095	−109.208412900006
02-017-05064	AZOGCC:0309	AZOGCC (2016)	−267	35.9635393	−110.479915000452
02-005-05083	AZOGCC:0321	AZOGCC (2016)	−138	35.9526073	−110.773939030486
02-017-05063	AZOGCC:0310	AZOGCC (2016)	−207	35.9344641	−110.315134990141
02-005-20003	AZOGCC:0474	AZOGCC (2016)	−105	35.9380184	−110.809629960017
02-017-05116	AZOGCC:0312	AZOGCC (2016)	−20	35.840583	−110.737898270046
02-005-05019	AZOGCC:0006	AZOGCC (2016)	1,118	35.768207	−112.357343900456
02-005-20035	AZOGCC:0922	AZOGCC (2016)	714	35.7336734	−111.44093909047
02-005-20034	AZOGCC:0914	AZOGCC (2016)	711	35.7226918	−111.427594529776
02-005-05016	AZOGCC:03-04	AZOGCC (2016)	722	35.7117942	−111.432044549884
02-017-05062	AZOGCC:0307	AZOGCC (2016)	39	35.6626681	−110.622287519329
02-005-05009	AZOGCC:03-02	AZOGCC (2016)	1,018	35.3249774	−111.312516670873
—	AZOGCC:ww011	AZOGCC (2016)	1,679	35.285962	−113.115739999844
02-005-05001	AZOGCC:0186	AZOGCC (2016)	810	35.1371181	−111.181593570052
02-025-05015	AZOGCC:0141	AZOGCC (2016)	1,585	35.1097338	−112.554964119081
02-025-05014	AZOGCC:0133	AZOGCC (2016)	1,580	35.1003798	−112.556860309683
02-005-05026	AZOGCC:0240	AZOGCC (2016)	951	35.0833428	−111.304557220225
—	Federal10	AZOGCC (2016)	−320	36.9689532	−113.470870625825
—	Federal1	AZOGCC (2016)	433	36.9253526	−113.272103915367
—	Federal19	AZOGCC (2016)	773	36.9396098	−112.332677475933
—	Federal24	AZOGCC (2016)	794	36.9394085	−112.350500659385
—	Federal2	AZOGCC (2016)	214	36.9106147	−113.018652680215
—	Federal2	AZOGCC (2016)	526	36.8678944	−113.302454321552
—	Antelope1	AZOGCC (2016)	451	36.8387409	−113.159617967494
—	Federal21	AZOGCC (2016)	1,438	36.8524115	−112.189151184713
—	Federal26	AZOGCC (2016)	188	36.8387507	−112.908170607699
—	Federal1	AZOGCC (2016)	386	36.8101346	−113.016455106771
—	Schreiber1	AZOGCC (2016)	465	36.739126	−113.66213441505
—	JacobLake1-32	AZOGCC (2016)	1,658	36.737036	−112.206923255841
—	Pigeon	AZDWR (2016)	889	36.7255499	−112.527729796591
—	Kanab	AZDWR (2016)	714	36.6852118	−112.643728590506
—	Hermit Mine	AZDWR (2016)	568	36.6895464	−112.751998302922
—	Federal1	AZOGCC (2016)	681	36.6508014	−112.871998273621
—	Federal15	AZOGCC (2016)	653	36.6080602	−113.571550703612
—	Pinenut	AZDWR (2016)	652	36.5028565	−112.733135447035
—	Federal1	AZOGCC (2016)	507	36.49129	−113.299224321049
43-015-11330	WASHBOARD WASH USA 1-A	UDOGM (2016)	−1,200	39.4549935	−110.866158535981

Table 1. 2. Top surface elevation of the Redwall Limestone derived from driller's logs.—Continued

API number	Other ID	Source	Redwall Limestone top elevation (m)	Latitude	Longitude
43-015-10021	GREEN RIVER DESERT U 9-7	UDOGM (2016)	−1,267	38.9160189	−110.27294136557
43-015-10022	GREEN RIVER DESERT U 24-1	UDOGM (2016)	−561	38.8928687	−110.435700954723
43-019-11188	SALT WASH UNIT 22-34	UDOGM (2016)	−1,789	38.8581501	−110.034770028371
43-015-11031	GRUVERS MESA 1	UDOGM (2016)	−848	38.7125169	−110.200598471972
43-015-11033	GRUVERS MESA 2	UDOGM (2016)	−588	38.6576631	−110.137249249989
43-015-20367	LAST CHANCE UNIT 1	UDOGM (2016)	293	38.541684	−111.210121167186
43-055-30030	FISH LAKE 1-1	UDOGM (2016)	99	38.4901824	−111.535145626858
43-055-30032	HANKSVILLE UNIT 1	UDOGM (2016)	−571	38.4900766	−110.751496975706
43-037-30923	TXC/HUBER FEDERAL 1-15	UDOGM (2016)	−1,379	38.3649951	−109.155178507605
43-055-11273	THOUSAND LAKE MTN UNIT 2	UDOGM (2016)	1,289	38.3515703	−111.428535929082
43-055-30010	DIRTY DEVIL UNIT 1	UDOGM (2016)	−166	38.227744	−110.50029748362
43-037-30694	LISBON U D-610	UDOGM (2016)	−157	38.1997866	−109.269897653929
43-037-30695	LISBON B-94	UDOGM (2016)	−705	38.2019454	−109.295495848729
43-037-30693	LISBON C-99	UDOGM (2016)	−669	38.1875585	−109.29272596538
43-037-31014	LISBON UNIT A-911	UDOGM (2016)	−250	38.1896549	−109.265444817462
43-037-31323	LISBON C-910	UDOGM (2016)	−385	38.188578	−109.271864416626
43-037-31351	LISBON B-614A	UDOGM (2016)	−461	38.1860487	−109.258040555179
43-037-31433	LISBON B-810	UDOGM (2016)	−490	38.191964	−109.276602892206
43-001-30007	BEAVER FED 21-14	UDOGM (2016)	−229	38.180327	−112.658086514773
43-037-31034	LISBON UNIT D-716	UDOGM (2016)	−650	38.1807185	−109.289620619152
43-017-30118	ALLEN FEE 1	UDOGM (2016)	963	38.1350355	−112.004181980889
43-017-30008	BLOODY HANDS GAP UNIT 1	UDOGM (2016)	−262	38.066831	−111.080654481505
43-017-30074	FEDERAL HARVEY 1-10R	UDOGM (2016)	631	38.0437311	−111.783370861432
43-017-30115	DIXIE UNIT 2	UDOGM (2016)	−2,036	37.9678074	−112.292578195594
43-021-30005	TABLE BUTTE U 1	UDOGM (2016)	376	37.8961329	−113.489526589867
43-021-30005	TABLE BUTTE U 1	UDOGM (2016)	−3,982	37.8961329	−113.489526589867
43-017-30138	FEDERAL 28 1	UDOGM (2016)	1,028	37.9062562	−111.139107074307
43-037-30600	REDD RANCH 1-34	UDOGM (2016)	773	37.8619777	−109.703404110354

Table 1. 2. Top surface elevation of the Redwall Limestone derived from driller's logs.—Continued

API number	Other ID	Source	Redwall Limestone top elevation (m)	Latitude	Longitude
43-017-30112	CLAY CREEK FEDERAL 13-29	UDOGM (2016)	−1,522	37.8156003	−112.037886588561
43-037-30980	USA 32-1	UDOGM (2016)	291	37.7771724	−109.524393293843
43-017-30022	JOHNS VALLEY FED 1	UDOGM (2016)	−877	37.7209627	−111.977912803057
43-017-10190	UPPER VALLEY UNIT 1	UDOGM (2016)	−550	37.704947	−111.742111958307
43-021-30002	SHURTZ CREEK	UDOGM (2016)	424	37.6052126	−113.091486792518
43-037-30849	NIELSON “”A”” 1	UDOGM (2016)	−642	37.5475291	−109.455978397703
43-025-30014	FEDERAL 11-9	UDOGM (2016)	−959	37.5287921	−111.596094798177
43-025-30006	GOVT 1	UDOGM (2016)	39	37.4129008	−111.880517941305
43-025-11036	W-T STATE 2 1-B	UDOGM (2016)	−418	37.3659929	−111.11939233994
43-025-30025	REESE CANYON ST 32 2	UDOGM (2016)	−759	37.3730909	−111.3950412117
43-025-10633	RINCON DOME FED 1	UDOGM (2016)	111	37.3353056	−110.793004154732
43-053-30001	FEDERAL 30-B3X	UDOGM (2016)	−255	37.2810226	−113.250278207594
43-025-11296	UTAH FED A-1	UDOGM (2016)	1,027	37.1189055	−112.007898969895
43-025-20063	JUDD HOLLOW 1	UDOGM (2016)	−363	37.0600907	−111.740920952044
43-053-10214	ST GEORGE UNIT 1	UDOGM (2016)	−771	37.0388629	−113.576805772737
43-025-30022	KAIBAB 1-36	UDOGM (2016)	1,231	37.0324953	−112.074880105064
43-017-10904	ESCALANTE U 2	UDOGM (2016)	1,119	37.9911354	−111.598613429
43-021-30005	TABLE BUTTE U 1	UDOGM (2016)	429	37.8961329	−113.489526589867
43-017-10592	GOVT 1	UDOGM (2016)	1,083	37.8374353	−111.088801157833
43-017-20183	FEDERAL TRAVIS 2	UDOGM (2016)	343	37.768897	−111.396365790459
43-017-11220	AJ BUTTON FEE 2	UDOGM (2016)	−375	37.7424839	−111.591210931406
43-017-30082	FEDERAL A 1	UDOGM (2016)	−730	37.7402193	−111.771134024253
43-021-30003	CEDAR CITY 1	UDOGM (2016)	−1,503	37.6741159	−113.136878072898
43-017-16025	UPPER VALLEY U 2	UDOGM (2016)	−498	37.6847342	−111.748567764753
43-017-30038	USA - AMOCO G 1	UDOGM (2016)	24	37.6742373	−111.276158773573
43-017-30021	UV 21	UDOGM (2016)	−747	37.611756	−111.730613124831
43-037-20359	FEDERAL 1	UDOGM (2016)	271	37.5991224	−110.458007472514
43-037-30509	MOQUI CANYON 1	UDOGM (2016)	3	37.4945025	−110.418275978486
43-037-30305	FEDERAL 23-29	UDOGM (2016)	564	37.4540756	−110.176905477262

Table 1. 2. Top surface elevation of the Redwall Limestone derived from driller's logs.—Continued

API number	Other ID	Source	Redwall Limestone top elevation (m)	Latitude	Longitude
43-037-10847	GRAND GULCH UNIT 1	UDOGM (2016)	399	37.4182354	−110.301278287757
43-053-10879	MARTIN-PINTURA U 1	UDOGM (2016)	−856	37.3515200	−113.325500000000
43-037-10376	GOVT 31-1	UDOGM (2016)	523	37.357471	−110.303918983582
43-025-20156	PARIA STATE UNIT 1-A	UDOGM (2016)	321	37.3334693	−112.033301893494
43-053-30007	FEDERAL 1-13	UDOGM (2016)	877	37.314024	−113.271097931077
43-053-20318	PEASE FED 1	UDOGM (2016)	−173	37.2841811	−113.263760167867
43-053-30001	FEDERAL 30-B3X	UDOGM (2016)	−164	37.2810226	−113.250278207594
43-037-20387	SKELLY OIL CO 1-A	UDOGM (2016)	239	37.2882016	−110.582560344566
43-037-20401	1	UDOGM (2016)	1,039	37.2832509	−109.931356968017
43-025-30015	FEDERAL 41-11	UDOGM (2016)	−312	37.2667495	−112.596070377555
43-037-11250	JOHNS CANYON UNIT 1	UDOGM (2016)	1,085	37.2479907	−109.979525497225
43-025-11189	KANAB CREEK UNIT 32-16	UDOGM (2016)	−85	37.1624091	−112.636554450465
43-053-30005	HIKO BELL FEDERAL 1	UDOGM (2016)	189	37.145167	−113.285288802231
43-037-11112	NAV TRIBAL 172 SJ 1	UDOGM (2016)	−305	37.1455034	−109.702280587902
43-037-11130	MEXICAN HAT 1	UDOGM (2016)	1,047	37.14637	−109.807871229286
43-025-10705	STATE 1	UDOGM (2016)	−307	37.0985975	−112.717264583222
43-037-10687	NAVAJO TRIB-AL 1-10	UDOGM (2016)	−227	37.0612769	−109.601546674579
43-037-15916	ENGLISH 7	UDOGM (2016)	−122	37.0579938	−109.508262013417
43-037-30247	NAVAJO TRIBAL DU-3	UDOGM (2016)	−250	37.0559459	−109.678163358968
43-053-20044	FEDERAL 1	UDOGM (2016)	440	37.0432854	−113.290201846052
43-037-15911	ENGLISH 1	UDOGM (2016)	−4	37.0425612	−109.488954071436
43-037-10278	CHINLE WASH 1	UDOGM (2016)	−310	37.0319511	−109.583758460597
43-037-11253	NAVAJO TRIBE AE-1	UDOGM (2016)	−233	37.0427291	−109.651540908905
43-037-15919	ENGLISH 10	UDOGM (2016)	11	37.0393282	−109.498406482741
43-037-31476	RABBIT EARS 1	UDOGM (2016)	−251	37.0402305	−109.527937138144
43-037-10701	NAVAJO B 1	UDOGM (2016)	−255	37.008592	−109.669755106989

Table 1. 3. Top surface elevation of the Bright Angel Shale, coincident in most places with the bottom of the Cambrian Muav Limestone, derived from driller's logs.

[API, American Petroleum Institute; AZOGCC, Arizona Oil and Gas Conservation Commission; ID, identification; m, meter; UDOGM, Utah Department of Natural Resources Division of Oil, Gas and Mining; —, not applicable]

API Number	Other ID	Source	Bright Angel Shale top elevation (m)	Latitude	Longitude
02-001-05187	AZOGCC:0248	AZOGCC (2016)	−463	36.9649786	−109.77273031988
02-001-05177	AZOGCC:0245	AZOGCC (2016)	−561	36.9500952	−109.680621070266
02-001-05179	AZOGCC:0266	AZOGCC (2016)	−541	36.9503208	−109.668143120257
02-017-00283	AZOGCC:0283	AZOGCC (2016)	−357	36.6830089	−110.24782078994
02-017-00281	AZOGCC:0281	AZOGCC (2016)	−373	36.6777864	−110.102405850327
02-005-05030	AZOGCC:03-06	AZOGCC (2016)	12	36.5789511	−110.840177909148
02-001-05318	AZOGCC:0325	AZOGCC (2016)	−189	36.5344456	−109.945755490816
02-005-05022	AZOGCC:03-05	AZOGCC (2016)	852	36.3017037	−111.50248308994
02-017-05064	AZOGCC:0309	AZOGCC (2016)	−462	35.9635393	−110.479915000452
02-005-05083	AZOGCC:0321	AZOGCC (2016)	−332	35.9526073	−110.773939030486
02-017-05063	AZOGCC:0310	AZOGCC (2016)	−416	35.9344641	−110.315134990141
02-017-05116	AZOGCC:0312	AZOGCC (2016)	−202	35.840583	−110.737898270046
02-005-05019	AZOGCC:0006	AZOGCC (2016)	887	35.768207	−112.357343900456
02-005-20035	AZOGCC:0922	AZOGCC (2016)	508	35.7336734	−111.44093909047
02-005-20034	AZOGCC:0914	AZOGCC (2016)	522	35.7226918	−111.427594529776
—	AZOGCC:ww011	AZOGCC (2016)	1462	35.285962	−113.115739999844
02-025-05015	AZOGCC:0141	AZOGCC (2016)	1,362	35.1097338	−112.554964119081
—	Federal24	AZOGCC (2016)	237	36.9394085	−112.350500659385
—	Federal2	AZOGCC (2016)	−545	36.9106147	−113.018652680215
—	Federal26	AZOGCC (2016)	−479	36.8387507	−112.908170607699
—	JacobLake1-32	AZOGCC (2016)	1,201	36.737036	−112.206923255841
—	Federal1	AZOGCC (2016)	130	36.6508014	−112.871998273621
—	Federal1	AZOGCC (2016)	315	36.49129	−113.299224321049
43-037-11250	JOHNS CANYON UNIT 1	UDOGM (2016)	770	37.2479907	−109.979525497225
43-025-11189	KANAB CREEK UNIT 32-16	UDOGM (2016)	−775	37.1624091	−112.636554450465
43-053-30005	HIKO BELL FEDERAL 1	UDOGM (2016)	−637	37.145167	−113.285288802231
43-037-11130	MEXICAN HAT 1	UDOGM (2016)	751	37.14637	−109.807871229286
43-025-11296	UTAH FED A-1	UDOGM (2016)	260	37.1189055	−112.007898969895
43-025-10705	STATE 1	UDOGM (2016)	−1,007	37.0985975	−112.717264583222
43-025-20063	JUDD HOLLOW 1	UDOGM (2016)	−934	37.0600907	−111.740920952044
43-025-30022	KAIBAB 1-36	UDOGM (2016)	621	37.0324953	−112.074880105064
43-017-30118	ALLEN FEE 1	UDOGM (2016)	19	38.1350355	−112.004181980889
43-017-10592	GOVT 1	UDOGM (2016)	475	37.8374353	−111.088801157833
43-037-15588	LIME RIDGE UNIT 1	UDOGM (2016)	568	37.2768739	−109.728511720126

References Cited

Arizona Department of Water Resources [AZDWR], 2016, Groundwater site inventory (GWSI) database: Arizona Department of Water Resources database, accessed October 3, 2016, at https://azwatermaps.azwater.gov/gwsi.

Arizona Oil and Gas Conservation Commission [AZOGCC], 2016, Oil and Gas Viewer, accessed June 16, 2016, at http://welldata.azogcc.az.gov/.

Biek, R.F., Rowley, P.D., Hayden, J.M., Hacker, D.B., Willis, G.C., Hintze, L.F., Brown, K.D., 2010, Geologic map of the St. George and East Part of the Clover Mountains 30'x60' quadrangles, Washington and Iron Counties, Utah: Utah Geological Survey, scale 1:100,000.

Billingsley, G.H., Block, D.L., and Dyer, H.C., 2006a, Geologic map of the Peach Springs 30'x60' quadrangle, Mohave and Coconino Counties, northwestern Arizona: U.S. Geological Survey Scientific Investigations Map 2900.

Billingsley, G.H., Felger, T.J., and Priest, S.S., 2006b, Geologic map of the Valle 30'x60' quadrangle, Coconino County, northern Arizona: U.S. Geological Survey Scientific Investigations Map 2895.

Billingsley, G.H., and Hampton, H.M, 2000, Geologic map of the Grand Canyon 30'x60' quadrangle, Coconino and Mohave Counties, northwestern Arizona: U.S. Geological Survey Geologic Investigations Series I-2688, scale 1:100,000.

Billingsley, G.H., and Priest, S.S., 2013, Geologic map of the Glen Canyon Dam 30'x60' quadrangle, Coconino County, northern Arizona: U.S. Geological Survey Scientific Investigations Map 3268.

Billingsley, G.H., Priest, S.S., and Felger, T.J., 2007, Geologic map of the Cameron 30'x60' quadrangle, Coconino County, northern Arizona: U.S. Geological Survey Scientific Investigations Map 2977, scale 1:100,000.

Billingsley, G.H., Priest, S.S., and Felger, T.J., 2008, Geologic map of the Fredonia 30'x60' quadrangle, Mohave and Coconino Counties, northern Arizona: U.S. Geological Survey Scientific Investigations Map 3035, scale 1:100,000.

Billingsley, G.H., Stoffer, P.W., and Priest, S.S., 2012, Geologic map of the Tuba City 30'x60' quadrangle, Coconino County, northern Arizona: U.S. Geological Survey Scientific Investigations Map 3227, scale 1:50,000.

Billingsley, G.H., and Wellmeyer, J.L., 2003, Geologic map of the Mount Trumbull 30'x60' quadrangle, Mohave and Coconino Counties, northwestern Arizona: U.S. Geological Survey Geologic Investigations Series I–2766.

Billingsley, G.H., and Workman, J.B., 2000, Geologic map of the Littlefield 30'x60' quadrangle, Mohave County, northwestern Arizona: U.S. Geological Survey Geologic Investigations Series I–2628.

Utah Department of Natural Resources Division of Oil, Gas and Mining [UDOGM], 2016, State of Utah – Data Explorer, accessed June 22, 2016, at https://datamining.ogm.utah.gov/.

Appendix 2. Soil-Water-Balance (SWB) Model Input Data and Results

Model Inputs

Input data for the Soil-Water-Balance Model are available in Knight and Jones (2022).

Table 2. 1. Soil-Water-Balance (SWB) model lookup table values for runoff curve numbers, root zone depths, and maximum infiltration rates.

[Values are identical to those chosen for a SWB model created for the upper Colorado River Basin (Tillman, 2015). NLCD, National Land Cover Database (Multi-Resolution Land Characteristics Consortium, 2020); ft, feet; in/d, inches per day]

NLCD land cover value	NLCD land cover description	Curve number by hydrologic soil group (HSG)				Root zone depth (ft)
		HSG A	HSG B	HSG C	HSG D	
11	Open water	100	100	100	100	0
21	Developed open space	49	69	79	84	8.53
22	Developed, low intensity	77	86	91	94	8.53
23	Developed, medium intensity	89	92	94	95	8.53
24	Developed, high intensity	98	98	98	98	8.53
31	Barren land	77	86	91	94	1
41	Deciduous forest	32	48	57	63	9.5
42	Evergreen forest	39	58	73	80	12.8
43	Mixed forest	46	60	68	74	11.15
52	Shrub	49	68	79	84	3.5
71	Grassland, herbaceous	64	71	81	89	8.53
81	Pasture	49	69	79	84	8.53
82	Cultivated crops	71	80	87	90	2
90	Woody wetlands	88	89	90	91	4.5
95	Herbaceous wetlands	89	90	91	92	4.5
		Maximum infiltration rate (in/d)				
	All land cover classifications	1	0.6	0.24	0.12	

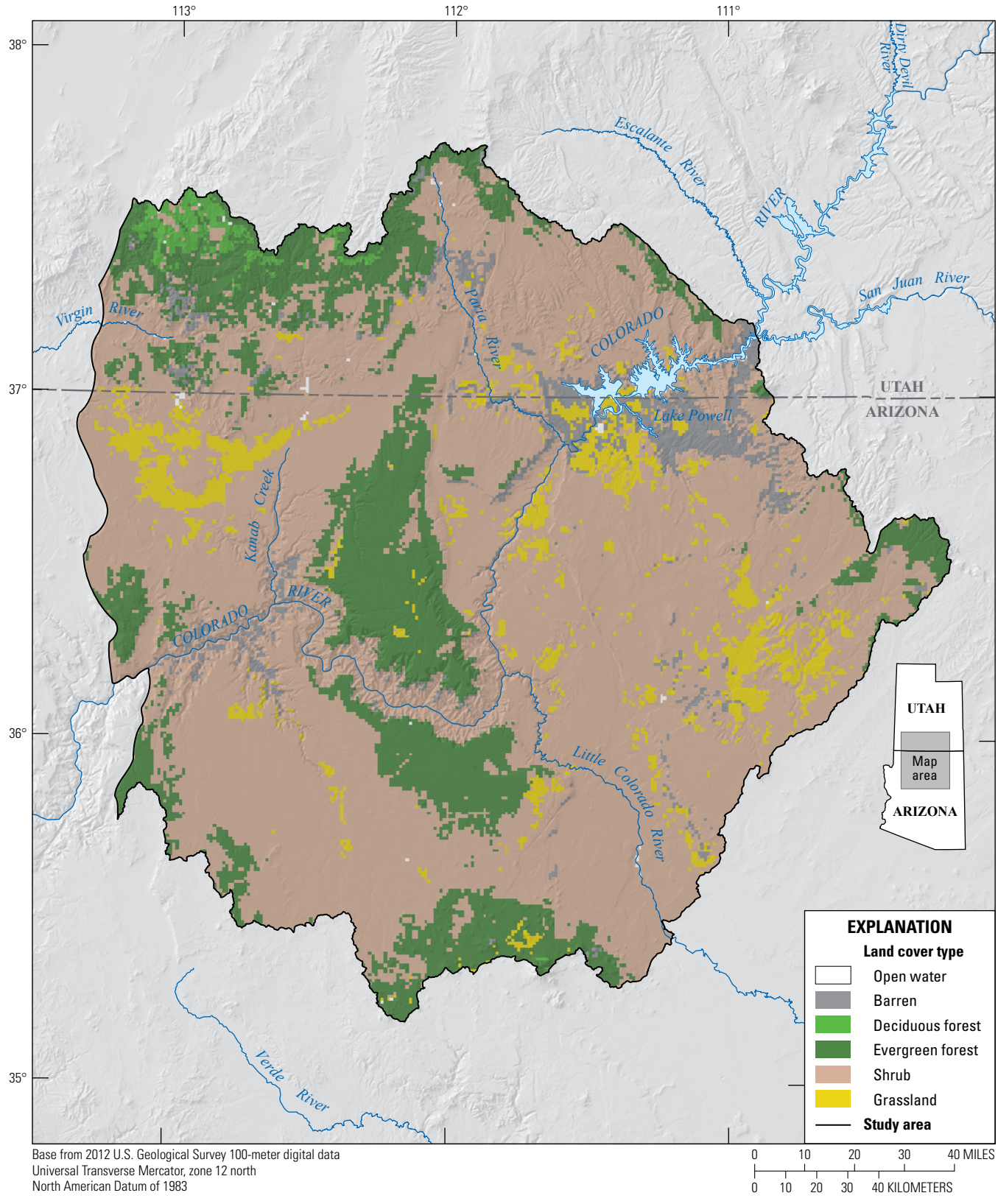

Figure 2.1. Map of land cover input dataset within the study area. Land cover data from Multi-Resolution Land Characteristics Consortium (2020).

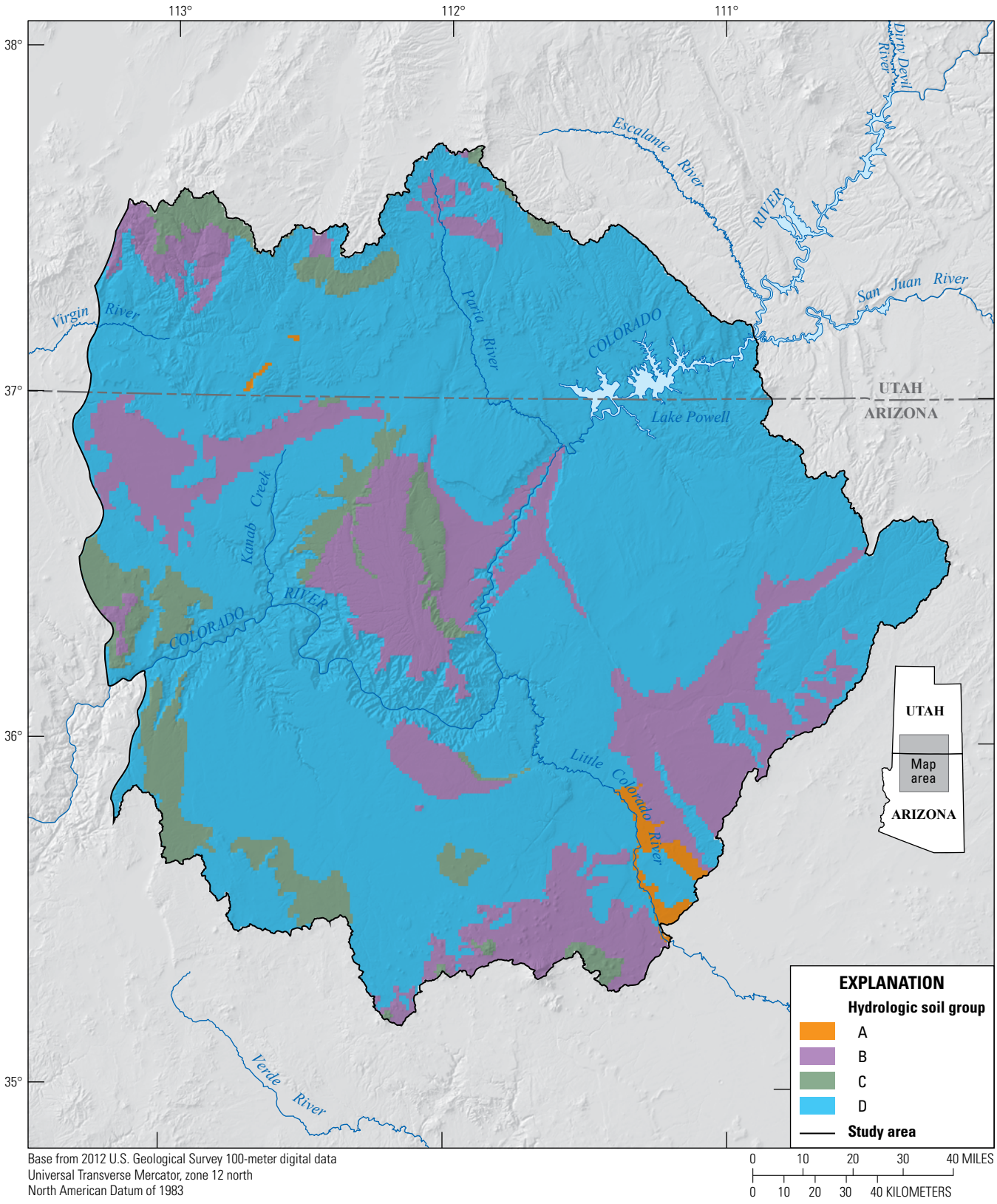

Figure 2.2. Map of hydrologic soil groups input dataset within the study area. Infiltration capacity decreases and overland flow potential increases from group A soils to group D soils. Data from National Resources Conservation Service (2020).

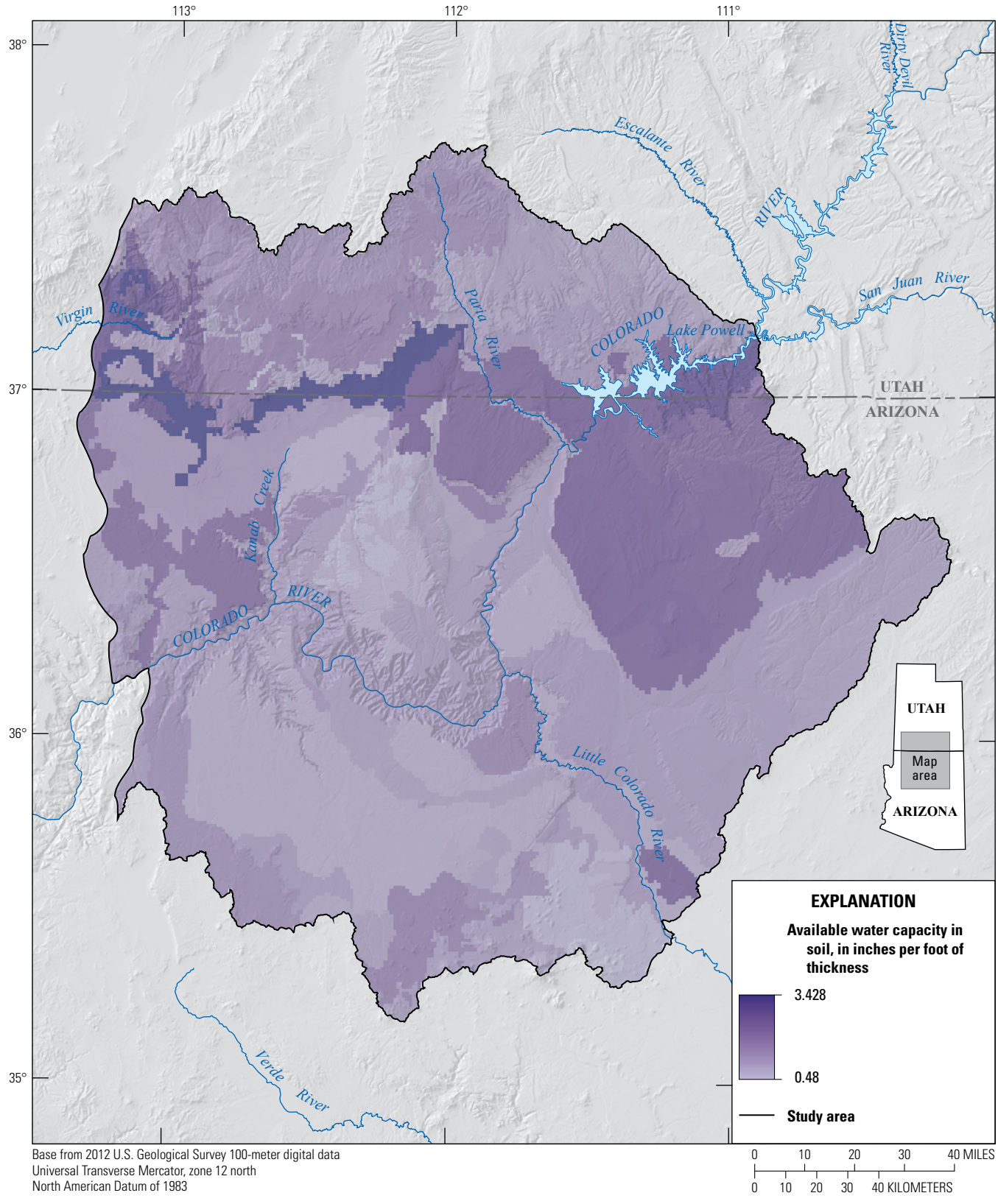

Figure 2.3. Map of available water capacity in soil input dataset, in inches per foot of thickness, within the study area. Data from National Resources Conservation Service (2020).

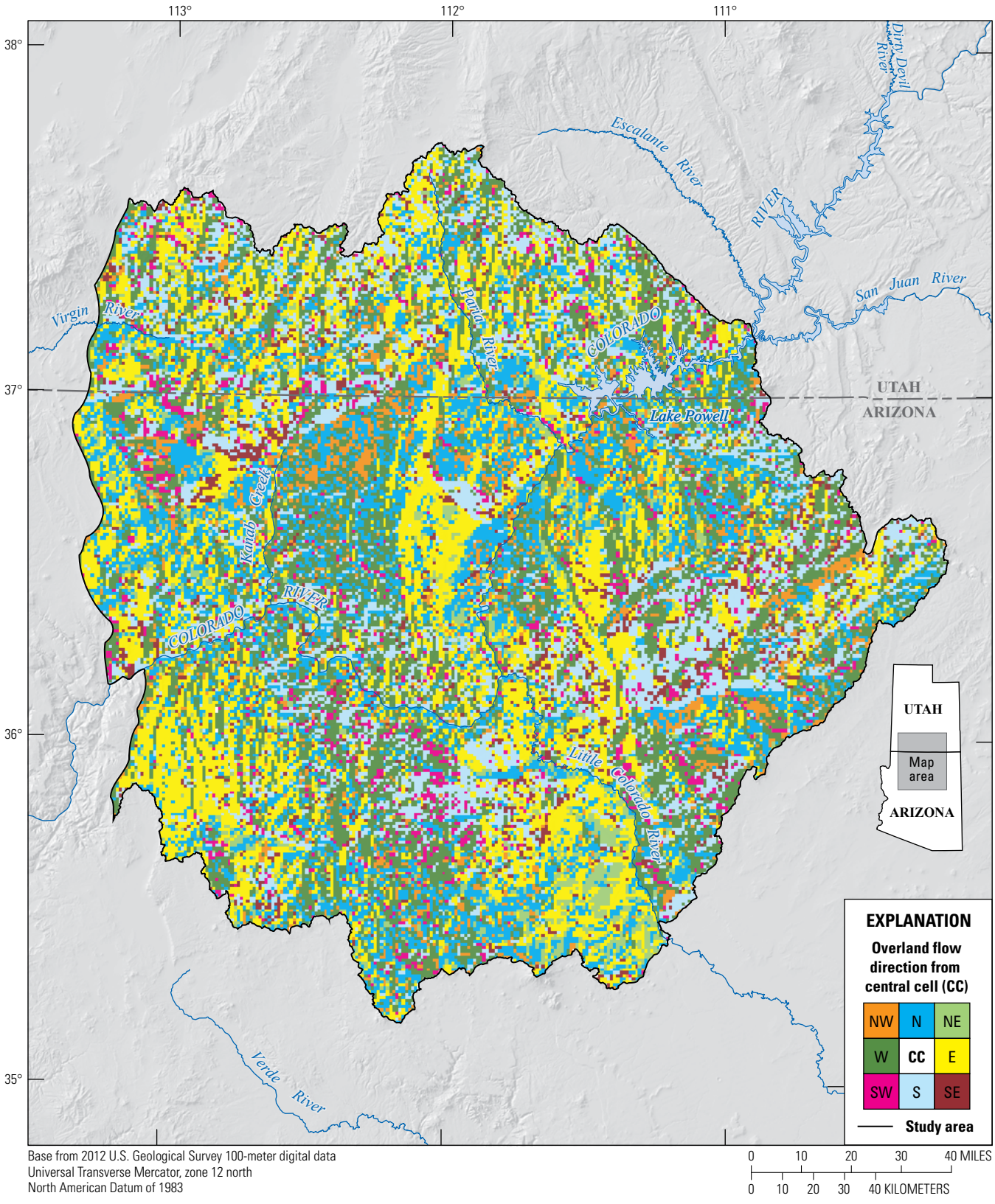

Figure 2.4. Map of overland flow direction within the study area. Colored polygons represent flow direction.

Model Results and Sensitivity Analysis

Table 2.2. Mean annual values of individual groundwater systems of the study area.

[Values in acre-feet]

Groundwater system	Potential evapotranspiration	Gross precipitation	Surface runoff	Net infiltration	Actual evapotranspiration	Recharge	Rejected recharge
Kaibab	3,342,820	1,447,050	30,695	1,415,895	1,224,667	171,690	28,943
Kanab	11,639,882	3,536,469	111,993	3,423,790	3,300,634	86,749	67,855
Marble-Shinumo	13,209,673	2,708,838	103,756	2,604,680	2,594,555	24,913	25,072
Cataract	9,571,485	3,007,196	77,670	2,929,529	2,824,650	60,063	59,290
Blue Spring	12,936,045	2,525,603	25,136	2,500,295	2,485,387	39,941	11,037

Table 2.3. Simulated mean annual recharge in study area resulting from adjusting model input values +/- 25 percent, in acre-feet, and percentage difference from mean annual recharge simulated using original model inputs.

[Curve number relates rainfall to surface runoff, with lower curve numbers meaning less runoff. Root depth is the depth below which water cannot be taken up by plant roots and transpired. Maximum recharge rate is used by the Soil-Water-Balance model to preclude rates of recharge greater than the expected saturated vertical conductivity of the soil; %, percent]

Model run	Mean annual recharge (acre-feet)	Percentage difference from original model
Base case	428,758	0
Curve number +25%	228,649	−47
Curve number −25%	460,385	7
Root depth +25%	340,711	−21
Root depth −25%	584,457	36
Maximum recharge rate +25%	474,320	11
Maximum recharge rate −25%	351,284	−18

References Cited

Knight, J.E., and Jones, C.J., 2022, Soil-Water-Balance (SWB) model archive used to simulate potential mean annual recharge in the Grand Canyon region, Arizona: U.S. Geological Survey data release, https://doi.org/10.5066/P9FQ7BSY.

Multi-Resolution Land Characteristics Consortium, 2020, National Land Cover Dataset 2016 Landcover (CONUS), accessed May 28, 2020, at https://www.mrlc.gov/data/nlcd-2016-land-cover-conus.

Natural Resources Conservation Service, Soil Survey Staff, 2020, SSURGO database—Web soil survey: U.S. Department of Agriculture database, accessed July 17, 2020, at https://websoilsurvey.nrcs.usda.gov/.

Tillman, F.D., 2015, Documentation of input datasets for the soil-water-balance groundwater recharge model of the Upper Colorado River Basin: U.S. Geological Survey Open-File Report 2015–1160, 17 p., accessed November 6, 2018, at https://doi.org/10.3133/ofr20151160.

Moffett Field Publishing Service Center, California
Manuscript approved April 01, 2022
Edited by Phil Frederick
Illustrative support by JoJo Mangano
Layout by Kimber Petersen

ISSN 2328-0328 (online)
https://doi.org/10.3133/sir20225037